MODE-LIKE PROPERTIES

AND IDENTIFICATION OF

NONLINEAR VIBRATING SYSTEMS

Thesis by

Liping Huang

In Partial Fulfillment of the Requirements

for the Degree of Doctor of Philosophy

California Institute of Technology

Pasadena, California

1995

(Submitted May, 1995)

ACKNOWLEDGMENTS

I would like to express my appreciation to my advisor, Professor W. D. Iwan, for his guidance while I pursued my Ph.D. at Caltech. His bright insight, continuous advice and helpful suggestions were essential for developing the ideas of this work. I consider myself fortunate for having the opportunity to share some of his knowledge and experience.

I am grateful to Caltech for the excellent education that I received and for the financial aid that made this thesis possible. I wish to thank Professor James L. Beck and John F. Hall for their encouragement and assistance in my graduate studies at Caltech. I appreciate the members of the examining committee, Professor John F. Hall, James L. Beck, Joel W. Burdick, and visiting Professor Konstantinos Papadimitriou from Texas A & M University for spending their time reviewing the dissertation.

I would also like to express my deep gratitude to my parents. Without their constant support and encouragement, this thesis could never have been completed. Special thanks must be given to my caring wife, Yingzi, for her help in typewritting and refining the thesis.

ABSTRACT

A study is made of mode-like properties and identification of nonlinear systems and their applications in structural seismic analysis.

In the thesis, mode-like behavior of nonlinear systems is examined. The modal frequencies and mode shapes of nonlinear systems are found to be dependent on the response. Based on approximation, amplitude-dependent mode shape is defined and approximate methods for calculation of modal frequencies and mode shapes (instantaneous and amplitude-dependent) are presented. Based on amplitude-dependent modal relationship, amplitude-dependent models of modal equations which are valid in large range of response and suitable for unique identification are proposed and the corresponding modal identification procedures are developed. The applicability of the new models and identification algorithms is tested through the analysis of an ideal 3DOF nonlinear system.

As applications, the seismic responses of a 47-story building and a 4-story building are investigated using the presented methods. The modal parameters and modal equations of the structures are identified.

Table of Contents

CHAPTER 1

INTRODUCTION

Dynamic behavior of systems is of considerable importance for the safety of structures. A major task of structural analysis is to find dynamic properties and to determine mathematical models of the system. Earthquake records provide much valuable information concerning the dynamic behavior of structures. They are an important resource for structural analysis. Since the San Fernando earthquake of 1971 the quality and quantity of seismic records have increased markedly. Increasing needs for seismic analysis have led considerable progress in the field of structural dynamics identification. Over the past 20 years, various techniques for seismic analysis [1-20] and more general system identification methodologies [21-52] have been developed.

Since many structural seismic responses are in the nonlinear (large amplitude) range and many civil engineering structures possess hysteretic nonlinearities, seismic analysis often requires the use of nonlinear system identification techniques. Among the nonlinear system identification techniques, most approaches analyze only single-degree-of-freedom (SDOF) system. The used models are hysteretic or polynomial. For application to multi-degree-of-freedom (MDOF) system, some approaches assume that the response of the system is dominated by the first mode and that the system can be described as SDOF system by

ignoring the effect of other modes. These approaches use the response data only at one degree of freedom. The approaches for MDOF system [38-44] assume the mathematical model of a system to be a set of second-order nonlinear ordinary differential equations in the physical coordinates domain, expressing all restoring force terms as polynomial, and determining the coefficients of this polynomial by response data. The method uses the complete response data of all degrees of freedom and allows any number of modes. However, if a system has many degrees of freedom, there will be many unknown coefficients to be determined. Furthermore, if the equations of motion have been determined, calculation of a new response requires solving the entire set of nonlinear differential equations even though the response of the system may be dominated by only a few modes.

As is well known, modal analysis is a powerful tool for dynamic analysis of linear systems. By modal analysis, a complicated N-dimensional problem can be reduced to a small number of independent one-dimensional problems. Modal analysis is especially efficient when a system is dominated only by its first few modes. For nonlinear problems, the same approach is of much interest for simplification of the analysis process. Furthermore, modal analysis is also needed to acquire the system natural frequencies and mode shapes which are very important information of structures.

In many dynamic responses of nonlinear systems mode-like behavior can often be observed. For example, resonant peaks are often observed in frequency spectra of the response, and the systems assume certain displacement configurations which are associated with those resonant frequencies. Therefore, there exists a practical basis for modal analysis of nonlinear systems. In the references of [53-55] modal analysis is extended to nonlinear

systems.

In many cases, linear modal identification methods are used to analyze nonlinear systems. Such approaches result in equivalent linear modes. Employing nonlinear models, several nonlinear modal identification procedures have also been developed [45-52]. These approaches fall into two categories. One is in the frequency domain in which equivalent natural frequencies and mode shapes are determined. Another is in the time domain in which modal equations are the identification target. In practice, modal equations are expressed as nonlinear functions with constant coefficients to be determined for response data.

For safety analysis of structures, a good model of the system is particularly important for response prediction. However, the models determined from existing modal identification techniques often fail to predict response of systems to a different loading. One reason is that the modal equations of the nonlinear systems are dependent upon the level of motion. Theoretically, a modal equation with constant coefficients determined from a specific response is only valid for the motion of same level. For motions with other level, such a model is invalid. If a system vibrates at a level which is close to the motion of a modal equation, the equation may be a good approximate model of the system. If the system vibrates at a different level which is far away from the level of the modal equation, the model may result in significant error in prediction of the response. Since a structure may vibrate in a wide amplitude range from small amplitude levels to the damage regime during earthquakes, an effective model which is applicable to a wider loading range is required to represent the system adequately. An important task of this thesis is to develop such a model in the modal domain.

For development of modal equation model and modal analysis of nonlinear systems, a good understanding of nonlinear modes is necessary. Basic properties of mode-like behavior of nonlinear system are to be studied. It is the first objective of this thesis to obtain more knowledge about nonlinear modes. To identify the modal quantities (modal frequencies and mode shapes) and the modal equations from recorded response data, a corresponding identification procedure needs to be developed, which is the final goal of the thesis.

The thesis starts with the concept of modes. Rosenberg's definition of modes of the nonlinear systems is given and mode shape is defined in Chapter 2. Examples of mode-like response of nonlinear system are shown.

In Chapter 3 approximate methods for calculation of nonlinear modal frequencies and mode shapes are proposed, and the properties of nonlinear modes are examined. The relationship between free vibration mode and resonance of forced vibration is shown. This relationship provides a basis for the use of free vibration mode in the analysis of forced vibration.

Chapter 4 mainly discusses model of modal equation. Based on the modal properties of the nonlinear system, amplitude-dependent modal equation is proposed. Since such modal equations are parametric differential equations, parameters need to be estimated *a priori* to solve the equations. An algorithm for amplitude estimation is presented in this chapter.

For feasible and unique determination from recorded data, two specific modal equation models and the corresponding identification methodologies are presented in chapter 5 and 6 respectively. To verify their efficiency, these models and identification procedures

are applied to identify modes of an ideal nonlinear system and the resulting models are used to predict the response of the system to another loading.

In chapter 7, the proposed models and identification procedures are applied to the analysis of response data recorded during the Loma Prieta earthquake in 1989. A forty-seven-story building and a four-story building are analyzed. The modal frequencies, mode shapes and modal equations of dominant modes of the system are determined.

The last chapter presents conclusions of this dissertation.

CHAPTER 2

NONLINEAR VIBRATION MODES

2.1 NONLINEAR VIBRATION MODES

2.1.1 Linear Modes

The vibration modes of a linear system are special states of motion of the system. These states are the natural ones of the system when it executes an undamped free vibration with a single frequency. When a linear system is in such a motion, the system will assume a certain displacement configuration (or shape). This displacement configuration is referred to as a mode shape of the system and the frequency is called a natural frequency (or modal frequency) of the system. A natural frequency and a corresponding mode shape constitute a so-called mode of the linear system and the system in a modal motion is said to be vibrating in a mode. When a linear system vibrates in a mode, the ratios of all displacement coordinates to a given coordinate (as a reference) remain constant throughout the motion and thereby all coordinates of the system can be determined from the reference coordinate at any instant of time.

2.1.2 Nonlinear Modes

Based on an analogy to linear modes, the concept of vibration in modes was

extended to nonlinear systems by Rosenberg in early 1960's [53-55]. According to Rosenberg, a nonlinear system is said to be vibrating in a mode when all masses execute undamped equiperiodic free motions, when all masses pass through their equilibrium positions at the same instant and reach their maximum positions at the same instant, and when the displacements of all the masses is uniquely determined, at any time t, by the displacement of any one mass. A state of the system represented by such a motion is known as a mode of the nonlinear system. Mathematically, a vibration in a mode of a nonlinear system is a motion which satisfies all of the following properties.

(i) There exists a constant, T, such that

$$x_i(t) = x_i(t+T), \quad i = 1, \cdots, n, \tag{2.1}$$

where x_i is the *ith* coordinate. That is, motion has period T.

(ii) If t_0 is any instant of time, there exists a single t_e in $t_0 \le t \le t_0 + T/2$ such that

$$x_i(t_e) = 0, \quad i = 1, \cdots, n. \tag{2.2}$$

(iii) There exists a single $t_p \neq t_e$ in $t_0 \le t \le t_0 + T/2$ such that

$$|x_i(t_p)| = |x_i(t)|_{max}, \quad i = 1, \cdots, n. \tag{2.3}$$

(iv) Let *r* (fixed) be any one of the $i = 1, \cdots, n$. Then every x_i can be represented by a real single-valued functional of x_r (called reference coordinate), for all t, in the form

$$x_i = \hat{x}_i(x_r), \quad i = 1, \cdots, n. \tag{2.4a}$$

Both x_i and x_r are functions of time. That is

$$x_i(t) = \hat{x}_i[x_r(t)], \quad i = 1, \cdots, n. \tag{2.4b}$$

In more general form, every x_i can be represented by a real single-valued functional of a single variable, u (called modal coordinate), for all t, in the form

$$x_i = \hat{x}_i (u) , \qquad i = 1, \cdots, n. \tag{2.5a}$$

As functions of time, equation (2.5a) may be expressed as

$$x_i (t) = \hat{x}_i [u (t)] , \qquad i = 1, \cdots, n. \tag{2.5b}$$

Such a motion is also called a vibration-in-unison. In other words, modal vibrations of a nonlinear system are the vibration-in-unison of the system. Such a vibration is called a normal mode by Rosenberg [55].

2.1.3 Modal Frequency and Mode Shape

According to the definition, when a nonlinear system vibrates in a mode, there exists a functional relation between any one coordinate and the reference one, represented by equation (2.4). This relation is called the modal relation [53]. The frequency of the modal vibration is referred to as the nonlinear natural frequency (or modal frequency). A mode of a nonlinear system is constituted by the modal relation and modal frequency.

When a nonlinear system vibrates in a mode, the system will assume a certain displacement configuration (or shape). This displacement configuration or shape of system is defined as the mode shape of the system associated with that mode.

The mode shape can be represented by the ratios of all displacements of masses to a given coordinate (as a reference). If a system vibrates in a mode, the mode shape of the system is determined by

$$\phi_i(x_r) = \frac{x_i}{x_r} = \frac{\hat{x}_i(x_r)}{x_r}, \quad i = 1, \cdots, n;\ r\text{---fixed}. \qquad (2.6a)$$

In this equation, $x_r = 0$ is a singular point. If $\phi_i(x_r)$ is a continuous function at $x_r = 0$, the $\phi_i(0)$ is defined as the limit of $\phi_i(x_r)$ as x_r tends to zero. If the function of $\phi_i(x_r)$ is not continuous at this point, the mode shape value at $x_r = 0$ can be defined as

$$\phi_i(0) = \frac{\phi_i(0+) + \phi_i(0-)}{2}, \quad i = 1, \cdots, n. \qquad (2.6b)$$

It is obvious that $\phi_r = 1.0$ and all other ϕ_i are functions of x_r. Therefore, the mode shape will depend upon displacement. Since eventually all ϕ_i except ϕ_r vary with time, a mode shape of a nonlinear system is also called an instantaneous mode shape.

If a mode shape is known, the modal relation (2.4) can be expressed as

$$x_i = \phi_i(x_r)\, x_r . \qquad (2.7)$$

The mode shape vector is formed as $\Phi = (\phi_1, \cdots, \phi_n)^T$. If there are several modes, each mode is denoted by a subscript based on the order of modal frequencies. For example, the mode shape associated with *jth* modal frequency is denoted as Φ_j. The *ith* component of *jth* mode shape is donated as ϕ_{ij}.

2.2 EXAMPLES OF NONLINEAR MODE-LIKE BEHAVIOR

Nonlinear modes have been studied by many researchers since it was first defined. Several different nonlinear systems have been examined [53-66]. However, the above

rigorously-defined nonlinear modes may not be found for general nonlinear systems due to the complexity of the nonlinear problems. On the other hand, even if such modes could be found, they could not be isolated since the superposition principle is in theory inadmissible for nonlinear systems. Therefore, their performance in a general vibration (non-pure mode vibration described in section 2.1) of the system cannot be studied analytically.

However, mode-like behavior can be observed in the response of many nonlinear systems. Practically, the mode-like states of such nonlinear systems may be regarded as "modes." By approximate methods, such modes can be approximately isolated and examined. Further, these nonlinear systems can be analyzed approximately using a modal analysis approach.

In order to have some intuitive knowledge of modal behaviors of nonlinear systems, a 3DOF elastically nonlinear system is examined. The system is shown in Figure 2.1. It has softening springs, linear dampers and is subjected to a base acceleration $\ddot{z}(t)$. The example problem simulates a dynamic shaking table test.

The governing equations of motion are

$$m_1 \ddot{x}_1 + c_1 x_1 - c_2 (x_2 - x_1) + k_1 x_1 - \tilde{k}_1 x_1^3 - k_2 (x_2 - x_1) + \tilde{k}_2 (x_2 - x_1)^3 = -m_1 \ddot{z}$$

$$m_2 \ddot{x}_2 + c_2 (x_2 - x_1) - c_3 (x_3 - x_2) + k_2 (x_2 - x_1) - \tilde{k}_2 (x_2 - x_1)^3 - k_3 (x_3 - x_2)$$

$$+ \tilde{k}_3 (x_3 - x_2)^3 = -m_2 \ddot{z}$$

$$m_3 \ddot{x}_3 + c_3 (x_3 - x_2) + k_3 (x_3 - x_2) - \tilde{k}_3 (x_3 - x_2)^3 = -m_3 \ddot{z} \qquad \textbf{(2.8a)}$$

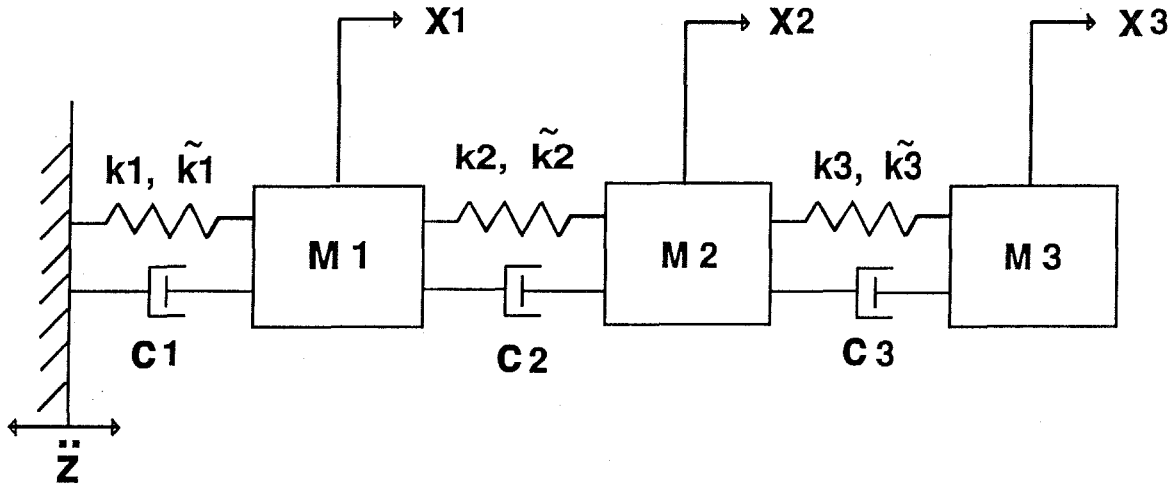

Figure 2.1. 3DOF system with cubic springs and viscous dampers

In matrix form, equation (2.8a) may be written as

$$\mathbf{M}\ddot{\mathbf{x}} + \mathbf{C}\dot{\mathbf{x}} + \mathbf{K}\mathbf{x} + \mathbf{f}(\mathbf{x}) = -\mathbf{M}\mathbf{I}\ddot{z}(t) \qquad \textbf{(2.8b)}$$

where

$$\mathbf{M} = \begin{pmatrix} m_1 & 0 & 0 \\ 0 & m_2 & 0 \\ 0 & 0 & m_3 \end{pmatrix}, \qquad \mathbf{C} = \begin{pmatrix} c_1 + c_2 & -c_2 & 0 \\ -c_2 & c_2 + c_3 & -c_3 \\ 0 & -c_3 & c_3 \end{pmatrix}$$

$$\mathbf{K} = \begin{pmatrix} k_1 + k_2 & -k_2 & 0 \\ -k_2 & k_2 + k_3 & -k_3 \\ 0 & -k_3 & k_3 \end{pmatrix}, \qquad \mathbf{f}(\mathbf{x}) = \begin{pmatrix} -\tilde{k}_1 x_1^3 + \tilde{k}_2 (x_2 - x_1)^3 \\ -\tilde{k}_2 (x_2 - x_1)^3 + \tilde{k}_3 (x_3 - x_2)^3 \\ -\tilde{k}_3 (x_3 - x_2)^3 \end{pmatrix}$$

(2.8c)

and the vector is $\mathbf{I} = (1, 1, 1)^T$.

The physical parameters of the example system are given as

$$m_1 = 1000 \text{ kg}, \quad m_2 = 750 \text{ kg}, \quad m_3 = 500 \text{ kg}$$

$$k_1 = \tilde{k}_1 = 3\times10^5 \text{ kg/cm}, \quad k_2 = \tilde{k}_2 = 2\times10^5 \text{ kg/cm}, \quad k_3 = \tilde{k}_3 = 10^5 \text{ kg/cm}.$$

Two cases of damping coefficients will be given later.

A swept sinusoidal excitation is applied to this system. The input function (base acceleration) is $\ddot{z} = Z \sin(at^2)$. This function provides a wide-band frequency signal which is frequently used in fast sweep sinusoidal testing using an electro-magnelic or hydraulic shaker. The magnitude of the force can be selected so that the amplitude of response is large enough to generate significant nonlinear behavior. The frequency band can also be selected. If v_{max} and v_{min} are the highest and lowest frequencies respectively, the parameter *a* is defined as $a = \pi(v_{max} - v_{min})/T$, where T is the sweep period. The corresponding time

history and Fourier Amplitude Spectrum of the excitation are shown in Figure 2.2. In the examples, v_{max} = 25 (Hz) and v_{min} = 0 (Hz). T = 40.96 *sec*. So a = 1.917.

2.2.1 Undamped System

Consider an undamped system, i.e., $c_1 = c_2 = c_3 = 0$ or **C** = O. The corresponding equation of motion is then

$$\mathbf{M\ddot{x} + Kx + f(x) = -MI\ddot{z}}(t) \; . \qquad (2.9)$$

The function of base acceleration is given as $\ddot{z} = 8\sin(1.917t^2)$.

By Newmark's method, the response of the system is calculated. Inter-mass restoring forces are shown in Figure 2.3. In the figure, nonlinearities of the system and their distribution are shown. The strongest nonlinearity is located near the free end where the restoring force curve becomes almost horizontal at about maximal relative displacement. It is clear that the system vibrates in the nonlinear range.

For a linear system, the Frequency-Response-Function (FRF) is defined as the ratio of the Fourier Amplitude Spectra of the output and input of a system. This represents the dynamic response properties of the system in the frequency domain. For a nonlinear system, a similar function, referred to as Fourier Amplitude Ratio (FAR), may be used. This function is defined as the ratio of the Fourier Amplitude spectra of the output and input of the system. For the given input (base acceleration), the FAR is defined as

$$\mathrm{FAR}(f) = \frac{\mathrm{FAS}\,[x(t)]}{\mathrm{FAS}\,[\ddot{z}(t)]} \qquad (2.10)$$

where FAS = Fourier Amplitude Spectra. It should be noted that a FRF of a linear system

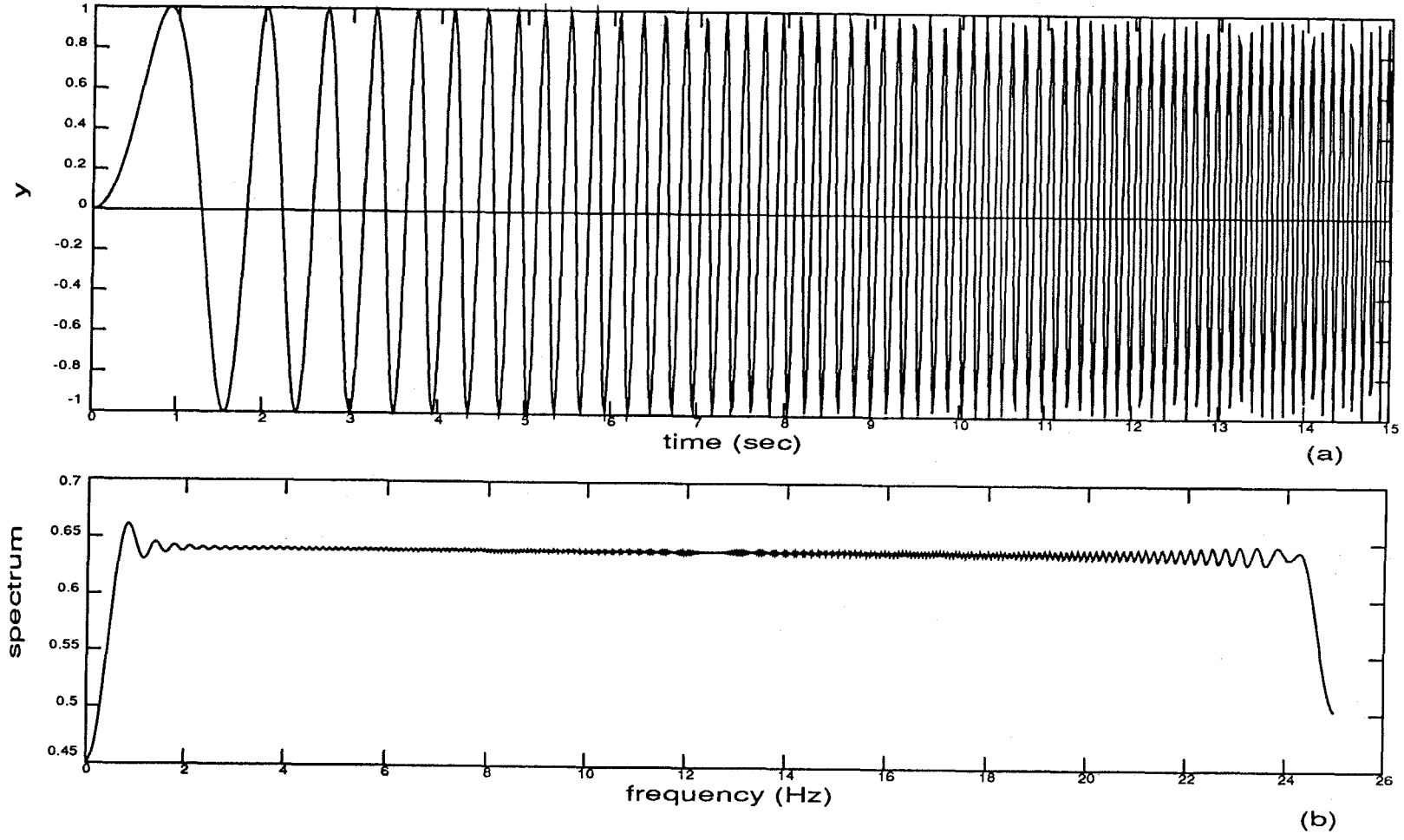

Figure 2.2. Time history of $y = \sin(at^2)$ and spectrum. (a) time history; (b)spectrum.

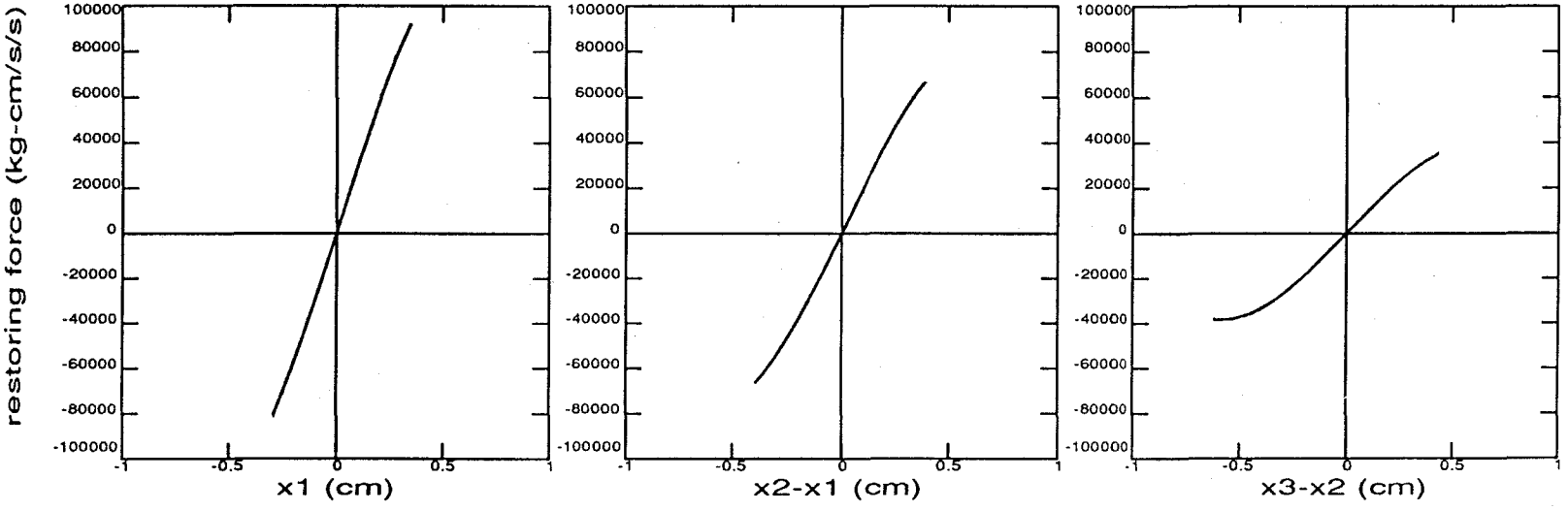

Figure 2.3. Inter-mass restoring forces of undamped 3DOF nonlinear system subjected to a swept sinusoidal input.

is dependent only upon the system itself and that the FAR of a nonlinear system will be dependent upon system response as well as on the system properties. Even so, it is still a useful measure of the dynamic frequency response properties of nonlinear system.

FARs of three coordinates of the system are shown in Figure 2.4. In the figure, mode-like behavior can be observed very clearly. Three peak (resonant) frequencies can be seen. They are *1.29Hz*, *2.64Hz* and *3.86Hz* respectively. The mode-like frequencies are well separated. Compared with linear natural frequencies of the system which are *1.33Hz*, *2.85Hz* and *4.24 Hz* respectively (calculated by letting $\mathbf{f}(\mathbf{x}) = 0$), the nonlinear resonant frequencies are lower than the corresponding linear ones, as expected since the system is softening. The first peak has the biggest amplitude, the second is smaller and the third is very small. Therefore, in the response of the system, the first mode is dominant, the second mode has a small contribution and the third mode can almost be neglected.

Since the mode-like frequencies of the system are well separated, the modal responses of the system can be approximately estimated by band-pass filtering. In practice, the band-pass filtering is performed in three stages: (1) taking a forward Fourier Transformation on the response in the time domain, (2) eliminating the frequency components that are lower than the specified low frequency cutoff or higher than the specified high frequency cutoff in the frequency domain, (3) taking an inverse Fourier Transformation to obtain the filtered response in time domain. The first mode response of the system is approximately obtained by means of a band-pass filtering with the frequency band from *0 Hz to 2 Hz*. This is shown in Figure 2.5 where x_{i1} stands for the first modal displacement of *ith* mass.

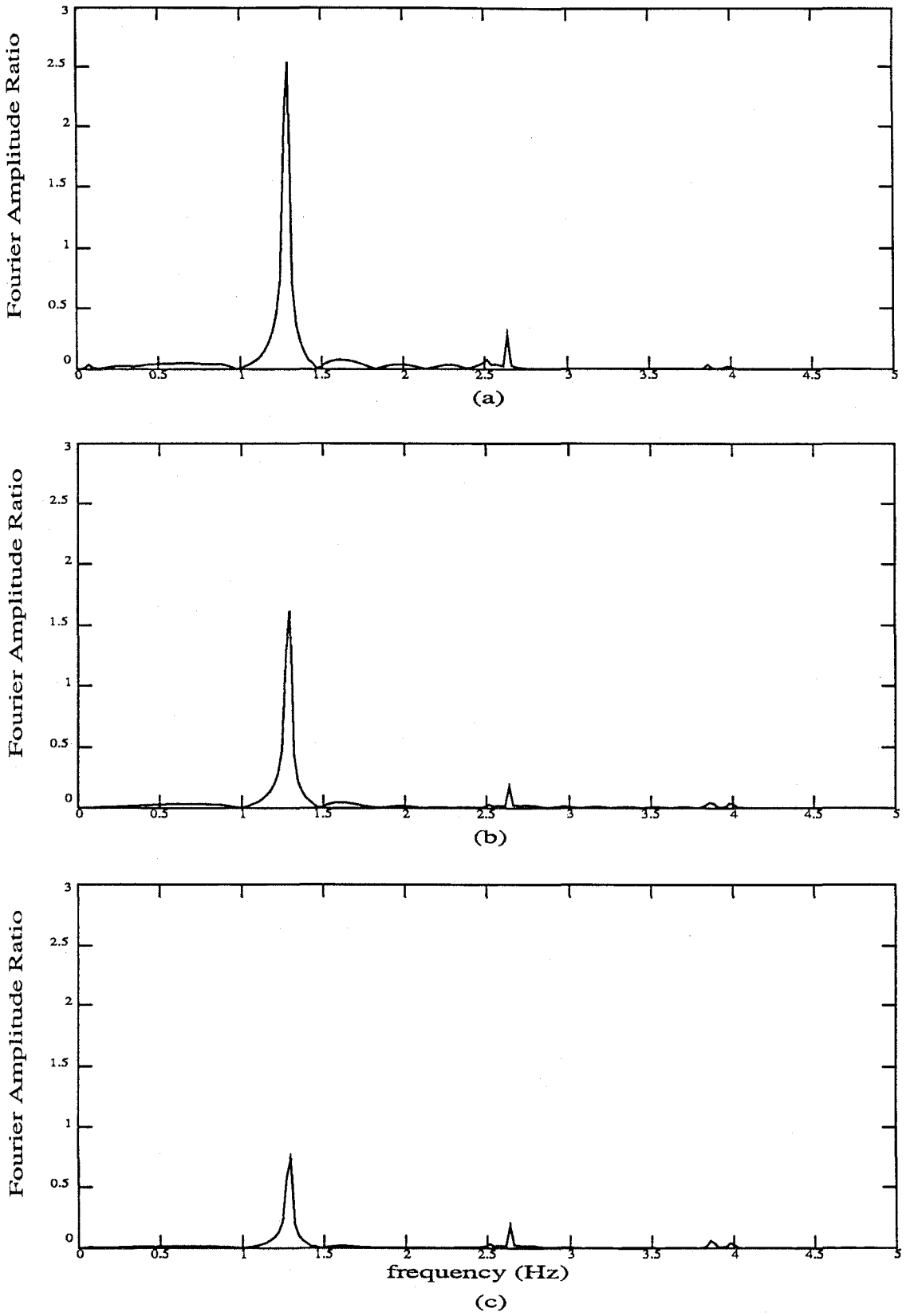

Figure 2.4. FARs of (a) mass 3; (b) mass 2; and (c) mass 1

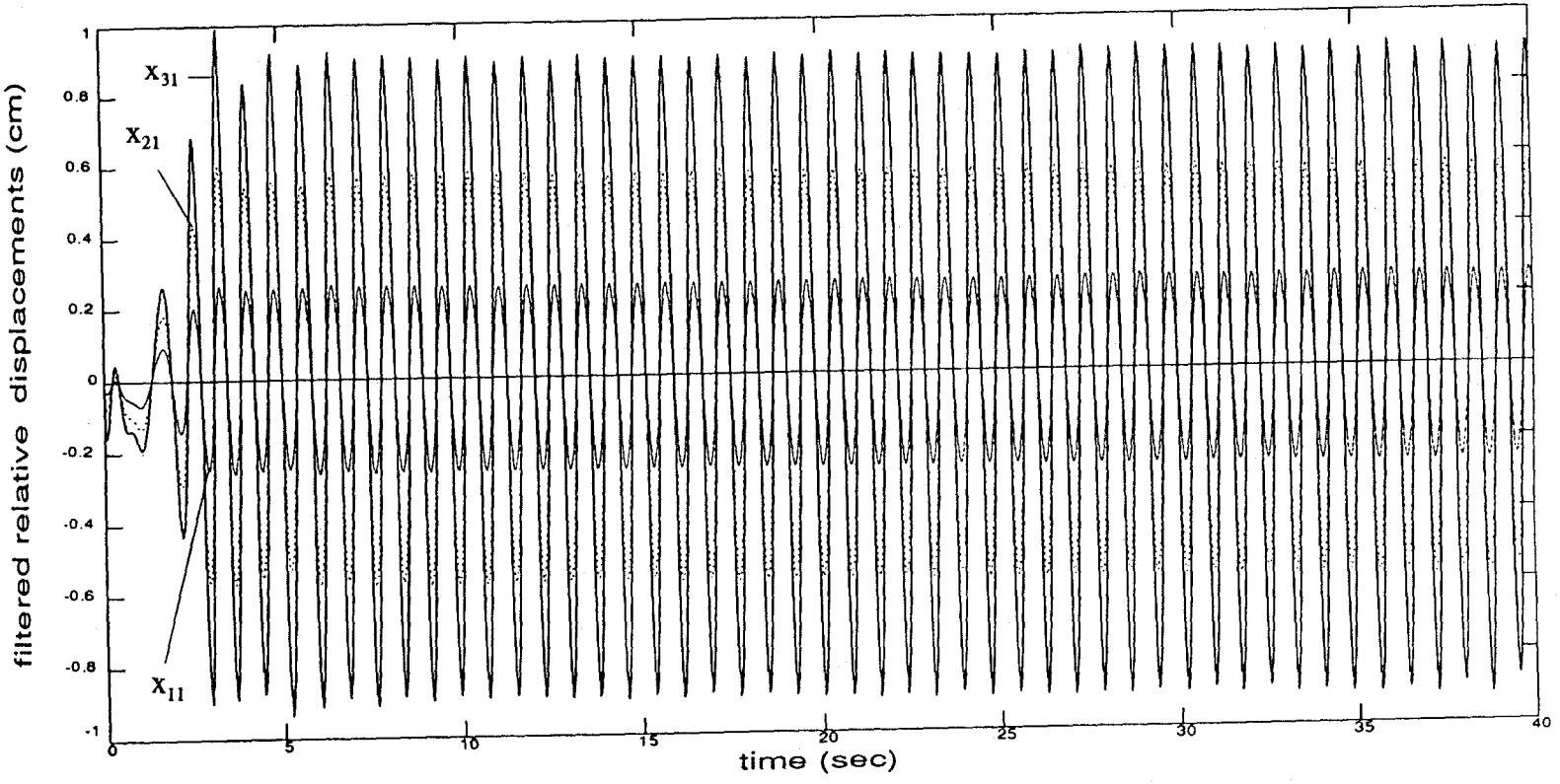

Figure 2.5. Filtered relative displacements of three masses of undamped 3DOF system.

As seen in the figure, after about 5 second, the mode response becomes stable and remains almost constant in amplitude. Since the driving (excitation) force is frequency-increasing, the system behaves in three stages. The first stage is the time range in which the driving frequency is lower than *1.1 Hz*. During this period, the response of the system is small since the driving frequency is far away from any natural frequencies of the system. The second stage is the system-resonance period of 3-5 second when the driving frequency is passing through the resonant (peak) frequency band (about *1.2 - 1.4Hz*). When the driving frequency is close to and passes *1.3 Hz*, the system experiences its first resonance. After this time period, the driving force has high frequency and little influence to the first mode of the system. The first mode of the system behaves like a free oscillation in this time period. Since the system has no damping, the mode vibration remains the response amplitude of resonance. Therefore, the modal response after 5 seconds can be regarded as a free response of a mode to the "initial" motion which is the first resonance of the system. In addition, it can be recognized that the mode-like vibration during *0 - 5* second is transient motion.

The instantaneous mode shape can be calculated approximately by equation (2.6). For this system, n = 3. Letting r = 3, $\phi_{11} = x_{11}/x_{31}$, $\phi_{21} = x_{21}/x_{31}$. The time histories of the instantaneous mode shape components (ϕ_{11}, ϕ_{21}) are shown in Figure 2.6 (a). $\phi_{31} \equiv 1$ is not shown in the figure. For comparison, the corresponding linear modeshape components are also plotted in this figure. The components of the linear mode shape remain constant at all times during the oscillation. The modal response x_{31} is given in below Figure (2.6b)

to show the relation of the mode shape and modal response.

In figure 2.6, the time histories of instantaneous mode shape components consist of many small curve segments. Each curve segment corresponds to a half-cycle of oscillation. Between any two adjoining segments, there is a jump or discontinuity of the mode shape value. These discontinuities occur around the instants of time when masses pass their equilibrium positions. Since the denominator (x_{31}) is near zero at these instants, it results in considerable numerical error in calculating x_{11}/x_{31} and x_{21}/x_{31}. In every segment (also in a half-cycle of oscillation), the mode shape components vary with time and the values are lower than the linear ones. This shows that the mode shape of the nonlinear system is different from the linear one and dependent on the displacement. However, it can be seen that the values in a segment change not much.

2.2.2 Damped System

As the second example, consider the system with linear damping. The coefficients of the viscous dampers are

c_1 = 300 kg sec/cm, c_2 = 200 kg sec/cm, c_3 = 100 kg sec/cm.

The base acceleration is given as $\ddot{z} = 10 \sin(1.917t^2)$.

Inter-mass restoring forces are plotted in Figure 2.7. The figure shows that the system has strong nonlinearity and the biggest nonlinearity is located between the second and third masses.

Using the same process described above, responses of the system and FARs of three coordinates are calculated. FARs are plotted in Figure 2.8. It can be seen that first

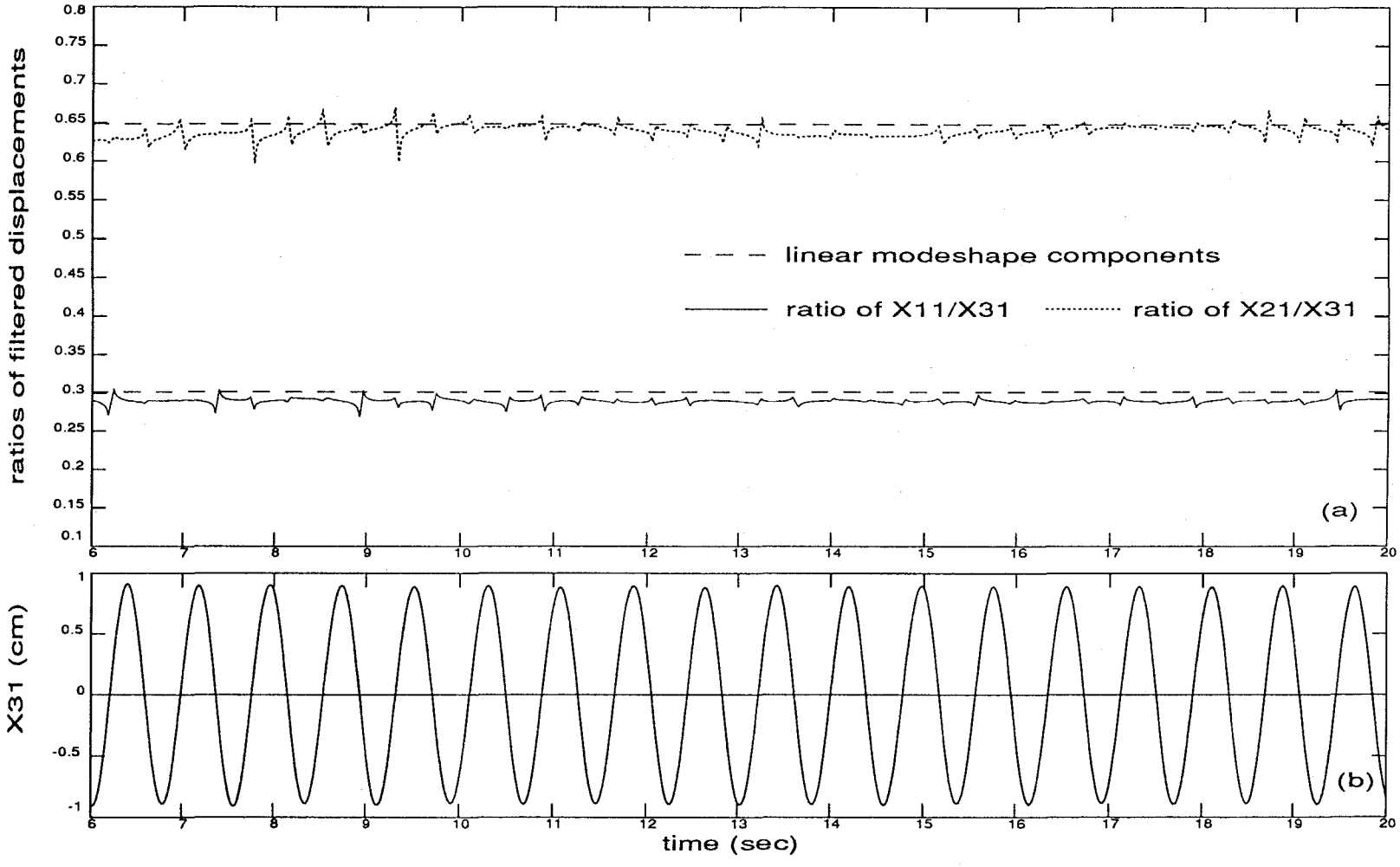

Figure 2.6. Ratios of filtered displacements and the filtered displacement of reference DOF.

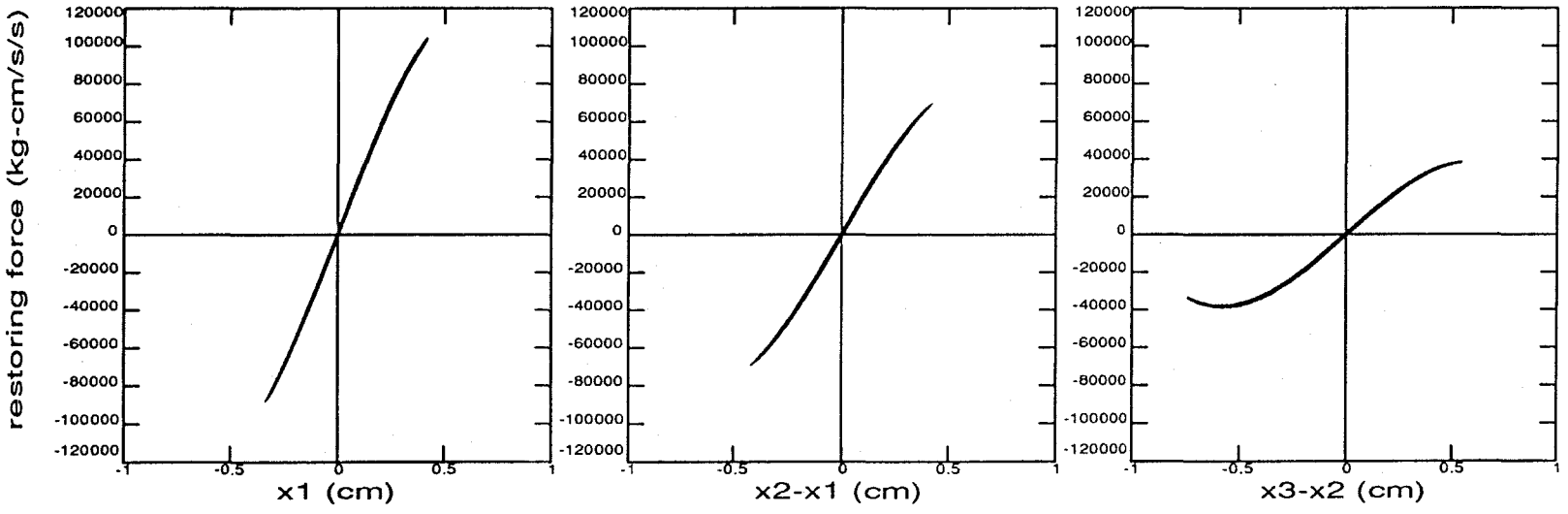

Figure 2.7. Inter-mass restoring forces of damped 3DOF nonlinear system subjected to a swept sinusoidal input.

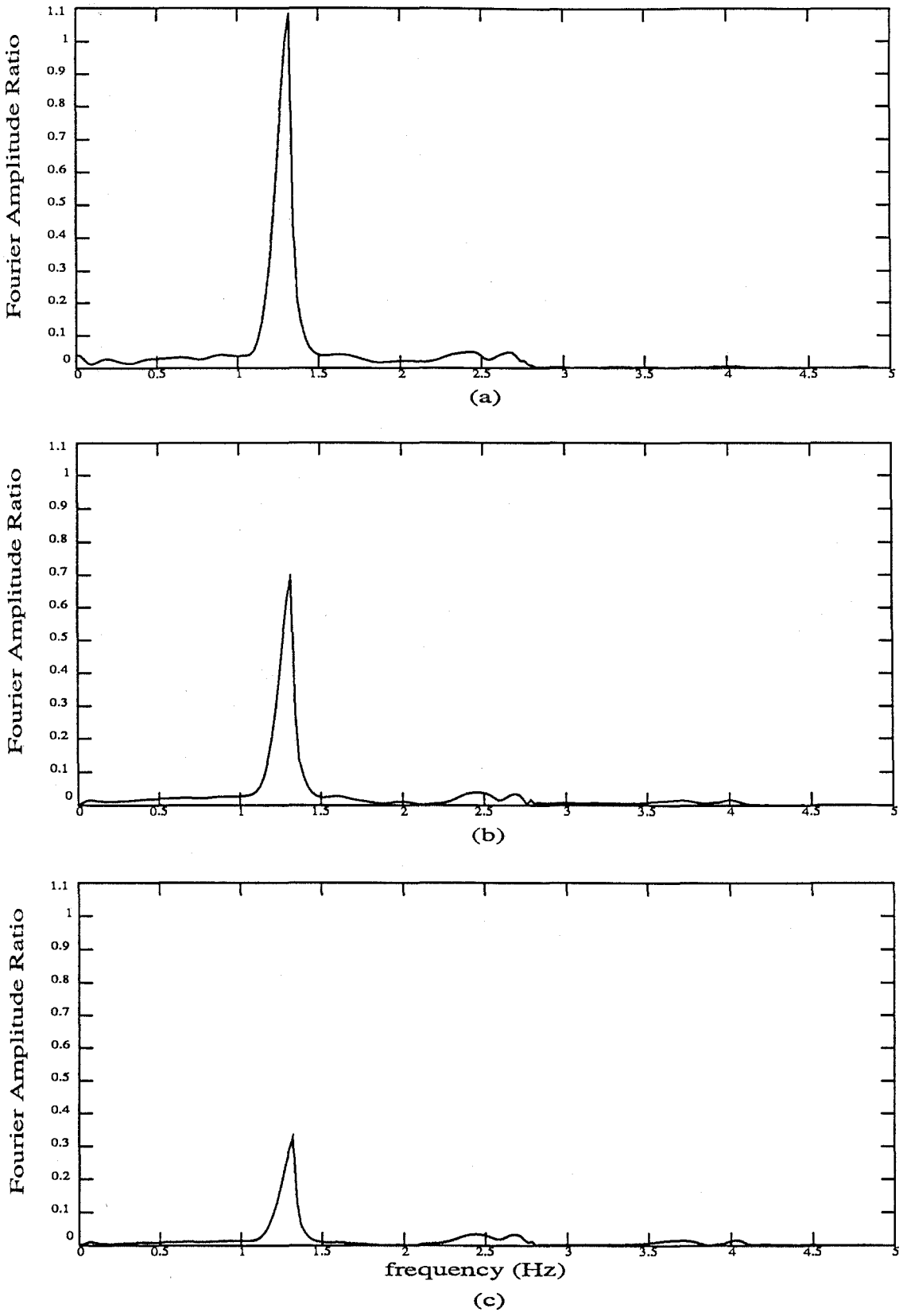

Figure 2.8. FARs of (a) mass 3; (b) mass 2; and (c) mass 1.

mode is very obvious and that the response of the mode is large. The others are small and not well identifiable. According to the FARs, the first mode dominates the response of the system.

The first mode responses at three masses are estimated by a filter of *0 - 2 Hz* and the instantaneous mode shape is estimated with $\phi_{11} = x_{11}/x_{31}$, $\phi_{21} = x_{21}/x_{31}$. The filtered responses of three masses are plotted in Figure 2.9 and the instantaneous mode shape components are plotted in Figure 2.10 in contrast with the modal response x_{31}. Same as the first case, after 5 seconds excitation force is in the high frequency range and has little influence on the first mode, so that the first mode response behaves like free vibration. However, the response amplitude decays with time due to the damping. From Figure 2.10, the change of mode shape with the response level can be seen. In the figure, when amplitude is large and in the nonlinear vibration range, the mode shape components differ from the corresponding linear values. As the amplitude decreases, the mode shape values tend to those of linear case.

2.2.3 Summary

In the above examples of nonlinear systems, mode-like motions were approximately extracted from a general vibration and instantaneous mode shapes were obtained. Through these examples, mode-like behavior is observed. Through direct observation of the mode-like motions, the following properties of nonlinear modes have been found.

(1). The frequencies of nonlinear modes differ from their corresponding linear

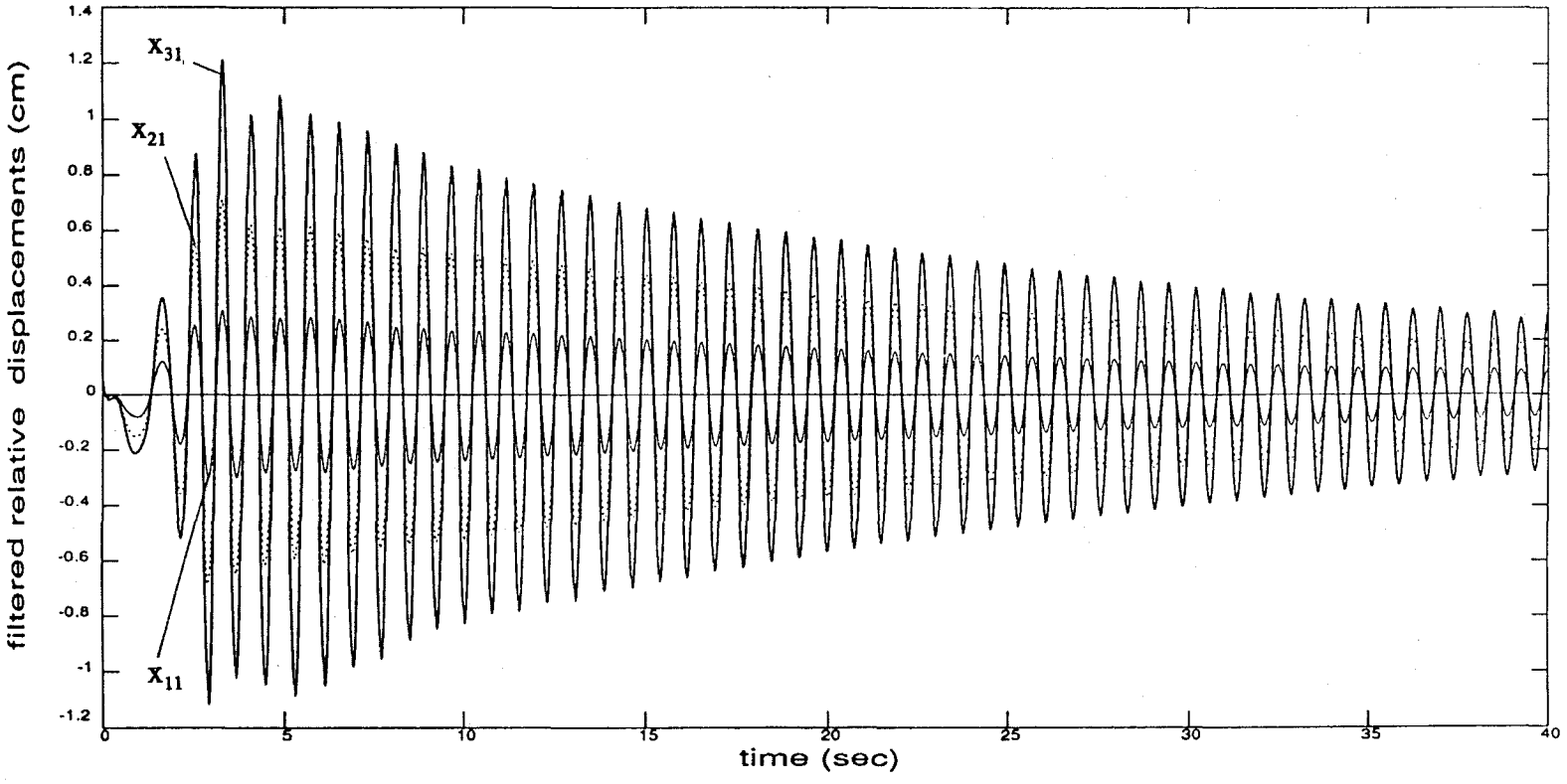

Figure 2.9. Filtered relative displacements of three masses of damped 3DOF system.

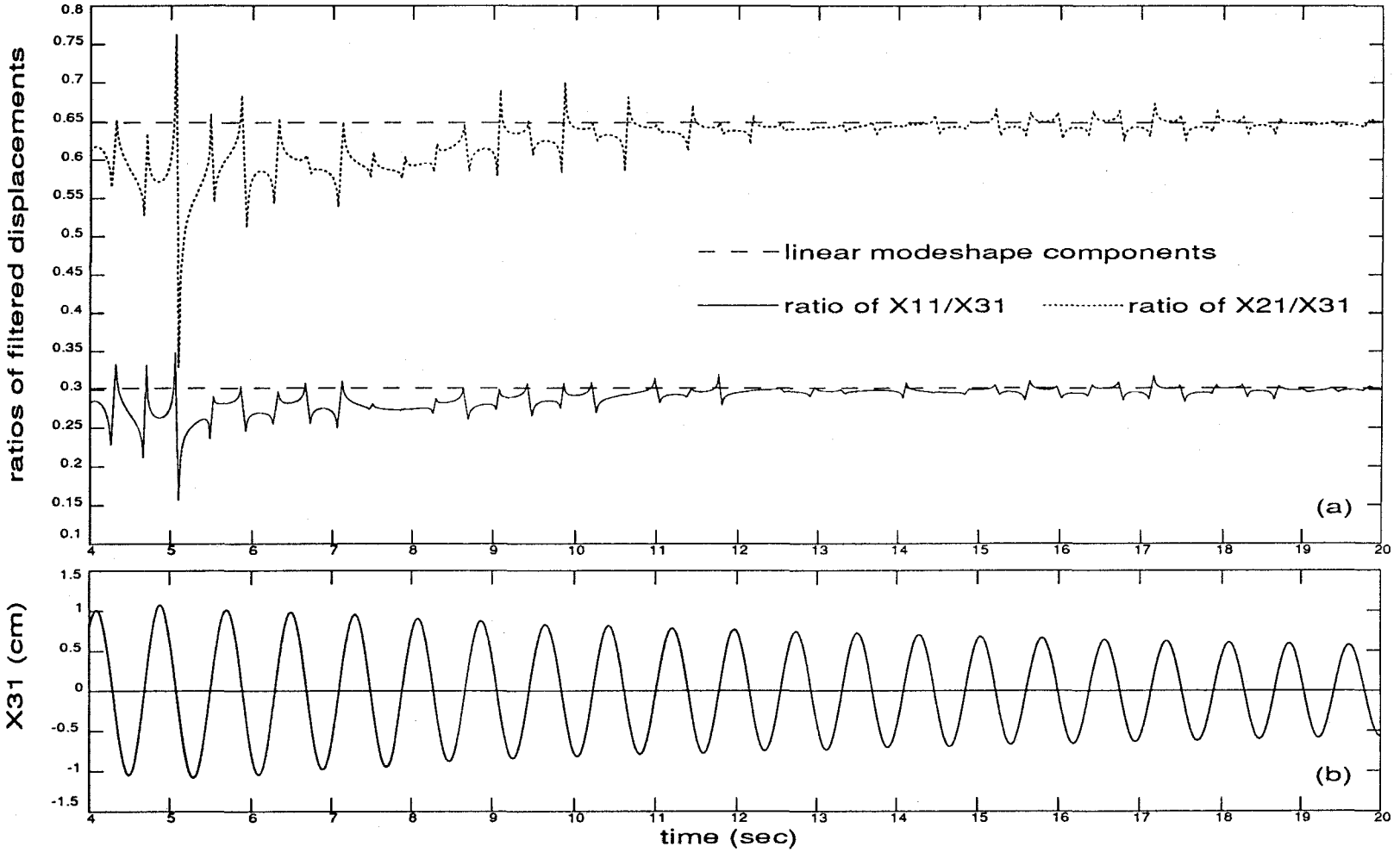

Figure 2.10. Ratios of filtered displacements and the filtered displacement of reference DOF.

ones. For the examined softening system, the frequency of each mode is lower than the corresponding linear natural frequency.

(2). The nonlinear mode shapes are dependent on the level of motion (or modal amplitude). The values of the nonlinear mode shapes differ from their linear counterparts. As modal amplitude decays, mode shape values tend to those of the corresponding linear mode.

(3). Nonlinear mode shapes do not remain constant during oscillation, even in a vibration cycle. Nonlinear mode shapes instantaneously depend on the modal displacement. However, the change of mode shape during a half cycle of oscillation is not much.

In fact, the first two properties were already shown by both rigorous and approximate analytical analyses of nonlinear modes by Rosenberg and Szemplinska-Stupnicka [55,69]. The examples show that a general nonlinear system may possess modal properties. Practically, the mode-like states are regarded as modes of the nonlinear system although it may not be confirmed in theory that the definition in the last section is satisfied rigorously.

Based on the observation of Figure 2.6 that instantaneous mode shape component values in a half-cycle of oscillation are very close, an instantaneous mode shape can be considered as an approximation of mode shape for half a period. As a result, the mode shape becomes constant over the half-cycle. There may be different choices to determine the approximate values of the mode shape. For examples, the average value of the instantaneous mode shape over a half-cycle may be regarded as an approximation or the

peak value of the instantaneous mode shape in the half-cycle may be defined as another approximation. More discussions will be given in the next chapter where approximate calculations of instantaneous and constant mode will be presented.

CHAPTER 3

MODE SHAPES OF NONLINEAR SYSTEMS

3.1 BACKGROUND

According to the definition in chapter 2, a nonlinear mode consists of a set of functionals $\hat{x}_i(\bullet)$ of modal relation (equation 2.4) and a corresponding modal frequency. If a modal relationship can be represented by mode shape, the mode consists of mode shape and the frequency instead. The task of determining a mode is to find the functionals of the modal relation (2.4) or a mode shape with a corresponding natural frequency. By these two calculation targets, existing approaches for evaluation nonlinear modes fall into two categories.

In the studies of the first category, functionals $\hat{x}_i(\bullet)$ of modal relation are calculated based on the original definition (2.4). A few special nonlinear systems were examined and nonlinear modes were found. Since in general it is very difficult or might be impossible to find exact solutions for modes of a nonlinear system, several studies have presented methodologies for calculating approximate solution [63-66].

Another category of mode calculation is the approximate evaluation of the mode shape and frequency. Szemplinska-Stupnicka [68-69] has presented an approach which is based on an approximate definition of the mode shape. In this approach, mode shapes

are assumed to be constant over a cycle of oscillation and Galerkin's method is used to determine the values of the constants.

In the studies of direct structural dynamic response integration [70-76], the instantaneous tangent stiffness matrix of a nonlinear system is used to calculate eigenvectors at a corresponding time. The resulting eigenvectors were also called instantaneous mode shapes, analogous to a linear system. The instantaneous mode shapes were calculated through an eigenvalue problem with an updated stiffness matrix. This approach was originally motivated by an attempt to reduce the computational effort of calculation of the system response by using the instantaneous mode shapes as a basis for response solution. Although the approach is originally not proposed for use of calculation of mode shapes, sometimes it may provide a good approximation of the instantaneous mode shape if the system is weakly nonlinear.

In this chapter, approximate methods for evaluating the mode shape will be presented and examples to illustrate these methods will be given. The properties of nonlinear mode shapes will be discussed.

3.2 CALCULATION OF INSTANTANEOUS MODE SHAPE

3.2.1 Normal Mode Method

In the first category, the functionals $\hat{x}_i(\bullet)$ in relation (2.4) are the targets of calculation. Most studies were accomplished by Rosenberg and his co-workers in the 1960's [53-65]. In their studies, modes were called *normal modes,* which is the same as the linear system. Rosenberg pointed out that the functions of $\hat{x}_i(x_r)$ constitute a trajectory,

namely the modal line, in the $(x_1, x_2, \cdots, x_n)$-space and that the trajectory is governed by the following differential equations:

$$2(U_0 + U(x_1, x_2, \cdots, x_n))\{ x_i''(1 + \sum_{j\neq i}^{n} x_j'^2) - \sum_{j\neq i}^{n} x_i' x_j' x_j'' \} +$$

$$(1 + \sum_{j=1}^{n} x_j'^2) \{ x_r' \frac{\partial U}{\partial x_i} + \sum_{j\neq i}^{n} x_i' x_j' \frac{\partial U}{\partial x_j} - (1 + \sum_{j\neq i}^{n} x_j'^2) \frac{\partial U}{\partial x_i} \} = 0$$

$$i, j = 1, 2, \cdots, n, \qquad i, j \neq r \tag{3.1}$$

where primes denote differentiation with respect to x_r and $U(x_1, x_2, \cdots, x_n)$ is the potential function of the autonomous system as described by the equation:

$$\dot{x}_i = \frac{\partial U}{\partial x_i}, \qquad i = 1, 2, \cdots, n. \tag{3.2}$$

in which $U_0 = -U((x_1)_{max}, \cdots, (x_n)_{max})$ is the maximum potential of the system that is obtained when all the masses reach their maximum positions. The solutions of equations (3.1), which satisfy the conditions that all $\dot{x}_i(0) = 0$ and that the trajectory of the solution intersects the surface defined by $U((x_1)_{max}, (x_2)_{max}, \cdots, (x_n)_{max})$ orthogonally, are the desired modal relation functions.

For some special nonlinear systems, the modal relation functions are linear, i.e., $x_i = c_i x_r$. The corresponding trajectory is a straight line. Such a mode is called a similar nonlinear mode [55]. A few examples of such nonlinear systems have been given [53-55]. However, such nonlinear systems are very limited. For general nonlinear systems, the modal relations are nonlinear and the modal lines are curved. The corresponding modes are said to be non-similar. In general, equations (3.1) are so complicated that "the

prospect of finding the general solution may be confidently regarded as hopeless" [55]. In reference [66], an asymptotic solution of a mode, say the *jth* mode, is represented by the polynomial series

$$x_{ij} = (c_{ij}^{(0)} + c_{ij}^{(1)}(A_{rj}))x_{rj} + (c_{ij}^{(3)}(A_{rj}))x_{rj}^3 + (c_{rj}^{(5)}(A_{rj}))x_{rj}^5 + \cdots$$

$$i\text{ - station}, \quad i = 1, \cdots, n \quad r\text{--reference station} \qquad (3.3)$$

where A_{rj} is the amplitude of the modal displacement x_{rj} and $c_{ij}^{(k)}$, k = 1, 3, 5, ···, are amplitude-dependent coefficients which are determined by a perturbation method. Nevertheless, these approaches are still complicated so that their application is very limited. However, some properties of nonlinear modes have been found through these studies.

The following features are important characteristics of nonlinear modes.

(1) For a similar nonlinear mode, the natural frequency is dependent on the energy level of motion of the system but the modal line (represented by the functional) is not.

(2) For a nonsimilar nonlinear mode, the modal line as well as the natural frequency depend upon the energy level of motion.

It can be further seen through the definition of mode shape that the mode shape of a similar mode must be constant. For nonsimilar modes, a (*jth*) mode shape is represented using the asymptotic solution

$$\phi_{ij} = \frac{x_{ij}}{x_{rj}} = (c_{ij}^{(0)} + c_{ij}^{(1)}(A_{rj})) + (c_{ij}^{(3)}(A_{rj}))x_{rj}^2 + (c_{ij}^{(5)}(A_{rj}))x_{rj}^4 + \cdots \qquad (3.4)$$
$$i = 1, \cdots, n.$$

It can be seen that the mode shape is dependent not only upon amplitude but also on

instantaneous displacement. That is, the mode shape varies instantaneously with displacement. For example, the instantaneous mode shape corresponding to the time when the masses reach their maximum position (response peak) and the one corresponding to the time when the masses pass through their equilibrium positions ($x_i = 0$) are different. Therefore, the mode shapes of a nonlinear system are said to be instantaneous.

3.2.2 Approximate Method

It may be understood that it will be difficult to find the instantaneous mode shape analytically. A practical approach for approximate estimation of the instantaneous mode shape is needed. In this section, one approach is proposed, which is based on the following assumptions.

Assume that a mode shape can be separated and the modal relation can be represented as

$$\mathbf{x} = \Psi(u)\, u \tag{3.5}$$

where $\mathbf{x}$ is displacement vector, $\Psi(u) = (\psi_1(u), \cdots, \psi_n(u))^T$ is mode shape vector and u is a modal coordinate. From (3.5), the velocity and acceleration vectors can be obtained as

$$\dot{\mathbf{x}} = (\Psi' u + \Psi)\, \dot{u} \tag{3.6}$$

$$\ddot{\mathbf{x}} = (\Psi'' u + 2\Psi')\, \dot{u}^2 + (\Psi' u + \Psi)\, \ddot{u} \tag{3.7}$$

where the primes denote differentiation with respect to u, that is, $\Psi'(u) = (\psi_1'(u), \cdots, \psi_n'(u))^T$ and $\Psi''(u) = (\psi_1''(u), \cdots, \psi_n''(u))^T$. Assume that the values of mode shape vary

slowly with respect to u so that

$$\Psi'(u) \approx 0 \quad , \quad \Psi''(u) \approx 0 \quad . \tag{3.8}$$

Then, (3.7) is simplified as

$$\ddot{\mathbf{x}} = \Psi(u)\,\ddot{u} \, . \tag{3.9}$$

Consider an autonomous system described by

$$\mathbf{M}\ddot{\mathbf{x}} + \mathbf{K}\mathbf{x} + \mathbf{f}(\mathbf{x}) = \mathbf{0} \tag{3.10}$$

where **M**, **K** are mass and stiffness matrices respectively, and **f** is vector of the nonlinear part of restoring force.

According to the definition in chapter 2, modes of a nonlinear system are determined in the case when the system executes a vibration-in-unison. It is assumed that modal coordinate acceleration can be approximately expressed as

$$\ddot{u} = -\omega^2 u \, . \tag{3.11}$$

Then, (3.9) is approximated as

$$\ddot{\mathbf{x}} = -\omega^2\,\Psi(u)\,u \, . \tag{3.12}$$

Substituting (3.5) and (3.12) into equation (3.10) yields

$$-\omega^2\mathbf{M}\Psi u + \mathbf{K}\Psi u + \mathbf{f}(\Psi u) = \mathbf{0} \, . \tag{3.13}$$

If the system is cubic, *u* can be factored out. So equation (3.13) becomes

$$-\omega^2\mathbf{M}\Psi + \mathbf{K}\Psi + \mathbf{f}(\Psi)\,u^2 = \mathbf{0} \, . \tag{3.14}$$

As an example, for the system of Figure 2.1, $u = x_3$, $\psi_3 \equiv 1$ and

$$\Psi = \begin{pmatrix} \psi_1 \\ \psi_2 \\ 1 \end{pmatrix}, \quad \mathbf{f}(\Psi) = \begin{pmatrix} -\tilde{k}_1\psi_1^3 - \tilde{k}_2(\psi_1 - \psi_2)^3 \\ \tilde{k}_2(\psi_1 - \psi_2)^3 - \tilde{k}_3(\psi_2 - 1)^3 \\ \tilde{k}_3(\psi_2 - 1)^3 \end{pmatrix}. \qquad (3.15)$$

If $\mathbf{f}(\Psi)$ is a zero vector, (3.13) is a standard linear eigenvalue problem. It has *n* solutions (i.e., *n* linear natural frequencies and n natural modes), which can be found in a straight forward manner. When $\mathbf{f}(\Psi)$ is not zero, equation (3.13) is a set of n nonlinear algebraic equations.

Let the *nth* coordinate of mass be the reference coordinate and the value of the mode shape at this mass be unity. That is,

$$\psi_{nj} \equiv 1 \qquad \forall\, j \text{ (mode solution number)}. \qquad (3.16)$$

Hence, for each (*jth*) mode, there are *n* unknowns in the equation (3.13) or (3.14), which are $\omega_j, \psi_{1j}, \cdots, \psi_{(n-1)j}$. The *jth* mode shape vector is $\Psi_j = (\psi_{1j}, \cdots, \psi_{nj})^T$.

In general, the nonlinear algebraic equation (3.13) or (3.14) can not be solved in an explicit form and the number of solutions is *a priori* unknown. A numerical scheme is needed to solve these equations. In the equation (3.14), if *u* is small, the system is weakly nonlinear and the equations may have *n* solutions near the linear ones. It is assumed that the nonlinear equations have *n* solutions in the neighborhoods of the linear ones. According to the reference [77], once the neighborhood of a root or of a place where there might be a root is known, the Newton-Raphson method for nonlinear systems of equations can be effectively used to find the root, if it exists, or of spectacularly failing to converge, indicating (though not proving) that the expected nearby root does not exist. The Newton-Raphson method is used herein to solve the equation.

In the process of the Newton-Raphson method, initial values of ω and Ψ are given and the procedure will converge to a solution of ω and Ψ. If an appropriate set of initial values for a mode is given, the modal frequency and mode shape of that mode can be found. Based on the above discussion, if the linear natural frequencies are not close to each other, the regions of possible roots for nonlinear modes are well separated and the Newton-Raphson procedure can effectively converge to a solution. All nonlinear modal frequencies, $\omega_1, \cdots, \omega_n$, and mode shapes, $\Psi_1, \cdots, \Psi_n$, can be expected to be obtained respectively by independently performing the numerical procedure with corresponding initial values. If the modes are very close, there may be difficulty in converging for some modes. Therefore, the presented approach is intended for use in the case where modes of system are well separated. In the equation (3.13), u is a parameter. For any one of the given values of u, a run of the Newton-Raphson process gives a set of ω and Ψ. These parameters can be solved in an u-incremental manner. Therefore, the resulting ω and Ψ will be functions of the modal coordinate u, i.e., $\omega(u)$ and $\Psi(u)$.

In reference [68], the above n solutions (n modal frequencies, $\omega_1, \cdots, \omega_n$, and n mode shapes, $\Psi_1, \cdots, \Psi_n$) which are associated with the linear eigenvalues and eigenvectors are referred to as primary modes. Besides primary modes, there may exist some other additional modes (like subharmonic modes, etc. [78]) which were called secondary modes. In this thesis, only the above primary nonlinear modes are considered.

Time history of mode shape in a vibration event can be predicted as functions of the modal response. As an example, the time history of the first mode shape of the undamped nonlinear system given in last chapter is predicted using the first modal

displacement which was estimated in section 2.2.1. This is done by placing the modal response in equation (3.14) and solving the equation in a u-incremental manner. The result and the measured instantaneous mode shape of the system are shown in Figure 3.1 with the modal displacement (filtered displacements), u. As shown in Figure 3.1, the predicted values give an acceptable estimation of the real mode shape but the curves of the calculated value do not represent the measured ones. As seen, the calculated results of mode shape associated with the large displacement (close to the peak of response) give better approximation to the measured mode shape than those associated with small displacement (near equilibrium position). The calculated mode shape components associated with small displacement are nearly equal to the value of linear mode shape. In fact, this is expected from equation (3.13) or (3.14), which become linear when u approaches zero. It is indicated that the mode shape is the linear one when $u = 0$.

The observation shows that the real instantaneous mode shape in a half cycle (a coarse segment) does not change as much as calculated. It is suggested that a constant mode shape might be a good approximation. This leads to the following approaches.

3.3 AMPLITUDE-DEPENDENT MODE SHAPES

3.3.1 Galerkin Method

Based on the observation of the measured mode shapes, a mode shape which remains constant over a half-cycle can be assumed to be an approximate solution for the nonlinear mode shape. In the 1970's, Szemplinska-Stupnicka assumed that the mode shape is constant over a cycle of oscillation. Consequently, the general response of the system

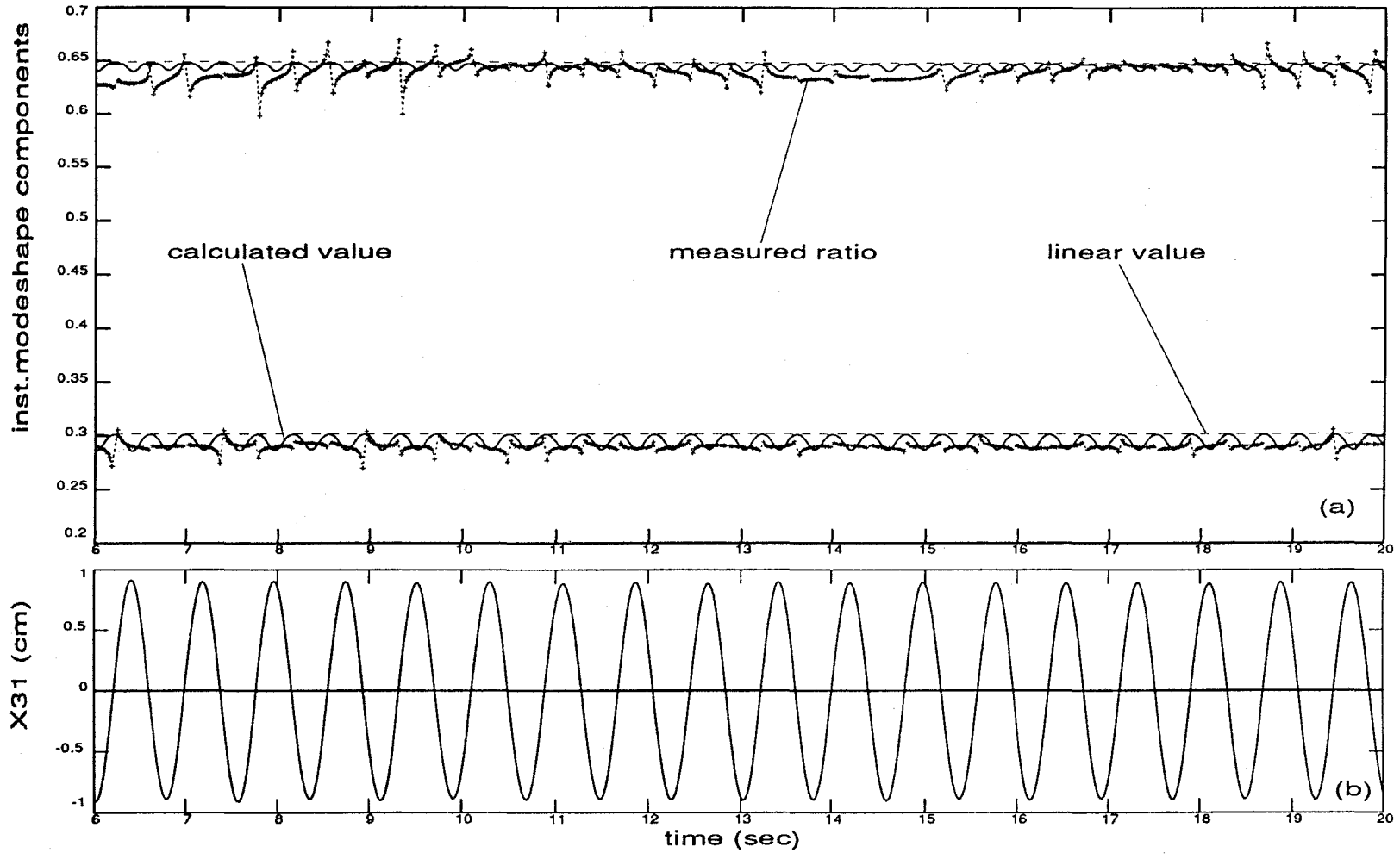

Figure 3.1. Calculated and measured instantaneous modeshape components.

vibrating in a mode can be represented as

$$\mathbf{x}(t) = \Phi u(t) \tag{3.17}$$

where Φ is a mode shape vector and u is a modal coordinate. The relation (3.17) is the modal relation in the case of a constant mode shape. In addition, Szemplinska-Stupnicka assumed that the free modal vibration is approximately harmonic. That is, the modal response solution has the approximate form:

$$\mathbf{x}(t) = \Phi A \sin(\omega t) \tag{3.18}$$

and the solution of the modal coordinate has the form

$$u(t) = A \sin(\omega t) . \tag{3.19}$$

In reference [68-69], the mode shape Φ and frequency ω are determined by the Galerkin method. According to the variational principle, an actual solution of $\mathbf{x}(t)$, is such that the functional

$$H(\mathbf{x}) = \int_0^T [T(\dot{\mathbf{x}}) - U(\mathbf{x})]\, dt \tag{3.20}$$

is an extremum for the path of motion, where T and U are kinetic and potential energies respectively.

As a trial solution, the approximation of (3.18) is substituted into the functional $H(\bullet)$, leading to a new functional, $\tilde{H}(\Phi, \omega)$. The optimal solutions are those Φ and ω which minimize the functional $\tilde{H}(\Phi, \omega)$, i.e.,

$$\tilde{H}(\Phi, \omega) = \int_0^T [T(\Phi, \omega, t) - U(\Phi, \omega, t)]\, dt = \text{minimum w.r.t. } \Phi, \omega. \tag{3.21}$$

According to the Galerkin method, the solution of the variational problem

$$\int_0^T e(\Phi, \omega, t) \sin(\omega t)\, dt = 0 \tag{3.22}$$

where $\mathbf{e}(\Phi, \omega, t)$ is the residual vector of the equation (3.10) after substitution of (3.18). In more detail, the equation is

$$\int_0^T [-\omega^2 \mathbf{M}\Phi A \sin(\omega t) + \mathbf{K}\Phi A \sin(\omega t) + \mathbf{f}(\Phi A \sin(\omega t))] \sin(\omega t)\, dt = 0. \tag{3.23}$$

In equation (3.23), the part within the square brackets represents the residual (or error) of equation (3.10) due to the approximation of the solution at time *t* and the functional part in the integral represents the weighted residual with the weighing function *sin*(ωt). The integral represents the sum of the weighted residual over a period of oscillation. The condition for determining the solution (3.18) is that the sum of the weighted residual is zero. Therefore, the solution determined by (3.23) is optimal in the sense that the sum of the weighted residual is minimized. Equivalently, the solution makes the functional $\tilde{H}(\Phi, \omega)$ a minimum. Since the functional is an integral over a period of oscillation, the optimization of the solution is based on the idea that the "global (or overall) error" of the solution over the whole period is a minimum.

After integration, (3.23) becomes

$$-\omega^2 \mathbf{M}\Phi + \mathbf{K}\Phi + \mathbf{S}(\Phi, A) = 0 \qquad (3.24)$$

where $\mathbf{S}(\Phi, A)$ is a vector given by

$$\mathbf{S}(\Phi, A) = \frac{2}{AT}\int_0^T \mathbf{f}(\Phi A \sin(\omega t))\sin(\omega t)\,dt . \qquad (3.25)$$

For a system with a cubic nonlinearity,

$$\mathbf{S}(\Phi, A) = \mathbf{f}(\Phi) A^2 \frac{3}{4} \qquad (3.26)$$

Equation (3.24) thus becomes

$$-\omega^2 \mathbf{M}\Phi + \mathbf{K}\Phi + \mathbf{f}(\Phi) A^2 \frac{3}{4} = 0 . \qquad (3.27)$$

Equations (3.24) and (3.27) are nonlinear algebraic equations in terms of the parameter A. They are similar to equation (3.13). The only difference lies in that the parameter in these equations is the modal amplitude A, instead of the modal displacement *u*. Similar to equation (3.13), these equations can also be solved with the Newton-Raphson method in A-incremental manner. As discussed in section 3.2.1, the mode shapes are amplitude-dependent, instead of varying with displacement instantaneously, they are constant over a cycle of oscillation.

3.3.2 Peak Approach

The Szemplinska-Stupnicka's approach provides one calculation of the constant

(amplitude-dependent) mode shape. In the approach, Φ and ω which are determined by (3.23) are optimal in the sense that the "global error" of modal solution (3.18) over the whole period is minimum. But this solution may not provide a minimized "local error" (the error between the approximate solution and the real response at one time t). For example, at the instant when the motion reaches its maximum position, the Φ evaluated by the Galerkin method may not be the displacement configuration, or shape, taken by the whole system at this time when the system executes a motion (modal vibration) with frequency ω.

Frequently, the shape that the system assumes, when all coordinates reach their extremum positions (response peak), may be more useful, and is easy to measure. Such a displacement configuration can be represented as

$$\phi_i = \frac{X_i}{X_r} \qquad (3.28)$$

$$i = 1, \cdots, n; \quad r\text{--fixed, reference}$$

where $X_i = (x_i)_{max}$ is maximum value (response peak) of displacement of *ith* mass. ϕ_i are ratios of displacement peak values. This displacement configuration is the instantaneous mode shape of the system at the time when all masses reach their maximum positions. This displacement configuration can be considered as another choice of approximation of constant mode shape. It may be approximately calculated as below.

Assume that all coordinates reach their extremum positions at the same instant of time, t_p, when the system vibrates in a mode with frequency ω. Let $\mathbf{X}_{max}$ and $\ddot{\mathbf{X}}_{max}$ be respectively the peak value vectors of displacement and acceleration, i.e. $\mathbf{X}_{max} = \mathbf{x}(t_p)$ and

$\ddot{\mathbf{X}}_{max} = \ddot{\mathbf{x}}(t_p)$. Then, at that instant, t_p, the equation of motion is

$$\mathbf{M}\,\ddot{\mathbf{X}}_{max} + \mathbf{K}\mathbf{X}_{max} + \mathbf{f}(\mathbf{X}_{max}) = \mathbf{0}\,. \qquad (3.29)$$

Assume that

$$\mathbf{X}_{max} = \mathbf{\Phi}_p A \qquad (3.30)$$

where A is the amplitude of modal response and Φ_p is the instantaneous mode shape at the instant t_p. Further assume that

$$\ddot{\mathbf{X}}_{max} = -\omega^2 \mathbf{X}_{max}\,. \qquad (3.31)$$

Then, substituting (3.30) and (3.31) into (3.29) yields

$$-\omega^2 \mathbf{M}\mathbf{\Phi}_p A + \mathbf{K}\mathbf{\Phi}_p A + \mathbf{f}(\mathbf{\Phi}_p A) = \mathbf{0}\,. \qquad (3.32)$$

The mode shape Φ_p is determined by this equation. If the system has a cubic nonlinearity, equation (3.32) becomes

$$-\omega^2 \mathbf{M}\mathbf{\Phi}_p + \mathbf{K}\mathbf{\Phi}_p + \mathbf{f}\,(\mathbf{\Phi}_p)\,A^2 = \mathbf{0}\,. \qquad (3.33)$$

It can be seen that equation (3.33) is different from equation (3.27) but has the same form as equation (3.14). Hence, Φ_p is different from Φ_s (subscript, s, denotes result of Szemplinska-Stupnicka process). As in the Szemplinska-Stupnicka method, these nonlinear algebraic equations can be solved with the Newton-Raphson method in the A-incremental manner. As assumed previously, if the system has *n* DOFs, equation (3.32) or (3.33) has *n* solutions for the set ω and Φ. Each ω and Φ is evaluated with initial values as before. A subscript, p, is added to ω (A) to indicated that it is calculated by the peak approach. The ω_p and Φ_p will be functions of the modal amplitude A.

In reference [48], it is assumed that the potential function $U(x_1, x_2, \cdots, x_n)$ is an even function since potential energy of a system is always positive and that restoring forces are odd functions of their arguments. Reference [66] pointed out that functions $\hat{x}_i(\bullet)$ must be odd functions of their arguments because of the symmetry of the potential function and expressed $\hat{x}_i(\bullet)$ as odd polynomial series (3.3). Therefore, the resulting mode shape ϕ_{ij} is even functions of the reference coordinate x_{rj} (equation 3.4). From the definition, the peak mode shape is obtained by letting $x_{rj} = A_j$ where A_j is the amplitude of x_{rj}. Therefore, the peak mode shape will be expressed as even polynomial series. Consequently, squared modal frequency from (3.32) will also be an even function. The modal frequency and mode shape components are expressed as

$$\omega_j^2 (A_j) = \sum_{k=0}^{p_\omega} \Omega_j^{(k)} A_j^{2k} \qquad (3.34)$$

$$\phi_{ij} (A_j) = \sum_{k=0}^{p_\phi} \phi_{ij}^{(k)} A_j^{2k} \qquad i=1, \cdots, n \qquad (3.35)$$

where A_j is the *jth* modal amplitude, p_ω and p_ϕ are truncated order numbers which are chosen for satisfactory curve-fittings of ω_p and Φ_p.

It can be found that the equation (3.32) or (3.33) will become a standard linear eigenvalue problem if the modal amplitude A tends to zero. The resulting eigenvalues and eigenvectors will be linear natural frequencies and mode shape vectors. Therefore, the limit values of the functions (3.34) and (3.35) will be linear natural frequencies and mode shape values as A tends to zero. These values are given by the constant terms of these functions.

For the 3DOF cubic system in Figure 2.1, the first two modes are calculated by the peak method. Figures 3.2 and 3.3 show $\omega_p(A)$ and components of $\Phi_p(A)$ for the first and second mode respectively. The modal frequency and mode shape of the first mode are expressed as

$$\omega_1^2(A_1) = 70.29 - 7.62A_1^2 + 0.0A_1^4 \qquad (3.36)$$

$$\phi_{11}(A_1) = 0.30 - 0.05A_1^2 - 0.007A_1^4 \qquad (3.37)$$

$$\phi_{21}(A_1) = 0.65 - 0.00A_1^2 - 0.008A_1^4 \qquad (3.38)$$

It is clear that the nonlinear modal frequency and mode shape change with the modal amplitude. As shown in the figures, when the modal amplitudes increase, the modal frequencies of both modes decrease, as expected since the nonlinear system is softening. As the modal amplitudes increase, the two components of the first mode shape, ϕ_{11} and ϕ_{21} , and the second component of the second mode shape, ϕ_{22} , decrease, but ϕ_{12} increases in a small amplitude range (about $A_2 < 0.3$) and decreases beyond that range.

It is clear that nonlinear mode shape is different from linear mode. For the first mode, whose linear natural frequency is *1.33 **Hz***, linear mode shape is $(0.30, 0.65, 1)^T$; when A_1 = *1.38 cm*, modal frequency becomes *1.19 **Hz*** and mode shape is $(0.25, 0.59, 1)^T$. The frequency changes *10.5%*, ϕ_{11} and ϕ_{21} change *16.7%* and *9.2%* respectively. For the second mode, the linear natural frequency is *2.85 **Hz*** and the mode shape is $(-0.67, -0.61, 1)^T$. When A_2 = *0.34 cm*, the modal frequency becomes *2.35 **Hz***, changing *17.5%*

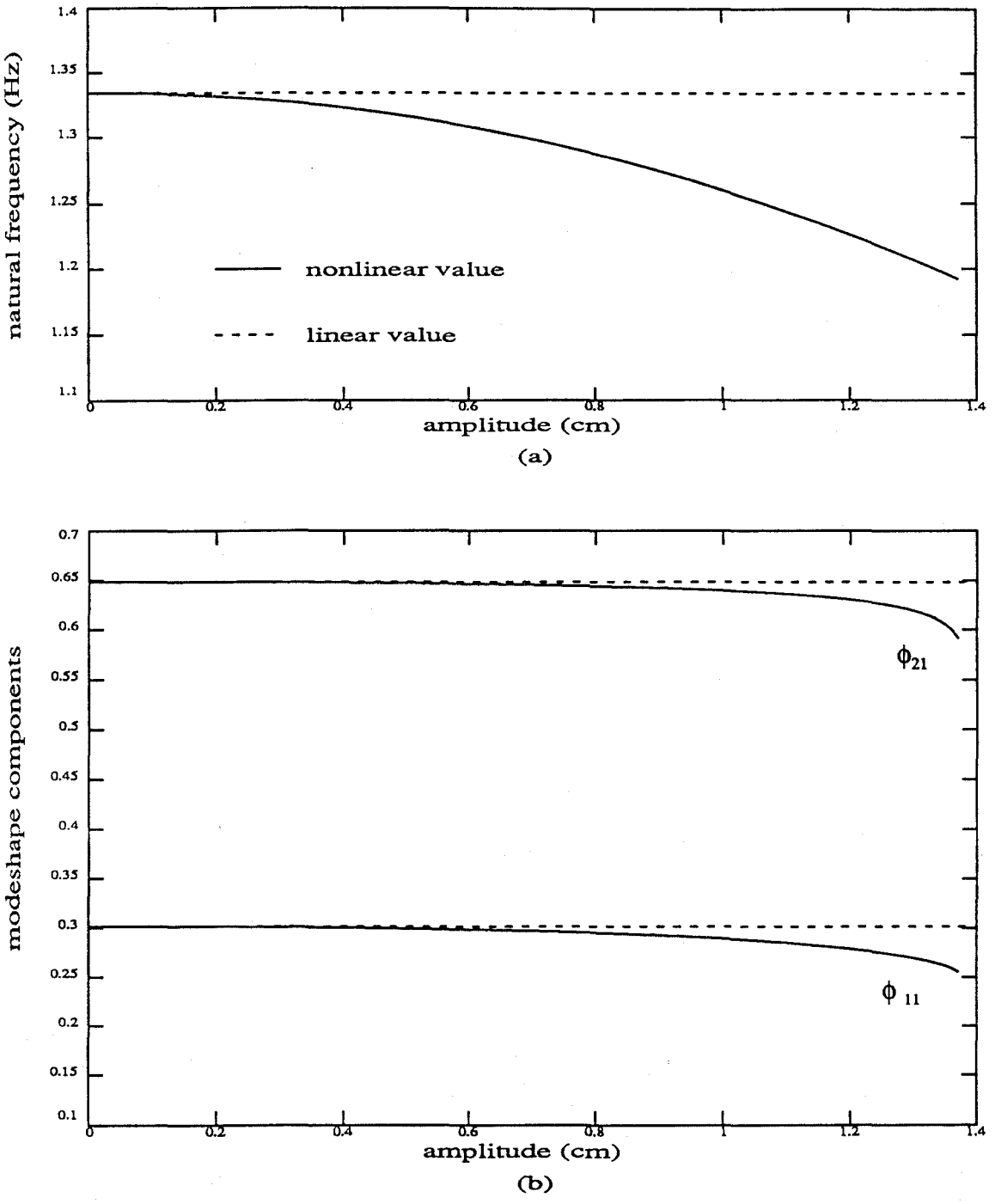

Figure 3.2. First natural frequency and modeshape calculated by peak approach. (a) natural frequency; (b) modeshape components.

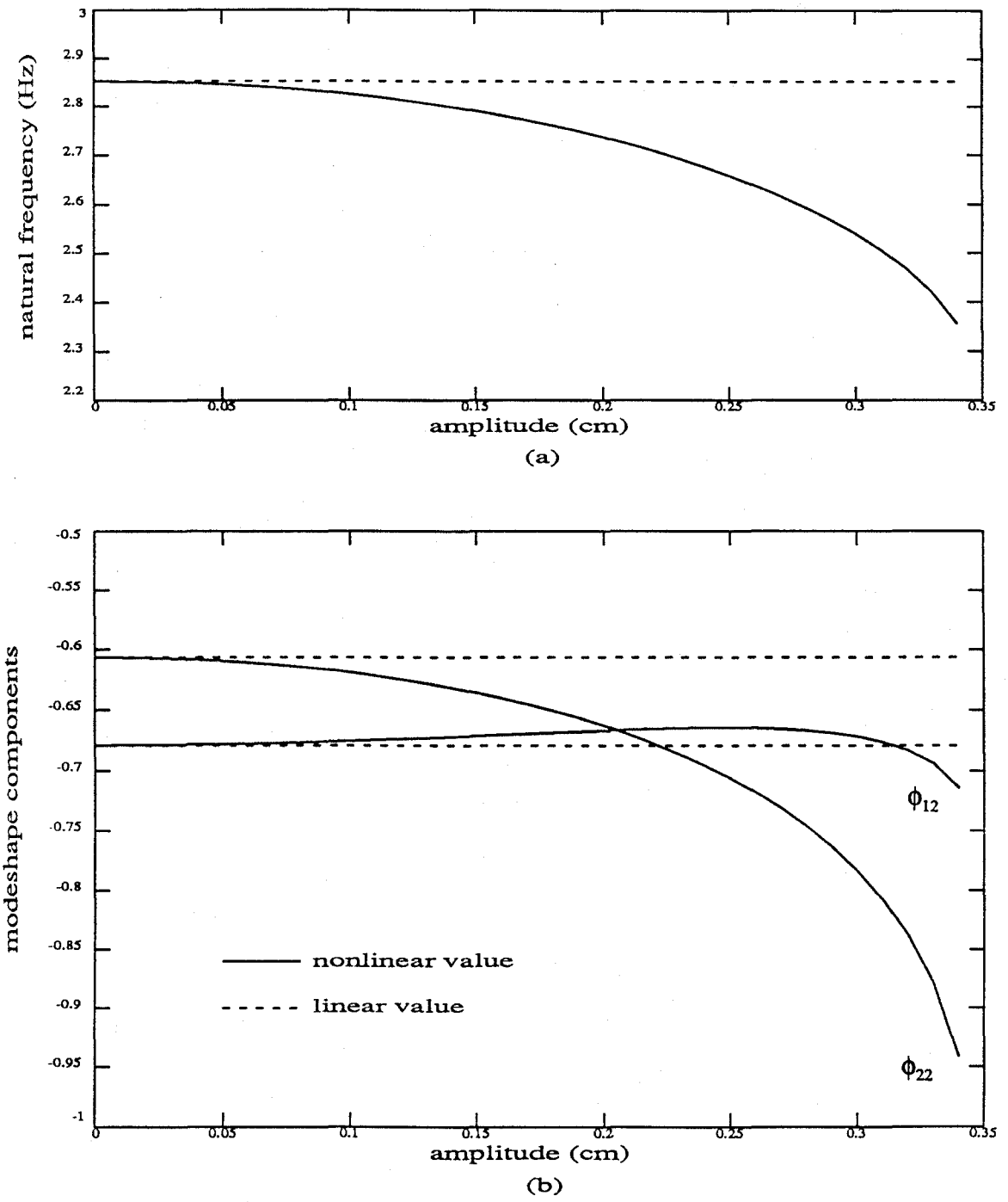

Figure 3.3. Second natural frequency and modeshape calculated by peak approach. (a) natural frequency; (b) modeshape components.

and mode shape becomes $(-0.71, -0.94, 1)^T$. ϕ_{12} and ϕ_{22} change *6%* and *54%* respectively. The linear and nonlinear mode shapes associated with the above amplitudes are shown in Figure 3.4. It can be seen that the change of modal quantities is significant.

3.3.3 Generalized Approach

Comparing equations (3.27) and (3.33), one can see that the coefficients of the last term in the two equations are different. Hence, the resulting mode shapes, Φ_p and Φ_s will be different. As known, Φ_p is determined at the time when the motion of the system reaches its maximum position. Physically, it represents the displacement configuration that the system assumes at that time. Therefore, it can be seen that this definition is based more on the point of view of observation or measurement. Following the same idea that the peak mode shape is a special measurement of the instantaneous mode shape, Φ_s can be also found to be a special measurement of the instantaneous mode shape and the "constant" mode shape can be defined with other choices. Extending the definition of the peak mode shape, a general definition of an amplitude-dependent mode shape can be given as below.

Assume that a nonlinear system is vibrating in a mode and the corresponding mode displacement is $\mathbf{x}(t)$. Let the modal coordinate be u ($u = x_n$ for pure mode vibrations) and A be the amplitude of u. Let t_α be such a time that $u(t_\alpha) = \alpha A$, $0 \leq \alpha \leq 1$. At the instant t_α, the displacement of the system vibrating in a mode is denoted by $\mathbf{x}(t_\alpha)$. Define the displacement configuration of the system at this time to be the mode shape for all time in the period and represent the mode shape as

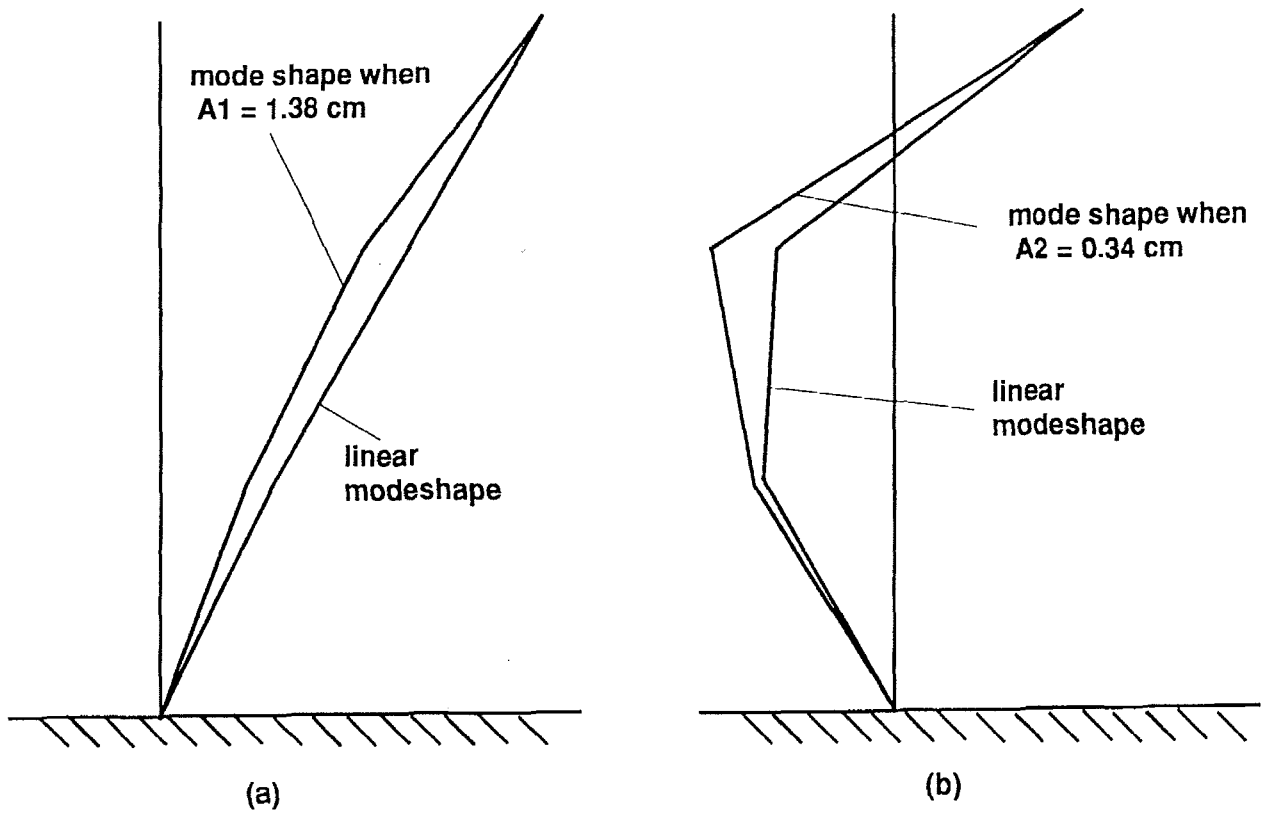

Figure 3.4. Difference of linear and nonlinear modeshapes. (a) First mode; (b) Second mode.

$$\Phi_\alpha(A) \equiv \frac{\mathbf{x}(t_\alpha)}{u(t_\alpha)} = \frac{\mathbf{x}(t_\alpha)}{\alpha A} . \qquad (3.39)$$

The modal relation for this mode over the period is approximated to be

$$\mathbf{x}(t) = \Phi_\alpha(A)\, u(t) . \qquad (3.40)$$

The mode shape is approximately evaluated at the time t_α. Assume that the system vibrates in a mode with frequency ω. At the instant t_α, the equation of motion is

$$\mathbf{M}\ddot{\mathbf{x}}(t_\alpha) + \mathbf{K}\mathbf{x}(t_\alpha) + \mathbf{f}(\mathbf{x}(t_\alpha)) = \mathbf{0} . \qquad (3.41)$$

Assume that the acceleration response of the system at the instant t_α is

$$\ddot{\mathbf{x}}(t_\alpha) = -\omega^2 \mathbf{x}(t_\alpha) . \qquad (3.42)$$

According to the definition (3.39)

$$\mathbf{x}(t_\alpha) = \Phi_\alpha(A)\, \alpha A . \qquad (3.43)$$

Substituting (3.42) and (3.43) into (3.41) yields

$$-\omega^2 \mathbf{M}\Phi_\alpha \alpha A + \mathbf{K}\Phi_\alpha \alpha A + \mathbf{f}(\Phi_\alpha \alpha A) = \mathbf{0} . \qquad (3.44)$$

For MDOF systems with cubic nonlinearity, the nonlinear algebraic equation for evaluating Φ_α and ω_α will be

$$-\omega^2 \mathbf{M}\Phi_\alpha + \mathbf{K}\Phi_\alpha + \mathbf{f}(\Phi_\alpha)\, \alpha^2 A^2 = \mathbf{0} . \qquad (3.45)$$

When $\alpha = 0$, Φ_α is the linear mode shape since the nonlinear term in equation (3.45)

vanishes so that the equation becomes a standard linear eigenvalue problem. When $\alpha = \sqrt{3}/2$, equation (3.45) becomes (3.27) which is the result of the Galerkin method, i.e., $\Phi_{\alpha=\sqrt{3}/2} = \Phi_s$. When $\alpha = 1$, equation (3.45) becomes (3.33) which corresponds to the peak approach, i.e., $\Phi_{\alpha=1} = \Phi_p$.

As before, n solutions of ω_α^2 and Φ_α are assumed to exist and can be evaluated independently one by one with appropriate initial values if the modes are well separated. For any $\alpha \neq 0$, the ω_α and Φ_α are functions of the modal amplitude. Therefore, the mode shape is amplitude dependent.

According to the above definition, the mode shape is the displacement configuration that the system assumes at the instant t_α when it vibrates in a mode. The mode shape can be easily measured from the modal response. For example, for a cubic system, $\Phi_{\alpha=\sqrt{3}/2}$ is measured by the ratios of the modal displacement at the instant t_s when $x_n = \sqrt{3}/2$ A, i.e.,

$$\Phi_{\alpha=\sqrt{3}/2} = \frac{\mathbf{x}(t_s)}{x_n(t_s)} . \qquad (3.46)$$

Similarly, $\Phi_{\alpha=1}$ is measured at the time t_p when all masses reach their maximum positions by the ratios

$$\Phi_{\alpha=1} = \frac{\mathbf{x}(t_p)}{x_n(t_p)} . \qquad (3.47)$$

Clearly, the peak mode shape $\Phi_{\alpha=1}$ is most easily measured. In later sessions, the peak

mode shape will be used for all analysis.

3.4 APPLICATION OF MODE SHAPE

3.4.1 Limitation of Application

In linear systems, mode shapes of free vibration can be used to decouple the equations of motion of forced vibrations. The response solution of the system can be expressed as a combination of mode shape vectors. With special conditions, the response solution can contain only one single mode shape vector, that is, the system vibrates in the shape of the free vibration mode and the whole system can be defined by any one coordinate of the system.

For nonlinear systems, the application of modes is restricted. First of all, this is due to the fact that the superposition principle is theoretically inadmissible in nonlinear systems. Hence modal solutions, even if they exist, can not be used to construct a general solution of the system as linear modal solutions do. Secondly, the modal relations for free mode vibration cannot in general be used to describe the coordinate relations for forced vibrations.

In reference [55], Rosenberg defined the steady-state vibration of forced nonlinear systems which is a vibration-in-unison of the systems. When a forced nonlinear system vibrates in a steady-state, all coordinates satisfy the relation

$$x_i = \tilde{x}_i (x_r) \qquad i = 1, \cdots, n, \quad r \text{ -- fixed.} \qquad \textbf{(3.48)}$$

Substitution of these functionals uncouples the equations of motion so that the equations of motion can be solved. However, in general, the functional $\tilde{x}_i [\bullet]$ for steady-state forced

vibration and $\hat{x}_i[\bullet]$ for free mode vibration are different and forced vibration equations cannot be uncoupled by $\hat{x}_i[\bullet]$. Rosenberg has already pointed out that nonlinear "normal-mode coordinates decouple the equations of motion for that mode only." In other words, the modal relation (2.4) exactly decouples the equations of motion only for the free mode of vibration itself, but not for other motions. Therefore, in general, the nonlinear modes can not be used to solve the steady-state forced vibration problem.

At present, for nonlinear systems, there is no theory to show a general relation between a free vibration mode shape and a shape of steady-state forced vibration. Therefore, based on the existing studies, nonlinear modes can not be used to analyze a general forced vibration of nonlinear systems. However, in some case, nonlinear modes can be used in analysis of nonlinear forced vibration, as will be shown below.

3.4.2 Resonant Vibration Shape

It was shown by Rosenberg that a nonlinear system exhibits resonance as the frequency of external force tends to a natural frequency of the system. It can further be shown that the system assumes the configuration of the free vibration mode shape, when it is in resonance.

Consider the nonlinear system (3.10), which is acted upon by a periodic force $\mathbf{p}(t)$, with driving frequency ν. The equation of motion is

$$\mathbf{M}\ddot{\mathbf{x}} + \mathbf{K}\mathbf{x} + \mathbf{f}(\mathbf{x}) = \mathbf{p}(t) . \qquad (3.49)$$

According to the peak approach, the mode shape of the system is determined by equation (3.32) which can be written as

$$-m_i \omega^2 \frac{X_i}{X_r} + \sum_{s=1}^{n} \kappa_{is} \frac{X_s}{X_r} + \frac{1}{X_r} f_i \left(\frac{X_1}{X_r} X_r, \cdots, \frac{X_n}{X_r} X_r\right) = 0 \qquad (3.50)$$

where $X_i / X_r = \phi_i$, i = 1, $\cdots$, n ; r -- fixed and ω is a natural frequency of the system.

Assume that the acceleration of the system (3.49) can be represented in the form of

$$\ddot{x}_i (t) = -\nu^2 x_i (t), \quad i = 1, \cdots, n. \qquad (3.51)$$

Then the *ith* equation of motion is

$$-m_i \nu^2 x_i + \sum_{s=1}^{n} \kappa_{is} x_s + f_i (x_1, \cdots, x_n) = p_i (t) \qquad (3.52)$$

$$i = 1, \cdots, n.$$

Let A_i be the amplitude of $x_i(t)$ (i = 1, $\cdots$, n). Dividing the above equation by the amplitude A_r of the reference coordinate yielding

$$-m_i \nu^2 \frac{x_i}{A_r} + \sum_{s=1}^{n} k_{is} \frac{x_s}{A_r} + \frac{1}{A_r} f_i (x_i, \cdots, x_n) = \frac{p_i (t)}{A_r} \qquad (3.53)$$

$$i = 1, \cdots, n, \quad r -- \text{fixed}.$$

The system configuration at the time when all masses reach their maximum position is represented by the ratios of displacement peak values (A_1 / A_r, $\cdots$, A_n / A_r) and determined by the following equation:

$$-m_i \nu^2 \frac{A_i}{A_r} + \sum_{s=1}^{n} k_{is} \frac{A_s}{A_r} + \frac{1}{A_r} f_i \left(\frac{A_1}{A_r} A, \cdots, \frac{A_n}{A_r} A\right) = \frac{p_i (t)}{A_r} \qquad (3.54)$$

When $\nu \rightarrow \omega$, the system goes to resonance. At resonance, A_r takes on a very large

value so that p_i (t) / A_r (i =1, ···, n), can be ignored. On rejecting the terms p_i (t) / A_r on the right hand side, this equation becomes the same as (3.50). It is concluded that the resonant configuration, called the resonant vibration shape, of a nonlinear system resembles the corresponding free vibration mode shape.

The above result is a useful property of a nonlinear mode. Using this property, free vibration mode shapes can be used in the analysis of resonant vibration. Hence, when a nonlinear system is in a resonant vibration, the mode shape vector of free vibration mode can be used to uncouple the equations of motion so that the system can be investigated as a set of SDOF systems.

3.4.3 Practical Problems

As pointed out above, free vibration modes of nonlinear systems can not in general be used in the analysis of forced vibration but can be used in resonant condition.

In actual nonlinear vibrations, mode-like behavior can often be observed. Resonance occurs in neighborhoods of some special frequencies. Associated with these frequencies, a system assumes certain shapes or configurations. These frequencies and configurations resemble the modal frequencies and mode shapes of a linear system. Therefore, although the system may not possess exact modes, it may possess mode-like properties near resonance. In a practical sense, a nonlinear system having mode-like states is said to have "modes of vibration." In many practical problems, the mode-like behavior physically exists, which is generally represented by resonances.

Two classes of nonlinear forced vibrations can be approximately analyzed using

the free vibration modes described previously. Systems of first class are those (undamped or lightly damped) subjected to exciting forces with a single driving frequency which is close to a natural frequency. In the second class, the systems (undamped or lightly damped) are subjected to wide-band excitations. The response of the latter system contains all frequency components in the excitation band. If the system has only one resonance in this range, those frequency components which are close to the resonant frequency dominate the response. If the damping of the system is small, the contributions of frequency components far from the resonant frequencies to the response are generally much smaller than those near the resonant frequencies. In this case, the system basically assumes the configuration of the free vibration mode shape.

In most practical problems, physical systems generally do not vibrate in one single mode but several modes appear in the response at same time. If the modes are not close to each other, the modal method can still be used. First of all, it is assumed that no secondary resonance, like harmonic resonances internal resonance [78], occur, or that such a resonance is so small compared with main resonances that they can be ignored. Hence, inter-mode influence will not be considered. The modal responses may be approximately isolated by "frequency windows," each of which contains the resonant and nearby frequency components. In each band, the response of the system can be approximately analyzed using the concept of modes. Although the superposition principle is not strictly valid in nonlinear systems, in many cases, a linear combination of nonlinear mode responses [49] can still give a good approximation to the response. Therefore, the whole response of the system may be expressed approximately as the sum of the nonlinear

modal responses.

Based on the above discussion, some complex vibrations of nonlinear systems, like earthquake response, can be investigated approximately as long as resonances of the systems are pronounced and well separated.

CHAPTER 4

MODAL EQUATIONS OF NONLINEAR SYSTEMS

4.1 BACKGROUND

In vibrations of a linear system, a complete set of mode shape vectors spans a solution space. The mode shape vectors are base vectors of the space. All response of the system can be expressed as a superposition of the mode shape vectors. A vibration component of the system associated with a mode shape vector is referred to as a modal vibration of the system and the equation which governs this motion is called a modal equation. For modal vibration, the mode shape determines the displacement relationship between degrees of freedom and a reference degree of freedom. A modal equation determines response of the reference degree of freedom. The modal vibration of the system is completely described by the solution of the modal equations along with mode shapes. The same idea will herein be extended to nonlinear systems.

4.1.1 Constant-coefficient Models

In linear systems, modal equations can be obtained rigorously using the orthogonality of the free vibration mode shapes. For nonlinear systems, all practical approaches are approximate since, in general, the nonlinear modal method is an

approximate approach. Most approaches employ linear mode shapes or equivalent mode shapes and assume that the modal equations have the form of a SDOF system. The coefficients of the equations are often assumed to be constant and determined equivalently in some sense. From the previous chapters, it has been already shown that the modal quantities of nonlinear systems are dependent on response level. Hence, it may be recognized that modal equations should also be response-level-dependent. This inference indicates that an equation with specific coefficients is only valid for a vibration at a special level. For a vibration of the system at another response level, it may not give an acceptable approximation. The following numerical test shows such an example.

The system considered is the damped system of chapter 2 which is shown in Figure 2.1. The system parameters were given in Chapter 2. The system is subjected to a ground motion excitation. The ground acceleration is generated using El Centro earthquake data which is scaled by 0.075. The inter-mass restoring forces and Fourier Amplitude Ratios are given in Figure 4.1 and 4.2 respectively. The nonlinear behavior and mode-like phenomena can be observed. The first mode-like response is obtained by filtering from 0 - 2 *Hz*. A constant-coefficient modal equation is obtained by "best" fitting of the response time history to be

$$\ddot{x} + 0.0778\dot{x} + 67.8536x - 4.6005x^3 = -1.5089\,\ddot{z}\,.$$

The time histories of the filtered modal displacement and of the displacement calculated by the equation are shown in Figure 4.3a. In order to test this equation, it is assumed that the system is subjected to another ground excitation which is the El Centro

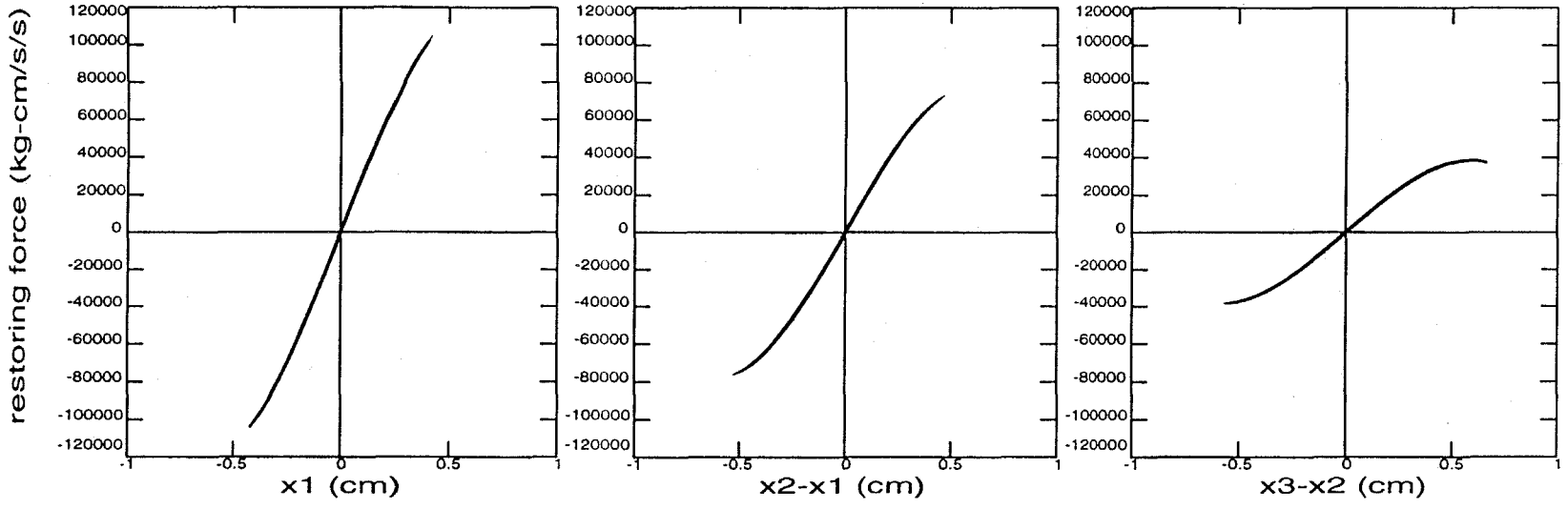

Figure 4.1. Inter-mass restoring force of 3DOF nonlinear system subjected to a scaled El Centro earthquake input (scale = 0.075) .

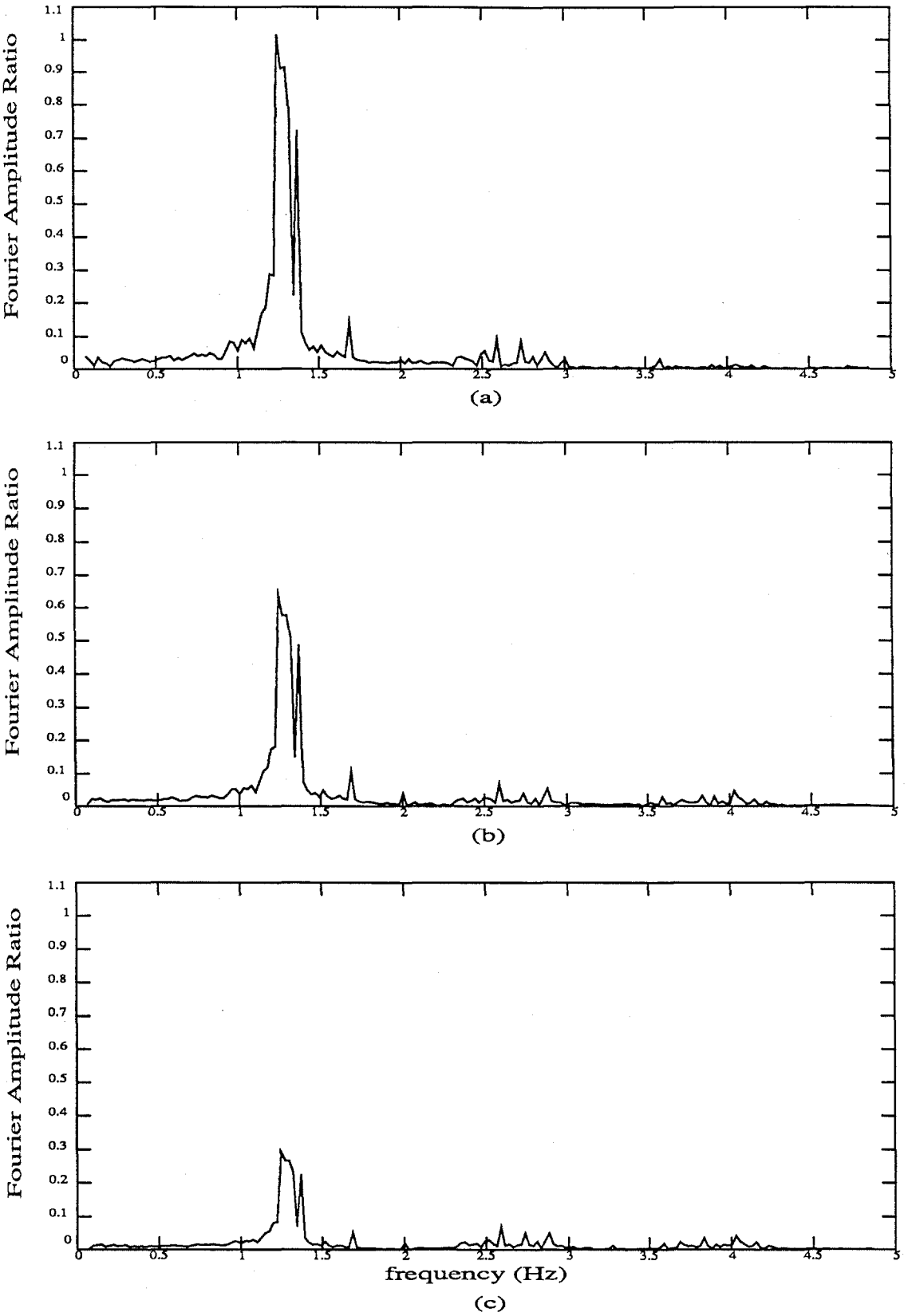

Figure 4.2. FARs of (a) mass 3; (b) mass 2; and (c) mass 1.

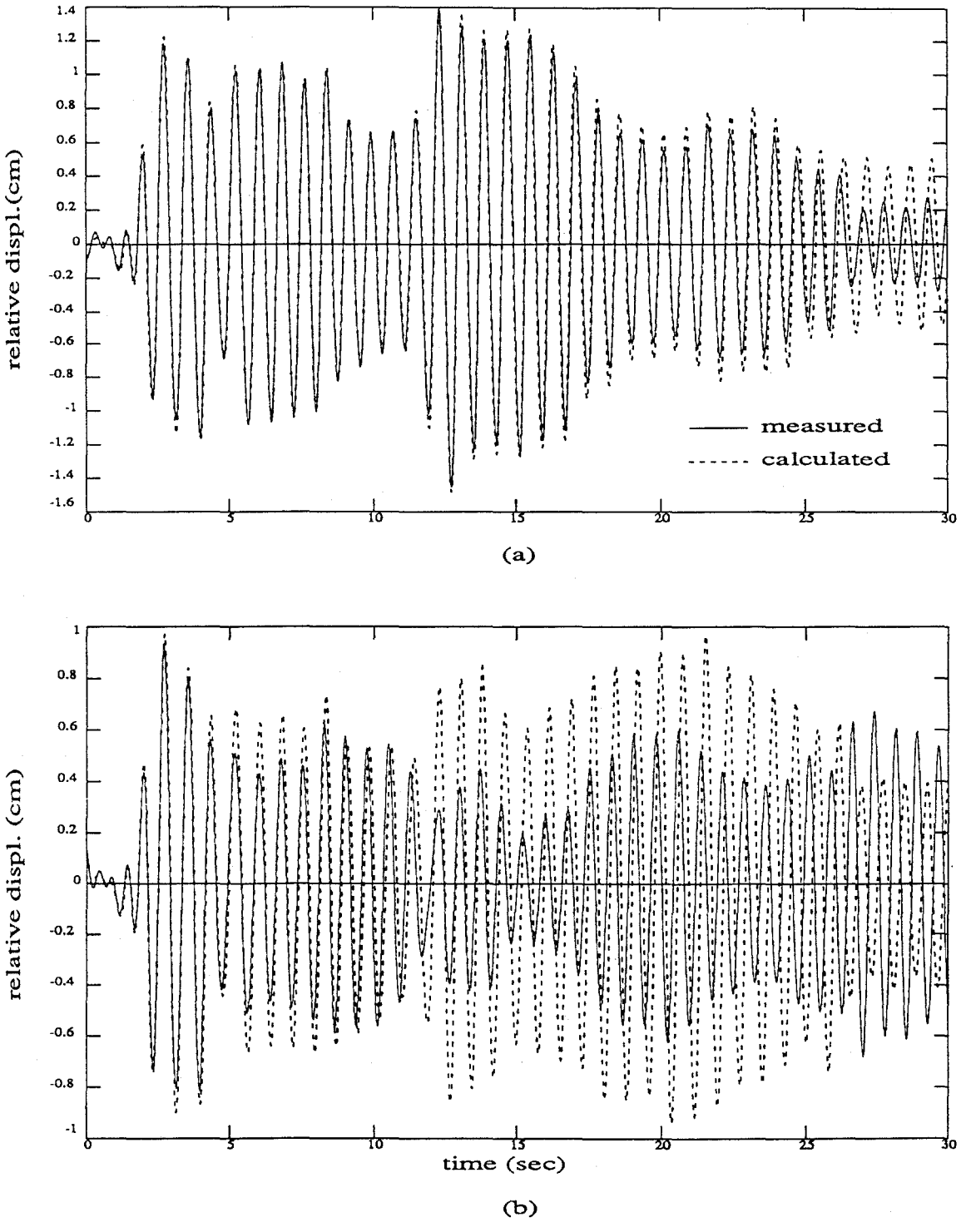

Figure 4.3. Calculated modal displacements by identified modal equation with (a) excitation one (scale = 0.075) and (b) excitation two (scale = 0.06)

earthquake ground acceleration scaled by 0.06. Since the excitation is lower than the first case, the system vibrates at a lower level. The filtered modal response and the predicted response by the above equation are plotted in Figure 4.3b. It is obvious that the equation fails to predict the modal response of the system to the new excitation. This example shows that a constant-coefficient modal equation is valid for a specific vibration level range, but may not be effective for other vibration levels. Hence, a constant-coefficient model of modal equation has limited range of application. In order to have a wider application, the modal equation of nonlinear systems needs a model which is applicable to various vibration levels.

4.1.2 Uncoupling of Equation of Motion

In linear systems, the response of a system can be described as the superposition of many modal responses. By means of the orthogonality of mode shapes, equations of motion can be uncoupled, leading to modal equations. However, nonlinear systems have no counterparts of superposition and orthogonality of mode shapes. Therefore, there is no basis for strictly uncoupling general nonlinear equations of motion and for decomposing the response of a system into components which can be defined by independent variables. In other words, no modal response is rigorously defined and decomposed, and no exact modal equations can be derived for general nonlinear vibrations. Therefore, in theory, equations of motion can be decoupled only in single-mode vibration. At present, there are three classes of single-mode vibration cases where equations of motion can be decoupled.

The first case is pure free mode vibration. When an autonomous nonlinear system vibrates in a single mode, a set of functional of a reference displacement, $\hat{x}_i(x_r)$, satisfying equation (2.4) can be found. Substituting these functional into the equations of motion uncouples them and results in a set of independent single-variable equations. The equation corresponding to the reference degree of freedom is the modal equation of the motion. The coefficients of the modal equation depend upon the response of the reference degree of freedom.

The second case is steady-state forced vibration, where all displacements of degrees of freedom can be determined by one of them and a set of functional (equation (3.48)). Equations of motion can be uncoupled by substitution of these functional and the number of independent variables is reduced to one. The steady-state motion of the system is determined by one independent variable. As mentioned previously, in general, the free vibration mode shape vector cannot be used to uncouple the equations of motion for steady-state forced vibration.

The third case is the forced vibration with single resonance. In this case, the configuration of a system is the same as a corresponding free vibration mode shape. The nonlinear mode shape vectors can be used to uncouple the equations of the system.

In this chapter, the modal equation of a single resonance will be derived and extended to the case of multiple resonance which has no exact modal equation in theory.

4.2 MODAL EQUATIONS OF SINGLE RESONANCE

Consider a lightly damped nonlinear system described by the following equation of motion

$$\mathbf{M}\ddot{\mathbf{x}} + \mathbf{C}\dot{\mathbf{x}} + \mathbf{K}\mathbf{x} + \mathbf{f}(\mathbf{x}) = \mathbf{p}(t) \qquad (4.1)$$

where **M, C, K** are mass, damping and linear stiffness matrices, **f** is the vector of nonlinear part of restoring force, **p**(t) is an external force vector. Assume that **p**(t) is a force with a single frequency which is close to the *jth* resonant frequency of the system so that only the *jth* resonance occurs. According to the last chapter, the free vibration modes are employed to generate modal equations for the resonant vibrations.

4.2.1 Direct Method

Since the solution (2.4) is the complete response of the system for single mode vibration, it can be directly substituted into the equation of motion. In the classical way [53,55,56], directly substituting the relation (2.4) into equations (4.1) leads to *n* independent single-variable equations. The equation associated with the reference degree of freedom is the modal equation. The coefficients of the equation depend upon the displacement x_r. Since the equation is displacement-dependent, there will be considerable difficulty in solving this equation or in identifying the coefficients in determining a system from a known response. Therefore, for practical application, it is necessary to simplify the modal equation by using the simplified mode shape. In this thesis, the amplitude-dependent modal models will be employed to obtain a modal equation.

Let the *jth* amplitude-dependent mode shape be Φ_j and the *jth* modal coordinate

be u_j. The response of the system may be approximately given by

$$\mathbf{x}(t) \approx \Phi_j(A_j)\, u_j(t) . \qquad (4.2)$$

where A_j is half-cycle amplitude of modal coordinate u_j and Φ_j is the *jth* amplitude-dependent mode shape vector. Substituting (4.2) into the equation of motion (4.1) yields

$$\mathbf{M}\Phi_j \ddot{u}_j + \mathbf{C}\Phi_j \dot{u}_j + \mathbf{K}\Phi_j u_j + \mathbf{f}(\Phi_j u_j) \approx \mathbf{p}(t) \qquad (4.3a)$$

or in component form

$$m_i \phi_{ij} \ddot{u}_j + \sum_s c_{is}\phi_{sj}\dot{u}_j + \sum_s k_{is}\phi_{sj}u_j + f_i(\phi_j u_j) \approx p_i(t) . \qquad (4.3b)$$

The equations (4.3b) can be written as

$$\ddot{u}_j + \frac{\sum c_{is}\phi_{sj}}{m_i\phi_{ij}}\dot{u}_j + \frac{\sum k_{is}\phi_{sj}}{m_i\phi_{ij}}u_j + \frac{f_i(\Phi_j u_j)}{m_i\phi_{ij}} = \frac{p_i(t)}{m_i\phi_{ij}} \qquad (4.3c)$$

$$i = 1, \cdots, n .$$

Equations (4.3) are *n* independent equations. They should be identical and any one of these equations can be used as the modal equation.

4.2.2 Szemplinska-Stupnicka's Method

In reference [68,69], Szemplinska-Stupnicka proposed a modal equation analogous to the modal equations of linear systems. Szemplinska-Stupnicka considered a case that the external force **p**(t) is harmonic and that the frequency of driving force is close to a natural frequency (say, the *jth* natural frequency) of the system. In this case, one (*jth*) resonance dominates the response of the system which can be regarded as vibrating in a

single mode. Szemplinska-Stupnicka assumed that the solution of u_j is also harmonic and has the same frequency as the driving force. Hence, in equation (4.2) u_j can be replaced by the harmonic function with the frequency of the driving force. Szemplinska-Stupnicka applied Galerkin's method to each equation, then, multiplied the *ith* equation by ϕ_{ij}, and added all equations with respect to the index *i*, yielding two algebraic equations for two unknowns (amplitude and phase). The solutions of the unknowns approximately determine the solution of u_j.

In Szemplinska-Stupnicka's process, the first step is applying Galerkin's method, while the later operation makes a transformation of *n* equations into a single equation. This process can also be presented in another way, by taking the transformation first, then applying Galerkin's method, as follows.

First, multiply the *ith* equation in (4.3) by ϕ_{ij}

$$\phi_{ij}\left(m_i\phi_{ij}\ddot{u}_j + \sum_s c_{is}\phi_{sj}\dot{u}_j + \sum_s k_{is}\phi_{sj}u_j + f_j(\Phi_j u_j)\right) \approx \phi_{ij}p_i(t)\,. \tag{4.4}$$

Sum all equations with respect to the index is

$$\sum_{i=1}^{n}\phi_{ij}\left(m_i\phi_{ij}\ddot{u}_j + \sum_s c_{is}\phi_{sj}\dot{u}_j + \sum_s k_{is}\phi_{sj}u_j + f_i(\Phi_j u_j)\right) = \sum_{i=1}^{n}\phi_{ij}p_i(t) \tag{4.5}$$

or, equivalently, equation (4.5) can be written in matrix form

$$\Phi_j^T\mathbf{M}\Phi_j\ddot{u}_j + \Phi_j^T\mathbf{C}\Phi_j\dot{u}_j + \Phi_j^T\mathbf{K}\Phi_j u_j + \Phi_j^T\mathbf{f}(\Phi_j u_j) = \Phi_j^T\mathbf{p}(t)\,. \tag{4.6}$$

Equation (4.5) is a SDOF nonlinear system. Inserting the assumed harmonic solution of u_j and applying Galerkin's method, leads to the same algebraic equations as those

obtained in the Szemplinska-Stupnicka's process.

Equations (4.5) are another approach for generating a modal equation for single resonance. Since this process leads to one equation, the solution of the modal response is unique. The process of obtaining equation (4.5) looks like an orthogonal operation, but it is only an analog to linear systems since no theory shows the existence of orthogonality of amplitude-dependent mode shapes. Hence, equation (4.5) is an approximation.

4.2.3 Discussion

In conclusion, by both the direct method and the Szemplinska-Stupnicka method, uncoupling the equations of motion using modal relation (4.2) results in a nonlinear amplitude-dependent modal equation. For a ground acceleration excitation, a modal equation can be represented in a normalized form

$$\ddot{u}_j + \alpha_j (A_j)\, \dot{u}_j + \tilde{f}_j (A_j, u_j) = -\beta_j (A_j)\, \ddot{z} \qquad (4.7)$$

where u_j is *jth* nonlinear modal coordinate, A_j is amplitude of u_j, $\tilde{f}_j$ is modal stiffness restoring force which is a nonlinear function of A_j and u_j , and $\alpha_j (A_j)$ and $\beta_j(A_j)$ are the modal damping coefficient and modal participation factor respectively, both of which are functions of modal amplitude A_j.

It is assumed that $\tilde{f}_j$ is an odd function of u_j. As an example, for a cubic system, the modal coordinate can be factored out, yielding a modal equation

$$\ddot{u}_j + \alpha_j (A_j)\, \dot{u}_j + \kappa_{1j} (A_j)\, u_j + \kappa_{3j} (A_j)\, u_j^3 = -\beta_j (A_j)\, \ddot{z} \qquad (4.8)$$

where $\alpha_j (A_j)$, $\beta_j (A_j)$, $\kappa_{1j} (A_j)$ and $\kappa_{3j} (A_j)$ are amplitude-dependent coefficients. Since

all components of Φ_j are even functions of modal amplitude as discussed in chapter 3, the coefficients of the resulting modal equation (4.3c) or (4.6) should also be even functions of modal amplitude. Hence, $\alpha_j(A_j)$, $\beta_j(A_j)$, $\kappa_{1j}(A_j)$ and $\kappa_{3j}(A_j)$ should be even functions of modal amplitude. More generally, the modal restoring force, $\tilde{f}_j(A_j, u_j)$, can be represented by a Taylor polynomial series with only odd terms (since $\tilde{f}_j$ is odd function) as

$$\ddot{u}_j + \alpha_j(A_j)\,\dot{u}_j + \kappa_{1j}(A_j)\,u_j + \kappa_{3j}(A_j)\,u_j^3 + \kappa_{3j}(A_j)\,u_j^5 + \cdots = -\beta_j(A_j)\,\ddot{z} \tag{4.9}$$

where all coefficients are functions of amplitude. It will be assumed that the coefficient functions are even functions.

Since the coefficients are amplitude-dependent, the modal equation will vary with amplitude. It indicates that a modal equation associated with a particular modal amplitude is only valid for the motion with that level. This can explain why in the example of 4.1.1 the constant-coefficient modal equation fails to predict modal response to another loading.

4.3 MODAL EQUATIONS FOR MULTIPLE RESONANCES

When **p**(t) is a general wide-band external excitation, the system may vibrate with many resonances. As mentioned previously, since nonlinear systems do not possess counterparts of the superposition principle and orthogonality of mode shapes, no exact modal equation can be defined and derived for multiple mode vibration. However, "modal equations" for nonlinear systems with multiple resonance can be proposed in an approximate sense as stated below.

First, for nonlinear systems with multiple resonances, each resonance is regarded as a "mode" and the resonant response is defined as a "modal response." It is approximately estimated by filtering in a "frequency window," called modal window, when the resonant frequencies are not close to each other. A second-order single-variable differential equation which can describe the above resonant response is defined as a modal equation. So-defined mode in the multiple resonance case should possess all the features of a single mode discussed before. Hence, the modal equation in the multiple resonance case is assumed to have the general form of (4.9). In the later two chapters, two specific amplitude-dependent models will be proposed.

For nonlinear systems with many resonances, when resonant frequencies are not close to each other, each mode is analyzed in a frequency band over which the system response is dominated by one mode (resonance). Let the mode under consideration be the *jth* mode. Over this frequency band, the system response can be approximately represented by

$$\mathbf{x}_j(t) \approx \mathbf{\Phi}_j(A_j)\, u_j(t) . \qquad (4.10)$$

The system is analyzed one mode at a time. Employing the approximation represented in reference [49], the full response of the system is expressed as a linear combination of nonlinear modes as:

$$\mathbf{x}(t) \approx \sum_{j=1}^{s} \mathbf{x}_j(t) \approx \sum_{j=1}^{s} \mathbf{\Phi}_j(A_j)\, u_j(t) \qquad (4.11)$$

where s is the number of modes included in the analysis.

In this thesis, the "modes" of nonlinear systems will be studied with the above

described idea.

4.4 AMPLITUDE ESTIMATION

Modal equation (4.9) is a differential equation with amplitude-dependent coefficients. Since it is a parametric differential equation and the modal amplitude is unknown *a priori*, an amplitude estimation is necessary in order to solve this equation. Therefore, a method for amplitude estimation must be developed before further examination of the modal equation.

To estimate the amplitude A_j, an energy equation is developed from the modal equation. Let A_j be changeable with time. For simplicity, consider the cubic equation (4.8). Multiplying by $\dot{u}_j$ and integrating from t_0 to t on both sides of equation, an energy equation can be derived. This yields

$$\frac{1}{2}\dot{u}_j^2(t) - \frac{1}{2}\dot{u}_j^2(t_0) + \int_{t_0}^{t} \alpha_j(A_j)\,\dot{u}_j^2(\tau)\,d\tau + \frac{1}{2}\kappa_{1j}(A_j)\,u_j^2(t) - \frac{1}{2}\kappa_{1j}(A_j)\,u_j^2(t_0)$$

$$+ \frac{1}{4}\kappa_{3j}(A_j)\,u_j^4(t) - \frac{1}{4}\kappa_{3j}(A_j)\,u_j^4(t_0) = -\int_{t_0}^{t} \beta_j(A_j)\,u_j(\tau)\,\ddot{z}(\tau)\,d\tau\,. \qquad \textbf{(4.12)}$$

In equation (4.12), the left-hand side is the increase in system energy (i.e., the sum of the increase in kinetic, viscous and potential energies) during the time interval t_0 to t. The right-hand side is the work done by the external force over the same time interval.

This equation can be simplified by choosing t_0 and t. In this thesis, the instants when the oscillators passes through its equilibrium portion (i.e., $u_j = 0$) are chosen as the

limits of integration. Consider two adjoining half-cycles numbered by k and k + 1, where the *kth* half-cycle is one with a known amplitude $A_{j,k}$ and the *(k+1)th* half-cycle is of unknown amplitude $A_{j,k+1}$ to be determined. Assume that t_k and t_{k+1} are respectively the starting time instants of the *kth* and *(k+1)th* half-cycles and that $T_k/2$ is the known period of the *kth* half-cycle and $T_{k+1}/2$ is the unknown period of (k+1)*th* half-cycle. Then $t_{k+1} = t_k + T_k/2$. Choose $t_o = t_k$, where $u_j(t_k) = 0$ and $t = t_{k+1} + T_{k+1}/2$. In this case, the stiffness terms do not appear in the equation since $u_j(t) = u_j(t_0) = 0$.

In the *(k+1)th* half-cycle, the response is unknown and is to be determined. Let the displacement and velocity in the *(k+1)th* half-cycle be respectively estimated by the approximation

$$u_j(\tau) = A_{j,k+1} \sin(\omega_j(A_{j,k+1})\,\tau) \qquad \textbf{(4.13a)}$$

$$\dot{u}_j(\tau) = \omega_j(A_{j,k+1})\,A_{j,k+1} \cos(\omega_j(A_{j,k+1})\,\tau)\,. \qquad \textbf{(4.13b)}$$

Substituting equations(4.13) into equation (4.12) yields

$$\frac{1}{2}\omega_j^2(A_{j,k+1})\,A_{j,k+1}^2 + \frac{\pi}{2}\alpha_j(A_{j,k+1})\,\omega_j(A_{j,k+1})\,A_{j,k+1}^2$$

$$+ \beta_j(A_{j,k+1})\,\omega_j(A_{j,k+1})\,A_{j,k+1} \int_0^{\frac{T_{k+1}}{2}} \cos(\omega_j(A_{j,k+1})\,\tau)\,\ddot{z}(t_{k+1}+\tau)\,d\tau$$

$$= \frac{1}{2}\dot{u}_j^2(t_k) - \alpha_j(A_{j,k}) \int_0^{\frac{T_k}{2}} \dot{u}_j^2(t_k+\tau)\,d\tau - \beta_j(A_{j,k}) \int_0^{\frac{T_k}{2}} u_j(t_k+\tau)\,\ddot{z}(t_k+\tau)$$

(4.14)

In equation (4.14), all quantities on the right-hand side belong to *kth* half-cycle

and are known; all quantities on the left-hand side belong to *(k+1)th* half-cycle and are unknown except for $\ddot{z}$. The equation (4.14) is a nonlinear equation for $A_{j,k+1}$. In order to simplify the equation, the value of T_{k+1} is approximately estimated and $\omega_j(A_{j,k+1})$ in the integral on the left-hand side is estimated from T_{k+1} so that the integral on the left-hand side can be calculated. For a harmonic driving force, T_{k+1} may be taken as the excitation period. For a broad-band input, T_{k+1} may be estimated from $\omega_j(A_j)$ as determined from the homogeneous system by a method presented in section 3.6, or some other appropriate method.

From equation (4.14), an approximate amplitude $A_{j,k+1}$ can be estimated. Thus, the coefficients, $\kappa_{1\,j}(A_j)$, $\kappa_{3\,j}(A_j)$, $\alpha_j(A_j)$, $\beta_j(A_j)$, of the modal equation (4.8) can be estimated and the response in the *(k+1)th* half-cycle can be predicted by any proper numerical procedure. During the initial (transient) stage of the response, the values of $\kappa_{1\,j}$ (0), $\kappa_{3\,j}$ (0), α_j (0), and β_j (0) can be used in solving the differential equation. In predicting the response from the modal equation (4.8), the amplitude needs to be updated for every vibration cycle (or half-cycle).

The energy equation (4.14) is a nonlinear algebraic equation, which must be solved numerically. It can be assumed that $A_{j,k+1} = A_{j,k} + \Delta A_{j,k}$. Substitute this into equation (4.14) so that it can be simplified by ignoring the terms in $\Delta A_{j,k}$ of higher order than quadratic, the resulting algebraic equation for $\Delta A_{j,k}$ can be easily solved.

In the above derivation, t and t_0 are chosen so that the stiffness terms do not appear in the equation to be solved. Consider the higher-order modal equation (4.9). If t and t_0 are chosen in the same way, stiffness terms will disappear in the equation and the

resulting algebraic equation will be the same as equation (4.14). Therefore, for higher-order modal equation, the equation for amplitude estimation is also equation (4.14).

CHAPTER 5

MODAL IDENTIFICATION USING SUCCESSIVE APPROXIMATION MODEL

5.1 BACKGROUND

In the last chapter, a general amplitude-dependent model of the modal equation was proposed to describe mode-like vibrations of nonlinear systems. If the modal equations of a system are known, modal responses of the system can be calculated. A reverse problem is how to determine a modal equation and modal parameters if a modal response is given. This problem is referred to as modal identification.

For linear systems, the modal theory and identification technology are mature. Modal equations in the time domain and transfer functions in the frequency domain can be expressed in modal parameters (frequencies, modal damping ratios and mode shapes). These parameters can be identified by fitting the modal equations or transfer functions using the recorded vibration response data. Many identification algorithms have been developed.

For nonlinear systems, however, since the modal theory is very limited, modal identification technology has not been well developed. Both mathematical models of modes and identification algorithms are current research subjects. In reference [49],

Frequency-Response-Function of nonlinear systems is expressed as a function of amplitude-dependent modal frequencies and mode shapes, and the modal frequencies and modal participation factors are identified in frequency domain by fitting experimental data. In general, there is a serious difficulty in identification of amplitude-dependent modal parameters and modal equations since, as mentioned previously, all nonlinear modal quantities and coefficients of modal equations are functions of amplitude. Many approaches use approximate constant models for simplicity. In those approaches, modal frequencies and mode shapes are identified as equivalent linear modes using linear modal algorithms and modal equations are determined by direct fit of response data in time domain. In many studies of seismic response, time-history-dependent models for hysteretic structural behavior were proposed and corresponding identification methods were presented. However, studies of use of amplitude-dependent models are rarely reported. Since amplitude-dependent models are necessary for nonlinear modal analysis with wide amplitude ranges, a goal of this work is to develop an adequate amplitude-dependent model of the modal equations and an effective methodology to identify the modal equations and modal parameters (modal frequencies, modal damping rations and mode shapes) using recorded response data.

In the last chapter, modal equations were expressed in the form of a polynomial with amplitude-dependent coefficients (equation (4.9)). Since this model has many stiffness restoring force terms and all coefficients to be determined are functions, numerically, this model cannot be directly determined uniquely. The amplitude-dependent model should be proper so that it is suitable for unique identification. There are a few

different ways to build such models. In this thesis, two approaches will be presented. Two amplitude-dependent polynomial models of the modal equation which are suitable for identification will be proposed in this and the next chapter respectively and two corresponding identification procedures will be presented.

5.2 SUCCESSIVE APPROXIMATION MODEL

In general, it is assumed that the *jth* (j = 1, ..., n) modal equation is given by the equation (4.7) in which $\alpha_j(A_j)$, $\beta_j(A_j)$ and $f_j(A_j, u_j)$ need to be determined. It is further assumed that the stiffness restoring force, f_j can be expressed in a form of successive approximation, that is

$$f_j(A_j, u_j) = \sum_{i=1,3,5\ldots}^{\infty} \varpi_{ij}(A_j)\, u_j^i . \qquad \textbf{(5.1a)}$$

It is assumed that the first-order term is much "larger" in magnitude that any other term. That is, the first-order term dominates the stiffness restoring force because the higher-order terms have smaller magnitude and give smaller contribution to the restoring force. Specifically, the order of magnitude of the terms is assumed to be the following:

$$O(\varpi_{1j}) = O(1),\ O(\varpi_{3j}) = O(\epsilon),\ O(\varpi_{5j}) = O(\epsilon^2) \qquad \textbf{(5.1b)}$$

where O(1) represents finite order, ε is a small number and $O(\varepsilon)$ represents that ϖ_{3j} is small compared with ϖ_{1j}, etc.

A modal equation is expressed as

$$\ddot{u}_j + \alpha_j (A_j)\, \dot{u}_j + \sum_{i=1,3,5,\cdots}^{\infty} \varpi_{ij} (A_j)\, u_j^i = -\beta_j (A_j)\, \ddot{z} \qquad (5.2)$$

where $\alpha_j(A_j)$, $\beta_j(A_j)$ and $\varpi_{ij}(A_j)$ need to be determined.

Physically, the model presents a weakly nonlinear system. Representing a nonlinear system by this model, system (5.2) may be called an equivalent weakly nonlinear system. If all $\varpi_{ij}(A_j)$ except ϖ_{1j} (i.e. i = 3, 5, ...) are zero, system (5.2) will be an equivalent linear system. It is clear that ϖ_{1j} is the *jth* equivalent linear natural frequency. Since higher order terms are very small so that their effect on the frequency of the mode can be neglected, ϖ_{1j} is a good approximation of modal frequency. That is

$$\varpi_{1j} (A_j) \approx \omega_j^2 (A_j) \,. \qquad (5.3)$$

In the equation (5.2), the ϖ_{ij}'s are functions of modal amplitude A_j. Using the previous assumption, the ϖ_{ij}'s are assumed to be even functions of A_j and are expressed as truncated polynomials. Let p_i be the truncation order for the function $\varpi_{ij}(A)$. $\varpi_{ij}(A)$ is expressed as

$$\varpi_{ij} (A_j) = \sum_{k=0}^{p_i} \varpi_{ij}^{(k)}\, A_j^{2k} \qquad i = 1,3,5,\cdots \qquad (5.4)$$

where $\varpi_{ij}^{(k)}$ (k = 0, 1, 2, ... , p_i) are constant coefficients.

5.3 "MODAL RESPONSE"

Assume that the response of a nonlinear system **x**(t) has been measured from an experiment or recorded from an actual vibration event (if $\ddot{\mathbf{x}}$(t) is measured, $\dot{\mathbf{x}}$(t) and **x**(t) can be obtained by integration). Based on the earlier discussion (Chapter 3), each

resonance is regarded as a mode and the modal response is given by corresponding resonant response. It is assumed that the resonances of the system are not close to each other and that the *jth* modal response, $\mathbf{x}_j(t)$, can be approximately estimated by band-pass filtering based on the frequency spectrum of the response.

It is assumed that the filtered response $\mathbf{x}_j(t)$ satisfy the modal relation (4.10). The modal coordinates are defined by this equation. Since $\phi_{nj}=1$, modal coordinates are given as: $u_j(t) = x_{nj}(t)$; $\dot{u}_j(t) = \dot{x}_{nj}(t)$; $\ddot{u}_j(t) = \ddot{x}_{nj}(t)$.

5.4 IDENTIFICATION OF MODAL EQUATIONS

A task of modal identification is to determine $\alpha_j(A_j)$, $\beta_j(A_j)$ and $\varpi_{ij}(A_j)$ (i = 1, 3, 5, ...) using the known modal response data. These unknowns all are functions of modal amplitude. With the model of (5.2), these functions can be determined successively. The methodology is outlined below.

1. Linear terms

First of all, linear terms will be determined. By the first-order approximation, the modal equation is

$$\ddot{u}_j + \alpha_j(A_j)\,\dot{u}_j + \varpi_{1j}(A_j)\,u_j = -\beta_j(A_j)\,\ddot{z}. \qquad (5.5)$$

This is an equivalent linear system. $\varpi_{1j}(A_j)$, $\alpha_j(A_j)$ and $\beta_j(A_j)$ are respectively the equivalent linear natural frequency, equivalent linear viscous damping coefficient and equivalent linear participation factor.

In equation (5.5), $\varpi_{1j}(A_j)$, $\alpha_j(A_j)$ and $\beta_j(A_j)$ are amplitude-dependent. They will vary with amplitude during entire vibration event. But they are defined to be constant

over a half-cycle of oscillation. Let t_k and t_{k+1} be the starting and ending times of the *kth* half-cycle of oscillation respectively and $A_j^{(k)}$ be the amplitude of this half-cycle. Over this half-cycle, the equation of motion is

$$\ddot{u}_j(t) + \alpha_j(A_j^{(k)})\,\dot{u}_j(t) + \varpi_{1j}(A_j^{(k)})\,u_j(t) = -\beta_j(A_j^{(k)})\,\ddot{z}(t), \quad t_k \le t \le t_k \tag{5.6}$$

The least-square method is used to determine $\varpi_{1j}(A_j^{(k)})$, $\alpha_j(A_j^{(k)})$ and $\beta_j(A_j^{(k)})$ using the measured data $u_j(t)$, $\dot{u}_j(t)$, $\ddot{u}_j(t)$ and $\ddot{z}(t)$ which belong to the *kth* half-cycle, $t_k \le t \le t_{k+1}$. From the least-square method, the equation for solving these unknowns is

$$\begin{pmatrix} \sum_{r=1}^{n_k} u_r^2 & \sum_{r=1}^{n_k} \dot{u}_r u_r & \sum_{r=1}^{n_k} \ddot{z}_r u_r \\ \sum_{r=1}^{n_k} u_r \dot{u}_r & \sum_{r=1}^{n_k} \dot{u}_r^2 & \sum_{r=1}^{n_k} \ddot{z}_r \dot{u}_r \\ \sum_{r=1}^{n_k} u_r \ddot{z}_r & \sum_{r=1}^{n_k} \dot{u}_r \ddot{z}_r & \sum_{r=1}^{n_k} \ddot{z}_r^2 \end{pmatrix} \begin{pmatrix} \varpi_{1j}(A_j^{(k)}) \\ \alpha_j(A_j^{(k)}) \\ \beta_j(A_j^{(k)}) \end{pmatrix} = \begin{pmatrix} \sum_{r=1}^{n_k} \ddot{u}_r u_r \\ \sum_{r=1}^{n_k} \ddot{u}_r \dot{u}_r \\ \sum_{r=1}^{n_k} \ddot{u}_r \ddot{z}_r \end{pmatrix} \tag{5.7}$$

where n_k is the data sample number over the *kth* half-cycle.

For each half-cycle, $\varpi_{1j}(A_j^{(k)})$, $\alpha_j(A_j^{(k)})$ and $\beta_j(A_j^{(k)})$ are determined by solving the above equation. The set of results (k = 1, ... , q) are used to determine the functions of $\varpi_{1j}(A_j^{(k)})$, $\alpha_j(A_j^{(k)})$ and $\beta_j(A_j^{(k)})$. Using curve fitting, these are approximately expressed as truncated even polynomial series of the form

$$\varpi_{1j}(A_j) = \sum_{k=0}^{p_1} \varpi_{1j}^{(k)} A_j^{2k} \tag{5.8}$$

$$\alpha_j (A_j) = \sum_{k=0}^{p_\alpha} \alpha_j^{(k)} A_j^{2k} \qquad (5.9)$$

$$\beta_j (A_j) = \sum_{k=0}^{p_\beta} \beta_j^{(k)} A_j^{2k} \qquad (5.10)$$

where p_1, p_α, p_β are determined for satisfactory accuracy of the curve-fittings.

2. Cubic Term

After the first-order approximation has been determined, the cubic term will be calculated by employing the model

$$\ddot{u}_j + \alpha_j (A_j)\, \dot{u}_j + \varpi_{1j} (A_j)\, u_j + \varpi_{3j} (A_j)\, u_j^3 = -\beta_j (A_j)\, \ddot{z} \qquad (5.11)$$

where $\varpi_{1j}(A_j)$, $\alpha_j(A_j)$ and $\beta_j(A_j)$ are already known. According to the expression of (5.4), ϖ_{3j} is written in the form

$$\varpi_{3j} (A_j) = \sum_{k=0}^{p_3} \varpi_{3j}^{(k)} A_j^{2k} . \qquad (5.12)$$

ϖ_{3j} is determined by minimizing the displacement error between the prediction by equation (5.11) and the measurement, with respect to all coefficients of the polynomial $\varpi_{3j}(A_j)$, which are $\varpi_{3j}^{(0)}$, $\varpi_{3j}^{(1)}$, ... , $\varpi_{3j}^{(P3)}$. The objective function of the optimization is

$$\epsilon (\varpi_{3j}^{(0)}, \varpi_{3j}^{(1)}, \cdots, \varpi_{3j}^{(p_3)}) = \sum_{i=1}^{s} [u(t_i; \varpi_{3j}^{(0)}, \varpi_{3j}^{(1)}, \cdots, \varpi_{3j}^{(p_3)}) - u_m (t_i)]^2 \qquad (5.13)$$

where *s* is the response sample number, t_i is the *ith* sample time, $u(t_i)$ is the modal displacement at instant t_i given by equation

$$\ddot{u}_j + \alpha_j (A_j)\, \dot{u}_j + \sum_{i=1,3} \sum_{k=0}^{p_3} \varpi_{ij}^{(k)} A_j^{2k} u_j^i = -\beta_j (A_j)\, \ddot{z} \qquad (5.14)$$

and $u_m(t_i)$ is the measured modal displacement at instant t_i.

The optimization process is performed with respect to $\varpi_{3j}^{(0)}, \varpi_{3j}^{(1)}, \ldots, \varpi_{3j}^{(P3)}$. The ranges and step-sizes of $\varpi_{3j}^{(0)}, \varpi_{3j}^{(1)}, \ldots, \varpi_{3j}^{(P3)}$ are specified. The scheme starts with zero initial values (since $O(\varpi_{3j}) = O(\varepsilon)$) and goes forward with the incremental $\varpi_{3j}^{(0)}, \varpi_{3j}^{(1)}, \ldots, \varpi_{3j}^{(P3)}$ until they reach the borders of their range. Response $u(t_i)$ is calculated at each step of $\varpi_{3j}^{(0)}, \varpi_{3j}^{(1)}, \ldots \varpi_{3j}^{(P3)}$ by equation (5.14) in which ϖ_{1j}, $\alpha_j(A_j)$ and $\beta_j(A_j)$ are given in the first stage of identification and $\varpi_{3j}^{(0)}, \varpi_{3j}^{(1)}, \ldots, \varpi_{3j}^{(P3)}$ are updated. The optimal values of $\varpi_{3j}^{(0)}, \varpi_{3j}^{(1)}, \ldots, \varpi_{3j}^{(P3)}$ are determined by taking those values associated with the minimum of ε. The process is formulated as follows

$$\begin{cases} E(\varpi_{3j\,opt}^{(0)}, \varpi_{3j\,opt}^{(1)}, \cdots, \varpi_{3j\,opt}^{(p_3)}) = \mathrm{Min}\, \epsilon(\varpi_{3j}^{(0)}, \varpi_{3j}^{(1)}, \cdots, \varpi_{3j}^{(p_3)}) \\ \\ \text{subjected to equation (5.14).} \end{cases} \qquad (5.15)$$

Final ϖ_{3j} will be given by the result of the optimization, that is

$$\varpi_{3j}(A_j) = \sum_{k=0}^{p_3} \varpi_{3j\,opt}^{(k)} A_j^{2k}. \qquad (5.16)$$

3. Higher-order terms

Assume that the *1st, 3rd, 5th, ..., (h-2)th*-order approximations of stiffness restoring force are known and that the functional coefficient of the *hth*-order term is expressed in the form

$$\varpi_{hj}(A_j) = \sum_{k=0}^{p_h} \varpi_{hj}^{(k)} A_j^{2k} . \qquad (5.17)$$

The *hth*-order approximation can be determined through a similar process performed for cubic term. In summary, the process is presented as follows

$$\epsilon(\varpi_{hj}^{(0)}, \cdots, \varpi_{1j}^{(p_h)}) = \sum_{i=1}^{s} [u(t_i; \varpi_{hj}^{(0)}, \cdots, \varpi_{hj}^{(p_h)}) - u_m(t_i)]^2 \qquad (5.18)$$

$$E(\varpi_{hj\,opt}^{(0)}, \cdots, \varpi_{hj\,opt}^{(p_h)}) = \mathrm{Min}\,\epsilon(\varpi_{hj}^{(0)}, \cdots, \varpi_{hj}^{(p_h)}) \qquad (5.19)$$

subjected to

$$\ddot{u}_j + \alpha_j(A_j)\dot{u}_j + \sum_{i=1,3,5,\cdots}^{h} \sum_{k=0}^{p_i} \varpi_{ij}^{(k)} A_j^{2k} u_j^i = -\beta_j(A_j)\ddot{z} \qquad (5.20)$$

$$\varpi_{hj\,init}^{(0)} = \varpi_{hj\,init}^{(1)} = \cdots = \varpi_{hj\,init}^{(p_h)} = 0 . \qquad (5.21)$$

The determined ϖ_{hj} is

$$\varpi_{hj}(A_j) = \sum_{k=0}^{p_h} \varpi_{hj\,opt}^{(k)} A_j^{2k)} . \qquad (5.22)$$

4. Final modal equation

Performing the above process for each progressively increased *h* (*h* = 3, 5, ...) using the previously determined lower-order approximations each time, until the response prediction by the model (5.2) is satisfactory, the following modal equation can be obtained

$$\ddot{u} + \alpha\,(A_j)\,\dot{u}_j + \sum_{i=1,3,5,\cdots}^{h} \sum_{k=0}^{p_h} \varpi_{hj\,opt}^{(k)} A_j^{2k} u_j^i = -\beta_j\,(A_j)\,\ddot{z}\,. \qquad (5.23)$$

In the above identification procedure, the first-order terms are determined uniquely by the least-square method. Higher-order terms are initially specified by zero initial condition. Therefore, the optimal results of these higher-order terms must be in the neighborhood of the origin.

5.5 IDENTIFICATION OF MODE SHAPE

For linear systems, a modal frequency and damping coefficient are given respectively by the coefficients of displacement and velocity terms of the modal equation. The mode shape can be calculated form the modal participation factors of all the stations since the mode shape is proportional to the vector of the modal participation factors associated with that modal frequency.

For nonlinear systems however, the modal parameters cannot be given directly by the modal equation. In the model (5.2), the damping term is assumed to be linear. Hence, the modal damping coefficient can be directly obtained by the coefficient of the velocity term. The modal frequency is approximately given by the coefficient of the linear term, that is equation (5.3).

If response of all degrees of freedom are available, mode shape can be estimated by definitions (2.6) for the instantaneous mode shape or (3.39) for the amplitude-dependent mode shape respectively. As mentioned previously, the peak mode shape will be used in this thesis. According to the definition (3.47), the mode shape is determined

by the ratios of the peak values of response at each degree of freedom to a reference degree of freedom, *n*. That is,

$$\phi_{ij} = \frac{x_{ij}\,(t_p)}{x_{nj}\,(t_p)}, \quad i=1,\ldots,n. \qquad (5.24)$$

The ϕ_{ij} defined above are also functions of amplitude but are assumed to be constant over a half-cycle. Therefore, $\phi_{ij}(A_j^{(k)})$ is calculated as the ratio of the peak value of displacement at one degree of freedom to the peak displacement at the reference degree of freedom in *kth* half-cycle. By curve-fitting, $\phi_{ij}(A_j)$ is expressed as a truncated even-order polynomial series of the form

$$\phi_{ij}\,(A_j) = \sum_{k=0}^{p_\phi} \phi_{ij}^{(k)}\, A_j^{2k} \qquad i = 1,\cdots,n \qquad (5.25)$$

where $\phi_{ij}^{(k)}$ (k = 0, 1, 2, ..., p_ϕ) are constant coefficients and p_ϕ is in the truncating order.

5.6 VERIFICATION WITH AN IDEAL SYSTEM

As an example, the outlined identification methodology is applied to identify the first mode of the three-degree-of-freedom ideal system which was studied using a constant-coefficient model in the last chapter (section 4.1.1).

The system is lightly damped and excited by a scaled EL Centro earthquake ground motion. The dynamic behavior of the system has been described in Chapter 4. The "first modal response," $x_1(t)$ (or x_{11}, x_{21}, x_{31},) filtered over the band of ***0-2 Hz*** is shown in Figure 4.3a. Setting $\phi_{31} \equiv 1$, the modal coordinate u_1 is approximately given by $u_1(t) = x_{31}(t)$, $\dot{u}_1(t) = \dot{x}_{31}(t)$, $\ddot{u}_1(t) = \ddot{x}_{31}(t)$.

All coefficient polynomials are truncated at fourth order, that is, $p_\alpha = p_\beta = p_1 = p_3 = ... = 4$. The linear terms are determined by the least-square method and curve-fitting. This yields

$$\varpi_{1j}(A_1) = 70.94 - 7.66A_1^2 + 0.95A_1^4 \qquad (5.26)$$

$$\alpha_1(A_1) = 0.07 - 0.10A_1^2 + 0.06A_1^4 \qquad (5.27)$$

$$\beta_1(A_1) = 1.48 + 0.12A_1^2 + 0.02A_1^4 . \qquad (5.28)$$

For the cubic term, process (5.15) is performed. With $p_3 = 4$, the process is a three-dimensional optimization with respect to the $\varpi_{31}^{(0)}$, $\varpi_{31}^{(1)}$ and $\varpi_{31}^{(2)}$. Through this process, the $\varpi_{31}(A_1)$ finally determined to be

$$\varpi_{31}(A_1) = 0.52 + 0.46A_1^2 - 0.08A_1^4 . \qquad (5.29)$$

Further calculation of the fifth-order term ($\varpi_{51}(A_1)$) is also made. However, little improvement of the objective function ε is shown. Therefore, no higher-order terms greater than 5 are needed. The modal equation (5.2) is truncated at the cubic order, that is,

$$\ddot{u}_1 + \alpha_1(A_1)\dot{u}_1 + \varpi_{11}(A_1)u_1 + \varpi_{31}(A_1)u_1^3 = -\beta_1(A_1)\ddot{z} \qquad (5.30)$$

where all coefficients, $\alpha_1(A_1)$, $\beta_1(A_1)$, $\varpi_{11}(A_1)$ and $\varpi_{31}(A_1)$, are given by (5.26-5.29) respectively. The modal displacement predicted from the identified equation is shown in Figure 5.1 and compared with the measured modal response. A satisfactory match between the two can be found. The modal frequency can be approximately estimated by ϖ_{1j}. That is

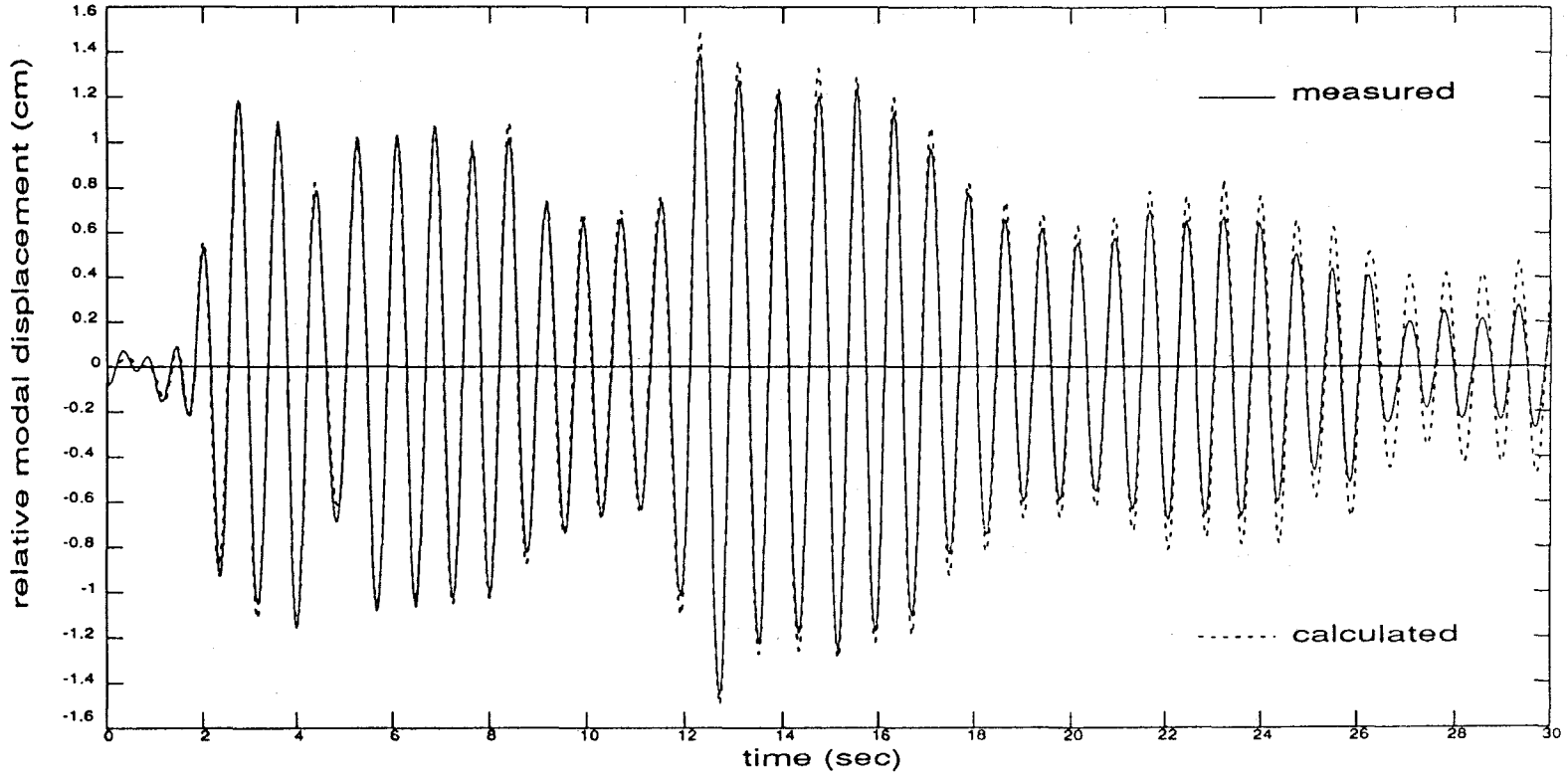

Figure 5.1. Comparison of calculated and measured relative modal displacements. Modal equation is identified by succesive approximation method.

$$\varpi_{1j}(A_1) = \omega_1^2(A_1) \ . \qquad (5.31)$$

The mode shape of the first mode is identified by using response data at other degrees of freedom. The result is

$$\phi_{11}(A_1) = 0.302 + 0.002A_1^2 - 0.009A_1^4 \qquad (5.32a)$$

$$\phi_{21}(A_1) = 0.649 - 0.002A_1^2 - 0.011A_1^4 \ . \qquad (5.32b)$$

The modal equation (5.30) is identified from the loading case associated with the scale of 0.075. In order to test the applicability of the identified modal equation, this equation is used to predict the modal response for a different loading. The same loading case as examined in section 4.1.1 is considered where the El Centro earthquake ground acceleration was scaled by 0.06. The response predicted by the modal equation (5.30) and the response calculated by Newmark-Method and filtering are shown in Figure 5.2. The result shows that the identified modal equation can well predict the modal response of different level.

5.7 SUMMARY

A successive approximation modal equation is proposed and a corresponding identification procedure is presented. The successive approximation model of modal equations is amplitude-dependent so that it will be applicable within a wider vibration range. In the model, the first-order term dominates the restoring force and higher-order terms have only a small contribution. By the identification process, the first-order term

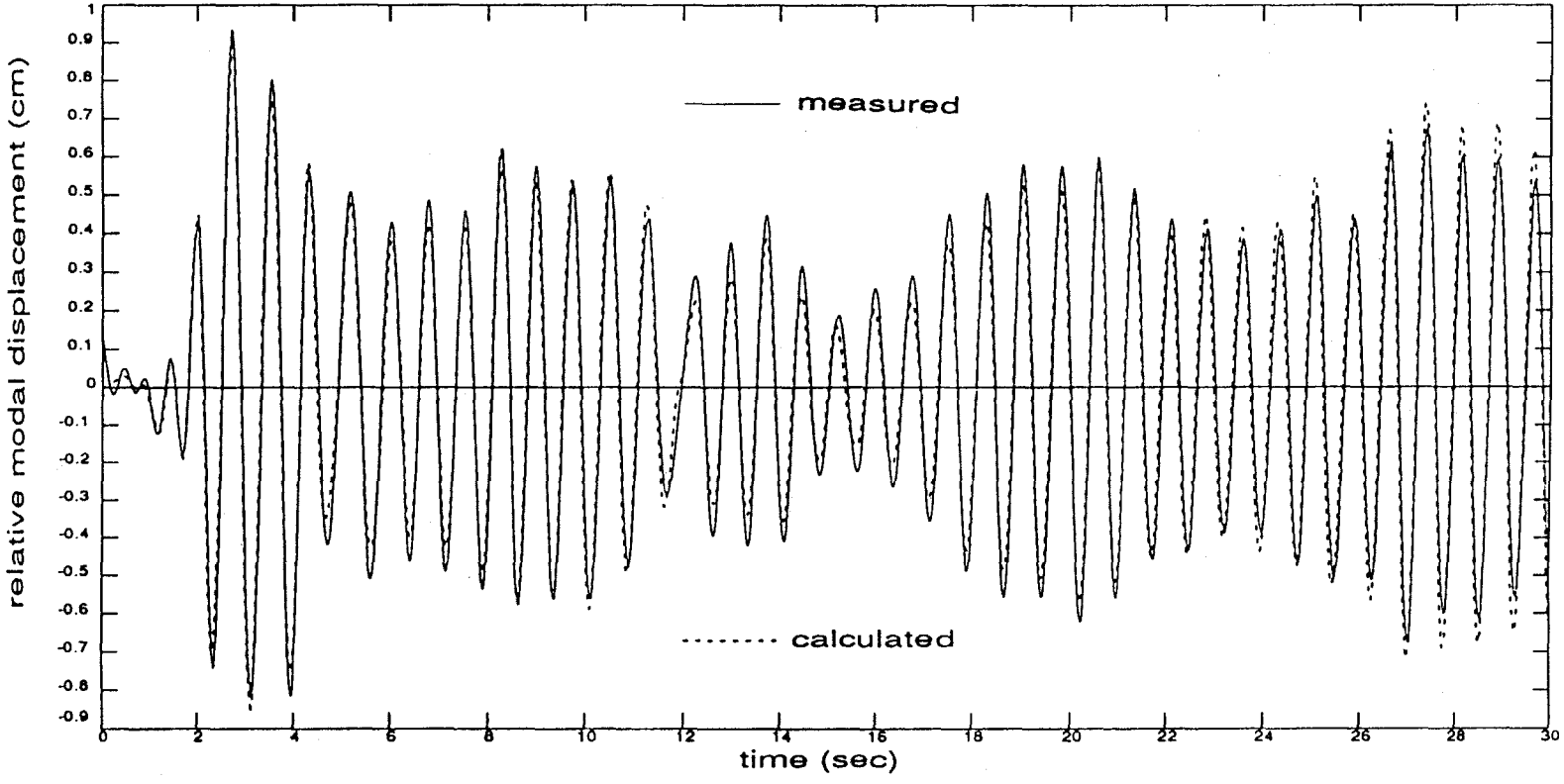

Figure 5.2. Comparison of the predicted and the measured relative modal displacements for a loading of different level.

is determined first and the higher-order terms are determined successively. Hence, the higher-order terms play a role of adjustment to the lower-order approximation in a small quantity. For approximation, only a few low-order terms are needed. So it can be expected that the successive approximation model is of low order.

CHAPTER 6

MODAL IDENTIFICATION USING SIMPLIFIED EXPANSION MODEL

6.1 SIMPLIFIED EXPANSION MODEL

The successive approximation approach is based on an asymptotic approximation of the modal restoring force. There is another approach which is based on a different approximate solution of the modal restoring force. As mentioned in chapter 4, the modal restoring force can be expanded in a Taylor polynomial series. As already pointed out, the model of the equation (4.9) obtained from direct expansion is not suited for unique identification since all coefficients to be determined are functions of amplitude and little is known regarding the properties of these functions. Numerically, these functions cannot be uniquely determined using the limited information obtained from data. For unique identification, the model will be modified below.

Consider equation (4.9). For approximation, the polynomial is truncated. Assume that h is the truncated order and that it is an odd number. It is determined based on the required accuracy of the analysis. Then the modal equation is

$$\ddot{u}_j + \alpha_j (A_j)\, \dot{u}_j + \kappa_{1j} (A_j)\, u_j + \kappa_{3j} (A_j)\, u_j^3 + \cdots + \kappa_{(h-2)j} (A_j)\, u_j^{(h-2)} + \kappa_{hj} (A_j)\, u_j^h$$

$$= -\beta_j (A)\, \ddot{z} \,. \tag{6.1}$$

The modification of the model is based on the simplification of the modal restoring force polynomial. The basic idea of the model simplification is leaving one coefficient amplitude-dependent and having the others to be constant so that the new model is amplitude-dependent and also simple for identification.

First, consider $\kappa_{1\,j}$, the coefficient of the term u_j. Let $\overline{\kappa}_{1\,j} \equiv \kappa_{1\,j}(0)$. This is an extreme case that $A_j = 0$. $\overline{\kappa}_{1\,j}$ will be constant. Split the coefficient into two parts - one amplitude-independent and the other amplitude-dependent - by writing $\kappa_{1\,j}(A_j)$ as

$$\kappa_{1j} (A_j) = \overline{\kappa}_{1j} + (\kappa_{1j} (A_j) - \overline{\kappa}_{1j}) = \overline{\kappa}_{1j} + \Delta\kappa_{1j} (A_j) \,. \tag{6.2a}$$

Similarly, let $\overline{\kappa}_{3\,j} \equiv \kappa_{3\,j}(0)$, $\cdots$, $\overline{\kappa}_{h\,j} \equiv \kappa_{h\,j}(0)$. Coefficients, $\kappa_{3\,j}(A_j)$, $\cdots$, $\kappa_{h\,j}(A_j)$, can be written as

$$\kappa_{3j} (A_j) = \overline{\kappa}_{3j} + \Delta\kappa_{3j} (A_j)$$

$$\cdots\cdots \tag{6.2b}$$

$$\kappa_{hj} (A_j) = \overline{\kappa}_{hj} + \Delta\kappa_{hj} (A_j) \,.$$

Then equation (6.1) becomes

$$\ddot{u}_j + \alpha_j (A_j)\, \dot{u}_j + \overline{\kappa}_{1j} u_j + \Delta\kappa (A_j)\, u_j + \overline{\kappa}_{3j} u_j^3 + \Delta\kappa_{3j} (A_j)\, u_j^3 + \cdots$$

$$+ \overline{\kappa}_{hj} u_j^h + \Delta\kappa_{hj} (A_j)\, u_j^h = -\beta_j (A_j)\, \ddot{z} \,. \tag{6.3}$$

The equation can be written as

$$\ddot{u}_j + \alpha_j (A_j)\, \dot{u}_j + \overline{\kappa}_{1j} u_j + \overline{\kappa}_{3j} u_j^3 + \cdots + \overline{\kappa}_{hj} u_j^h + \Delta\kappa_{1j} (A_j)\, u_j + \Delta\kappa_{3j} (A_j)\, u_j^3 + \cdots + \Delta\kappa_{hj} (A_j)\, u_j^h = -\beta_j (A_j)\, \ddot{z} . \tag{6.4}$$

In equation (6.4) the stiffness restoring force consists of two polynomials: the first one has constant coefficients and the second one has amplitude-dependent coefficients. According to the idea of simplification, the amplitude-dependent portion is to be merged into one term. There are multiple choices for selecting the remaining term. For example, a linear term, a highest-order term or any one term with an order between the linear and highest orders may be kept. Later on, in presenting identification procedure, it can be shown that only keeping the highest-order term will lead to a unique determination of the coefficient. Hence, equation (6.4) is written as

$$\ddot{u}_j + \alpha_j (A_j)\, \dot{u}_j + \overline{\kappa}_{1j} u_j + \overline{\kappa}_{3j} u_j^3 + \cdots + \overline{\kappa}_{hj} u_j^h + \left[\frac{\Delta\kappa_{1j} (A_j)}{u_j^{h-1}} + \frac{\Delta\kappa_{3j} (A_j)}{u_j^{h-3}} + \cdots + \frac{\Delta\kappa_{(h-2)j} (A_j)}{u_j^2} + \Delta\kappa_{hj} (A_j) \right] u_j^h = -\beta_j (A_j)\, \ddot{z} . \tag{6.5}$$

Define $\tilde{\kappa}_{hj}(A_j)$ to be an "equivalent" amplitude-dependent quantity such that it makes the equation

$$\ddot{u}_j + \alpha_j (A_j)\, \dot{u}_j + \overline{\kappa}_{1j} u_j + \overline{\kappa}_{3j} u_j^3 + \cdots + \overline{\kappa}_{hj} u_j^h + \tilde{\kappa}_{hj} (A_j)\, u_j^h = -\beta_j (A_j)\, \ddot{z} \tag{6.6}$$

"best" fit the solution of $\ddot{u}_j$, $\dot{u}_j$, u_j given by the equation (6.5).

Equation (6.1) is the Taylor expansion of modal stiffness restoring force. Equation (6.6) is a simplified version of equation (6.1). So it is named the simplified expansion model. Instead of having all coefficients of the stiffness terms be amplitude-dependent

in (6.1), only one term is amplitude-dependent and the others are amplitude-independent in (6.6).

As an example, the equation for a cubic system becomes

$$\ddot{u}_j + \alpha_j (A_j)\, \dot{u}_j + \overline{\kappa}_{1j} u_j + \overline{\kappa}_{3j} u_j^3 + \tilde{\kappa}_{3j} (A_j)\, u_j^3 = -\beta_j (A_j)\, \ddot{z} . \qquad (6.8)$$

Similarly, the equation for a fifth-order system becomes

$$\ddot{u}_j + \alpha_j (A_j)\, \dot{u}_j + \overline{\kappa}_{1j} u_j + \overline{\kappa}_{3j} u_j^3 + \overline{\kappa}_{5j} u_j^5 + \tilde{\kappa}_{5j} (A_j)\, u_j^5 = -\beta_j (A_j)\, \ddot{z} \qquad (6.9)$$

Comparing equations (6.1) and (6.6), it can be seen that the constants in (6.6) are equal to the values of amplitude-dependent coefficients in (6.1) with $A_j = 0$. Therefore, these constants can be obtained by setting $A_j = 0$ in equation (6.1). Physically, it may be regarded as a linear vibration case (small amplitude vibration) of nonlinear system. When the vibration amplitude of a nonlinear system is sufficiently small (A_j approaches to zero), dynamic behavior of the system will be linear and linear theory can be applied.

If ϕ_j is the *jth* linear mode shape vector normalized with respect to **M**, i.e. $\phi_j^T \mathbf{M} \phi_j = 1$, a modal equation of motion can be obtained as

$$\boldsymbol{\phi}_j^T \mathbf{M} \boldsymbol{\phi}_j \ddot{u}_j + \boldsymbol{\phi}_j^T \mathbf{C} \boldsymbol{\phi}_j \dot{u}_j + \boldsymbol{\phi}_j^T \mathbf{K} \boldsymbol{\phi}_j u_j + \boldsymbol{\phi}_j^T \mathbf{f} (\boldsymbol{\phi}_j u_j) = -\boldsymbol{\phi}_j^T \mathbf{M} \mathbf{I} \ddot{z} . \qquad (6.10)$$

Expanded in an odd polynomial of u_j, this nonlinear equation becomes

$$\ddot{u}_j + \overline{\alpha}_j \dot{u}_j + \overline{\kappa}_{1j} u_j + \overline{\kappa}_{3j} u_j^3 + \cdots + \overline{\kappa}_{(h-2)j} u_j^{(h-2)} + \overline{\kappa}_{hj} u_j^h = -\overline{\beta}_j \ddot{z} \qquad (6.11)$$

where $\overline{\alpha}_j = \alpha_j(0)$ and $\overline{\beta}_j = \beta_j(0)$. That is, all constants in (6.6) are the coefficients of (6.11) which are obtained through the transformation using the linear mode shape. Since the linear mode shape is constant, the coefficients are amplitude-independent. For a linear

vibration, the coefficient of linear stiffness term is equal to the squared natural frequency. So $\bar{\kappa}_{1j}$ gives the *jth* linear squared natural frequency of the system.

6.2 IDENTIFICATION PROCEDURE

Use of the model (6.6) for identification requires the determination of the truncating order *h* first. For this purpose, the identification procedure is performed in two stages.

In the *first stage*, equivalent modal frequency of the mode is evaluated from the data by employing an equivalent linear model. The purpose of this work is to identify overall properties of a mode and to obtain necessary information for estimation of the parameters since the modal frequencies can represent the properties of system stiffness. The corresponding equation is

$$\ddot{u}_j + \alpha_j (A_j)\, \dot{u}_j + \omega_j^2 (A_j)\, u_j = -\beta_j (A_j)\, \ddot{z} \qquad (6.12)$$

where $\omega_j(A_j)$, $\alpha_j(A_j)$ and $\beta_j(A_j)$ are respectively the equivalent linear natural frequency, equivalent linear viscous damping coefficient and equivalent linear participation factor. The equation is the same as (5.5). They are determined in the same way as the successive approximation method does.

From the resulting curve of $\omega_j^2(A_j)$, the properties of the *jth* modal stiffness can be observed since the behavior of $\omega_j^2(A_j)$ physically represents the nonlinear property of the mode. This information can be used to roughly estimate the order of the modal equation since the function of $\omega_j^2(A_j)$ and the order of modal equation have the following approximate relation.

Consider the *jth* undamped free mode of vibration. Assuming that the truncation order of the modal equation is h (an odd number), the equation is

$$\ddot{u}_j + \bar{\kappa}_{1j} u_j + \bar{\kappa}_{3j} u_j^3 + \bar{\kappa}_{5j} u_j^5 + \cdots + \bar{\kappa}_{(h-2)j} u_j^{h-2} + \bar{\kappa}_{hj} u_j^h + \tilde{\kappa}_{hj}(A_j)\, u_j^h = 0 \quad \textbf{(6.13)}$$

The *jth* modal frequency, $\omega_j^2(A_j)$, can be approximately evaluated by applying Galerkin's method. Then, it may be shown that

$$\omega_j^2(A_j) = \bar{\kappa}_{1j} + \frac{3}{4}\bar{\kappa}_{3j} A_j^2 + \frac{5}{8}\bar{\kappa}_{5j} A_j^4 + \cdots + \frac{(h-1)!}{2^{h-2}\left[\left(\frac{h-1}{2}\right)!\right]^2}\bar{\kappa}_{(h-2)j} A_j^{h-3}$$

$$+ \frac{(h+1)!}{2^h\left[\left(\frac{h+1}{2}\right)!\right]^2}\bar{\kappa}_{hj} A_j^{h-1} + \frac{(h+1)!}{2^h\left[\left(\frac{h+1}{2}\right)!\right]^2}\tilde{\kappa}_{hj}(A_j) A_j^{h-1}. \quad \textbf{(6.14)}$$

From (6.14), it can be seen that the order of $\omega_j^2(A_j)$ is determined by the highest order of last term which is equal to the sum of truncating order of $\tilde{\kappa}_{hj}(A_j)$ and h-1. If the orders of $\omega_j^2(A_j)$ and $\tilde{\kappa}_{hj}(A_j)$ are $2p_\omega$ and $2p_h$ respectively, $2p_\omega = 2p_h + h - 1$. In practice, $\tilde{\kappa}_{hj}(A_j)$ will be truncated at lower order. Therefore, the order of $\omega_j^2(A_j)$ is approximately equal to h-1 but it should be satisfied that $h\text{-}1 \le 2p_\omega$. Since the truncating order of $\omega_j^2(A_j)$ can be determined by a satisfactory curve-fitting with the result of $\omega_j^2(A_j)$, h can be approximately estimated based on the p_ω by temporarily ignoring $\tilde{\kappa}_{hj}(A_j)$ with the condition that $h\text{-}1 \le 2p_\omega$.

At this point, only $\alpha_j(A_j)$, $\beta_j(A_j)$ and the truncating order h of equation (6.6) have been determined. In the *second stage* of the identification, $\bar{\kappa}_{hj}$, ···, $\bar{\kappa}_{hj}$, $\tilde{\kappa}_{hj}(A_j)$ are to be determined. Since $\omega_j^2(A_j)$ is assumed to be an even polynomial function of A_j, it can be seen from (6.14) that $\tilde{\kappa}_{hj}(A_j)$ should also be an even polynomial function since h-1 is an

even number. Assume that $\tilde{\kappa}_{hj}(A_j)$ is truncated at $2p_h$.

$$\tilde{\kappa}_{hj}(A_j) = \sum_{i=1}^{p_h} \tilde{\kappa}_{hj}^{(i)} A_j^{2i}, \qquad (6.15)$$

where $\tilde{\kappa}_{hj}^{(i)}$ ($i = 1, 2, \ldots, p_h$) are constants. By substitution of (6.15), equation (6.14) becomes

$$\omega_j^2(A_j) = \bar{\kappa}_{1j} + \frac{3}{4}\bar{\kappa}_{3j} A_j^2 + \frac{5}{8}\bar{\kappa}_{5j} A_j^4 + \cdots + \frac{(h-1)!}{2^{h-2}[(\frac{h-1}{2})!]^2} \bar{\kappa}_{(h-2)j} A_j^{h-3}$$
$$+ \frac{(h+1)!}{2^h[(\frac{h+1}{2})!]^2} \bar{\kappa}_{hj} A_j^{h-1} + \frac{(h+1)!}{2^h[(\frac{h+1}{2})!]^2} \sum_{i=1}^{p_h} \tilde{\kappa}_{hj}^{(i)} A_j^{2i+h-1}. \qquad (6.16)$$

On the left side of the equation, $\omega_j^2(A_j)$ is already known from the identification of the first stage. It is expressed in the truncated polynomial as

$$\omega_j^2(A_j) = \sum_{i=0}^{p_\omega} \Omega_j^{(i)} A_j^{2i}, \qquad (6.17)$$

where $\Omega_j^{(i)}$ ($i = 0, 1, 2, \ldots, p_\omega$) are constants which are determined by curve fitting of identified values of $\omega_j^2(A_j)$. So, the equation (6.16) becomes

$$\sum_{i=0}^{p_\omega} \Omega_j^{(i)} A_j^{2i} = \bar{\kappa}_{hj} + \frac{3}{4}\bar{\kappa}_{3j} A_j^2 + \frac{5}{8}\bar{\kappa}_{5j} A_j^4 + \cdots + \frac{(h-1)!}{2^{h-2}[(\frac{h-1}{2})!]^2} \bar{\kappa}_{(h-2)j} A_j^{h-3}$$
$$+ \frac{(h+1)!}{2^h[(\frac{h+1}{2})!]^2} \bar{\kappa}_{hj} A_j^{h-1} + \frac{(h+1)!}{2^h[(\frac{h+1}{2})!]^2} \sum_{i=1}^{p_h} \tilde{\kappa}_{hj}^{(i)} A_j^{2i+h-1}. \qquad (6.18)$$

Equating like coefficients on both sides of equation, the following equations are obtained as

$$
\begin{aligned}
A^0 \quad &: \quad \bar{\kappa}_{1j} = \Omega_j^{(0)} \\
A^2 \quad &: \quad \bar{\kappa}_{3j} = \frac{4}{3}\Omega_j^{(1)} \\
A^4 \quad &: \quad \bar{\kappa}_{5j} = \frac{8}{5}\Omega_j^{(2)} \\
&\cdots\cdots \\
A^{h-3} \quad &: \quad \bar{\kappa}_{(h-2)j} = \frac{2^{1-2}[9\frac{h-1}{2})!]^2}{(1-1)!}\Omega_j^{(\frac{h-3}{2})} \\
A^{h-1} \quad &: \quad \bar{\kappa}_{hj} = \frac{2^h[(\frac{h+1}{2})!]^2}{(h+1)!}\Omega_j^{(\frac{h-1}{2})} \\
A^{h+1} \quad &: \quad \tilde{\kappa}_{hj}^{(1)} = \frac{2_h[(\frac{h+1}{2})!]^2}{(h+1)!}\Omega_j^{(\frac{h+1}{2})} \\
&\cdots\cdots \\
A^{2p_\omega} \quad &: \quad \tilde{\kappa}_{hj}^{(p_\omega-\frac{h-1}{2})} = \frac{2^h[(\frac{h+1}{2})!]^2}{(h+1)!}\Omega_j^{(p_\omega)}
\end{aligned}
\qquad \textbf{(6.19a)}
$$

If p_h has been chosen such that $p_h = p_\omega - (h-1)/2$, all constants, $\bar{\kappa}_{1j}$, ···, $\bar{\kappa}_{hj}$, and coefficients of $\tilde{\kappa}_{hj}(A_j)$ are given by these equations. If p_h is chosen such that it is greater than $p_\omega - (h-1)/2$, the coefficients of higher order terms of $\tilde{\kappa}_{hj}(A_j)$ are taken to be zero, that is

$$
\tilde{\kappa}_{hj}^{(p_\omega-\frac{h-3}{2})} = \tilde{\kappa}_{hj}^{(p_\omega-\frac{h-5}{2})} = \cdots = \tilde{\kappa}_{hj}^{(p_h)} = 0 . \qquad \textbf{(6.19b)}
$$

Thus, the remaining coefficients of modal equation (6.6) are completely given by (6.19).

Since the $\omega_j^2(A_j)$ is uniquely determined, all unknowns on the left-hand side of equations (6.19) are uniquely determined.

It can be seen that there is only one unknown (on the left-hand side) in each equation of (6.19). The items on the right-hand side of the equations are known from the first identification stage. Therefore, all unknowns can be determined uniquely.

Now, returning to the earlier discussion of the selection of the remaining amplitude-dependent term. As in the above process, each selection of the remaining amplitude-dependent term will result in a similar set of equations like (6.19). However, it can be shown that each other selection will lead to two unknowns on the left-hand side in some of equations of (6.19). For the choice of the remaining linear term, all resulting equations, the counterparts of (6.19), will have two unknowns on the left-hand side. So, the unknowns cannot be determined uniquely.

According to the previous discussion, $\bar{\kappa}_{1j}$ is the square of the *jth* linear natural frequency of the system. It is given by the value of constant term in (6.16) or the limit value of $\omega_j^2(A_j)$ as A_j approaches zero. That is

$$\bar{\kappa}_{1j} = \Omega_j^{(0)} = \omega_j^2(0) . \qquad (6.20)$$

Generally, the linear natural frequency estimated in this way is satisfactory.

In order to increase the accuracy of the model, the initial estimation of equivalent coefficient $\tilde{\kappa}_{hj}(A_j)$ given by (6.19) is further modified by a p_h-dimensional optimization process. The objective function of the optimization is

$$\epsilon(\tilde{\kappa}_{hj}^{(1)}, \cdots, \tilde{\kappa}_{hj}^{(p_h)}) = \sum_{i=1}^{s} [u(t_i; \tilde{\kappa}_{hj}^{(1)}, \cdots, \tilde{\kappa}_{hj}^{(p_h)}) - u_m(t_i)]^2 \quad \textbf{(6.21a)}$$

where s is the response sample number, t_i is the *ith* sample time, $u(t_i, \tilde{\kappa}_{hj}^{(1)}, \cdots, \tilde{\kappa}_{hj}^{(Ph)})$ is the modal displacement at instant t_i given by equation

$$\ddot{u}_j + \alpha_j(A_j)\dot{u}_j + \overline{\kappa}_{1j}u_j + \overline{\kappa}_{3j}u_j^3 + \cdots + \overline{\kappa}_{hj}u_j^h + \sum_{i=1}^{p_h} \tilde{\kappa}_{hj}^{(i)} A_j^{2i} u_j^h = -\beta_j(A_j)\ddot{z} \quad \textbf{(6.22)}$$

and $u_m(t_i)$ is the measured modal displacement at instant t_i.

The optimization process is performed with respect to $\tilde{\kappa}_{hj}^{(1)}, \cdots, \tilde{\kappa}_{hj}^{(Ph)}$. The ranges and step-sizes of $\tilde{\kappa}_{hj}^{(1)}, \cdots, \tilde{\kappa}_{hj}^{(Ph)}$ are specified. The scheme starts with the initial values given by (6.19) and goes forward with the incremental $\tilde{\kappa}_{hj}^{(1)}, \cdots, \tilde{\kappa}_{hj}^{(Ph)}$ until they reach the borders of their ranges. The response $u_j(t)$ is calculated at each step of $\tilde{\kappa}_{hj}^{(1)}, \cdots, \tilde{\kappa}_{hj}^{(Ph)}$ by equation (6.22) where $\alpha_j(A_j)$, $\beta_j(A_j)$, $\overline{\kappa}_{hj}, \cdots, \overline{\kappa}_{hj}$ are given in the first stage of identification and the optimal $\tilde{\kappa}_{hj}^{(1)}, \cdots, \tilde{\kappa}_{hj}^{(Ph)}$ are determined by taking those values associated with the minimum of ϵ. The process is formulated as follows

$$\begin{cases} E(\tilde{\kappa}_{hj\,opt}^{(1)}, \cdots, \tilde{\kappa}_{hj\,opt}^{(p_h)}) = \text{Min}\,\epsilon(\tilde{\kappa}_{hj}^{(1)}, \cdots, \tilde{\kappa}_{hj}^{(p_h)}) \\ \\ \text{subjected to equation (6.22)} . \end{cases} \quad \textbf{(6.23a)}$$

Finally, the identified modal equation is given by

$$\ddot{u}_j + \alpha_j(A_j)\dot{u}_j + \overline{\kappa}_{1j}u_j + \overline{\kappa}_{3j}u_j^3 + \cdots + \overline{\kappa}_{hj}u_j^h + \sum_{i=1}^{p_h} \tilde{\kappa}_{hj\,opt}^{(i)} A_j^{2i} u_j^h = -\beta_j(A_j)\ddot{z} \quad \textbf{(6.24)}$$

If the accuracy of the model is still unsatisfactory, more coefficients of higher-order terms

should be modified to improve the accuracy of the equation. For an example, $\bar{\kappa}_{hj}$ is involved in optimization

$$\epsilon(\bar{\kappa}_{hj}, \tilde{\kappa}_{hj}^{(1)}, \cdots, \tilde{\kappa}_{hj}^{(p_h)}) = \sum_{i=1}^{s} [u(t; \bar{\kappa}_{hj}, \tilde{\kappa}_{hj}^{(1)}, \cdots, \tilde{\kappa}_{hj}^{(p_h)}) - u_m(t_i)]^2 \qquad \textbf{(6.21b)}$$

$$E(\bar{\kappa}_{hjopt}, \tilde{\kappa}_{hjopt}^{(1)}, \cdots, \tilde{\kappa}_{hjopt}^{(p_n)}) = \text{Min}\epsilon(\bar{\kappa}_{hj}, \tilde{\kappa}_{hj}^{(1)}, \cdots, \tilde{\kappa}_{hj}^{(p_h)}) \qquad \textbf{(6.23b)}$$

subjected to equation (6.22).

6.3 VERIFICATION WITH AN IDEAL SYSTEM

This identification procedure is also applied to identify the first mode of the same 3DOF ideal system same as examined in the last chapter.

In the first stage of identification, the functions of $\omega_1^2(A_1)$, $\alpha_1(A_1)$ and $\beta_1(A_1)$ are identified using the modal response data. In that process, p_ω is selected to be 2 for a satisfactory curve-fitting of $\omega_1^2(A_1)$, that is, the polynomial of $\omega_1^2(A_1)$ is truncated at fourth order. h is chosen as $h = 3$. So, the model of the modal equation is (6.8). The polynomials of $\alpha_1(A_1)$ and $\beta_1(A_1)$ are also truncated at fourth order, i.e. $p_\alpha = p_\beta = 2$. These functions are identified by the least-square method and curve-fitting as before in the first stage of successive approximation method. The results, which are the same as equations (5.25-27), are listed below

$$\omega_1^2(A_1) = 70.94 - 7.66A_1^2 + 0.95A_1^4 \qquad (6.25)$$

$$\alpha_1(A_1) = 0.07 - 0.10A_1^2 + 0.06A_1^4 \qquad (6.26)$$

$$\beta_1(A_1) = 1.48 + 0.12A_1^2 + 0.02A_1^4 . \qquad (6.27)$$

According to the previous discussion, the coefficients $\bar{\kappa}_{11}$ and $\bar{\kappa}_{31}$ of the modal equation are determined by (6.19) as

$$\bar{\kappa}_{11} = \Omega_1^{(0)} = 70.9 \qquad (6.28)$$

$$\bar{\kappa}_{31} = \Omega_1^{(1)} = -7.66 \qquad (6.29)$$

$\bar{\kappa}_{11}$ is equal to the corresponding linear squared natural frequency. The coefficient, $\tilde{\kappa}_{31}$, is a function of A_1. It is expressed as

$$\tilde{\kappa}_{31}(A_1) = \sum_{i=1}^{p_h} \tilde{\kappa}_{31}^{(i)} A_1^{2i} . \qquad (6.30)$$

According to (6.19), the coefficients of this polynomial are initially given by

$$\tilde{\kappa}_{31\,init}^{(1)} = \frac{4}{3}\Omega_1^{(2)}, \quad \tilde{\kappa}_{31\,init}^{(2)} = \frac{4}{3}\Omega_1^{(3)}, \ \cdots, \ \tilde{\kappa}_{31\,init}^{(p_h)} = \frac{4}{3}\Omega_1^{(p_h+1)} . \qquad (6.31)$$

This polynomial is truncated at fourth order, i.e., $p_h = 2$. Equations (6.31) provide an initial estimation of the coefficients of $\tilde{\kappa}_{31}(A_1)$. They are further modified by the following three-dimensional optimization with respect to the $\tilde{\kappa}_{31}^{(1)}$ and $\tilde{\kappa}_{31}^{(2)}$

$$\epsilon(\tilde{\kappa}_{31}^{(1)}, \tilde{\kappa}_{31}^{(2)}) = \sum_{i=1}^{s} [u_1(t_i; \tilde{\kappa}_{31}^{(1)}, \tilde{\kappa}_{31}^{(2)}) - u_{m1}(t_i)]^2 \tag{6.32}$$

$$E(\tilde{\kappa}_{31opt}^{(1)}, \tilde{\kappa}_{31opt}^{(2)}) = \text{Min}\, \epsilon(\tilde{\kappa}_{31}^{(1)}, \tilde{\kappa}_{31}^{(2)}) \tag{6.33}$$

subjected to

$$\ddot{u}_1 + \alpha_1(A_1)\dot{u}_1 + \bar{\kappa}_{11}u_1 + \bar{\kappa}_{31}u_1^3 + \sum_{i=1}^{2} \tilde{\kappa}_{31}^{(i)} A_1^{2i} u_1^3 = -\beta_1(A_1)\ddot{z} \tag{6.34}$$

where s is the response sample number, t_i is the *ith* sample time, $u_1(t_i)$ is the modal displacement at instant t_i predicted by equation (6.34) with the known $\alpha_1(A_1)$, $\beta_1(A_1)$, $\bar{\kappa}_{11}$ and $\bar{\kappa}_{31}$ (6.26-29), and $u_{m1}(t_i)$ is the measured modal displacement at instant t_i.

Through the above process, the optimally determined $\tilde{\kappa}_{31}(A_1)$ is

$$\tilde{\kappa}_{31}(A_1) = 2.95A_1^2 - 2.70A_1^4. \tag{6.35}$$

The modal displacement predicted from the identified model, the equation (6.34) with the coefficients given by (6.26-29) and (6.35), is shown in Figure 6.1 and compared with the modal response. A satisfactory match between the two is found.

This equation is applied to predict modal response of the system to the El Centro earthquake ground acceleration data scaled by 0.06. The predicted modal response and the simulated modal response are shown in Figure 6.2. The result shows that the identified modal equation obtained from special response level can well predict the modal response of different level. Such a model is useful in a wide range of loading.

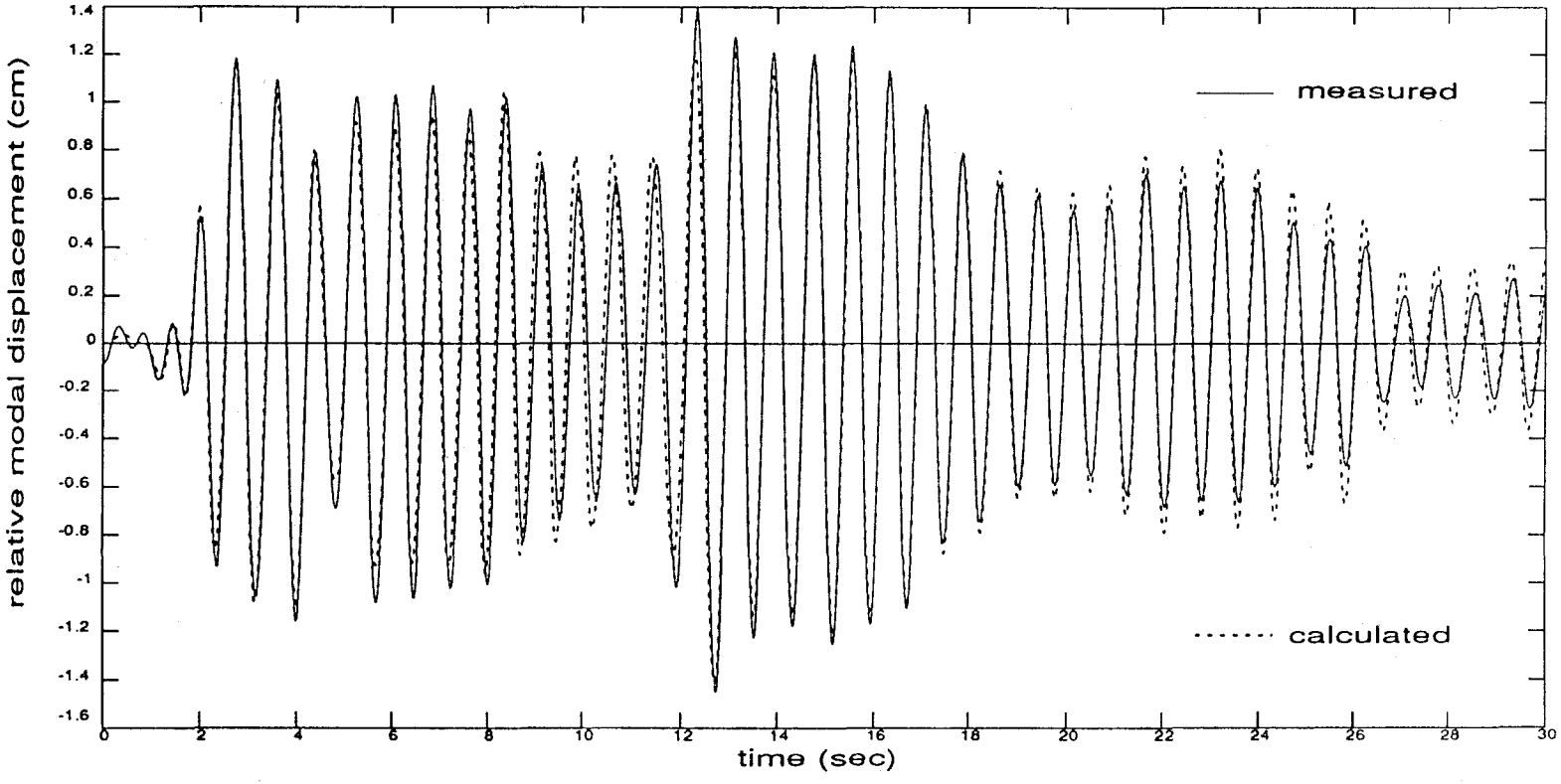

Figure 6.1. Comparison of calculated and measured relative modal displacements. Modal equation is identified by simplified model method.

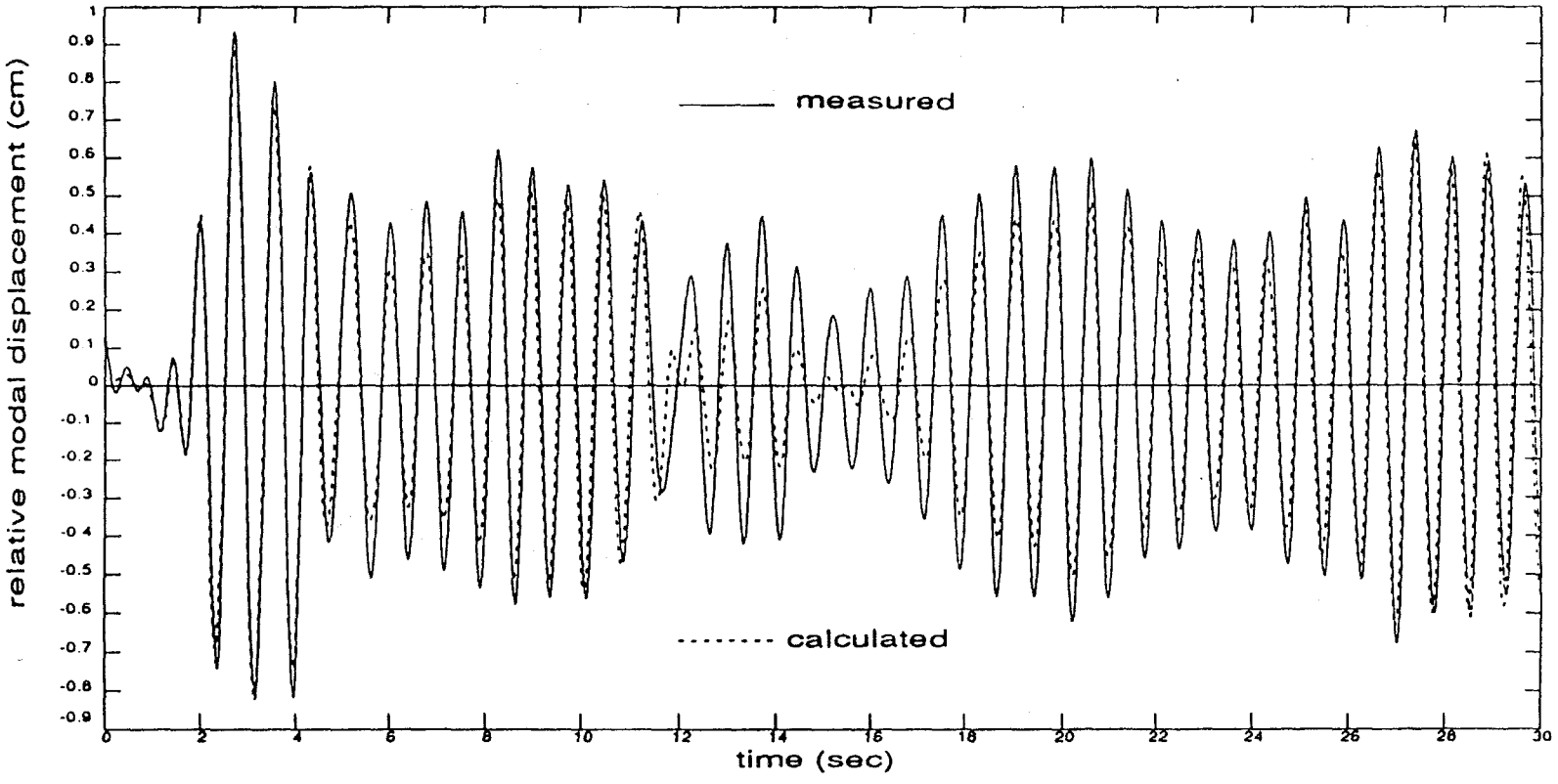

Figure 6.2. Comparison of the predicted and the measured relative modal displacements for a loading of different level.

6.4 SUMMARY

The amplitude-dependent modal equations based on the Taylor expansion is simplified for identification and a parameter estimation methodology is presented. Application of the identification procedure to a verification example gives accurate modal parameters and the response prediction from the identified modal equation gives satisfactory results for different vibration levels. It shows that the approach is feasible and that the model and identification procedure are effective and useful. In the next chapter, the proposed model and identification approach will be used in the analysis of two real structures subjected to earthquake excitation.

CHAPTER 7

APPLICATION TO TWO BUILDINGS

It has been pointed out that the modal analysis approach can be used in the approximate analysis of resonance-dominant vibrations of nonlinear systems. As is well known, mode-like characteristics can be observed in the earthquake response of many structures and the response is often dominated by a few lower modes. In such cases, the modal approach is an effective and convenient tool for describing the system.

In this chapter, modal identification is performed on two buildings whose seismic response data recorded during the 1989 Loma Prieta earthquake are used to determine the major modal parameters and modal equations of the systems, using the methods presented in last two chapters. In the analysis, all the assumptions regarding the models used for the ideal elastic nonlinear systems will be employed for approximation even though the real structures differ from the ideal systems.

The two buildings investigated are a forty-seven-story office building located in San Francisco and a four-story commercial building in Watsonville respectively. Both buildings were subjected to the Loma Prieta earthquake in 1989. The response data were obtained by the California Department of Mines and Geology [67].

7.1 FOUR-STORY BUILDING (E-W Direction)

7.1.1 Building Description and Measurement

The first structure investigated is a 4-story commercial building. It is located at 340 Rodriguez Street in the city of Watsonville, California. It was constructed in 1948 with a total of three stories. The fourth story was added in 1955. It houses equipment for telephone communications operations.

The building is approximately 70 feet by 74 feet in plan, and about 66 feet high. It is supported by spread footings or partial base mats. The building carries vertical load by composite concrete/steel beams, girders and columns, and concrete slabs. Lateral loads are resisted primarily by the reinforced concrete shear walls. Plan views of the ground floor, third floor and roof, which identify structural walls and columns, are shown in Figure 7.1.

Thirteen accelerometers were installed at the basement, third floor and roof levels of the building. The locations of the accelerometers installed are shown in Figure 7.1. The instrumentation is able to record seismic responses in all three directions and allows calculation of torsional response.

The epicenter of Loma Prieta earthquake was approximately 18 km to the northwest of the building site. The building experienced significant shaking during this earthquake. The acceleration time histories recorded at the roof and basement in the E-W direction are shown in Figure 7.2. The roof peak acceleration in this direction is *1.24g*.

This structure was thoroughly investigated by P. Hashimoto, J. Beck *et al.*[79] by performing elastic analysis and modal identification in which the equivalent linear model

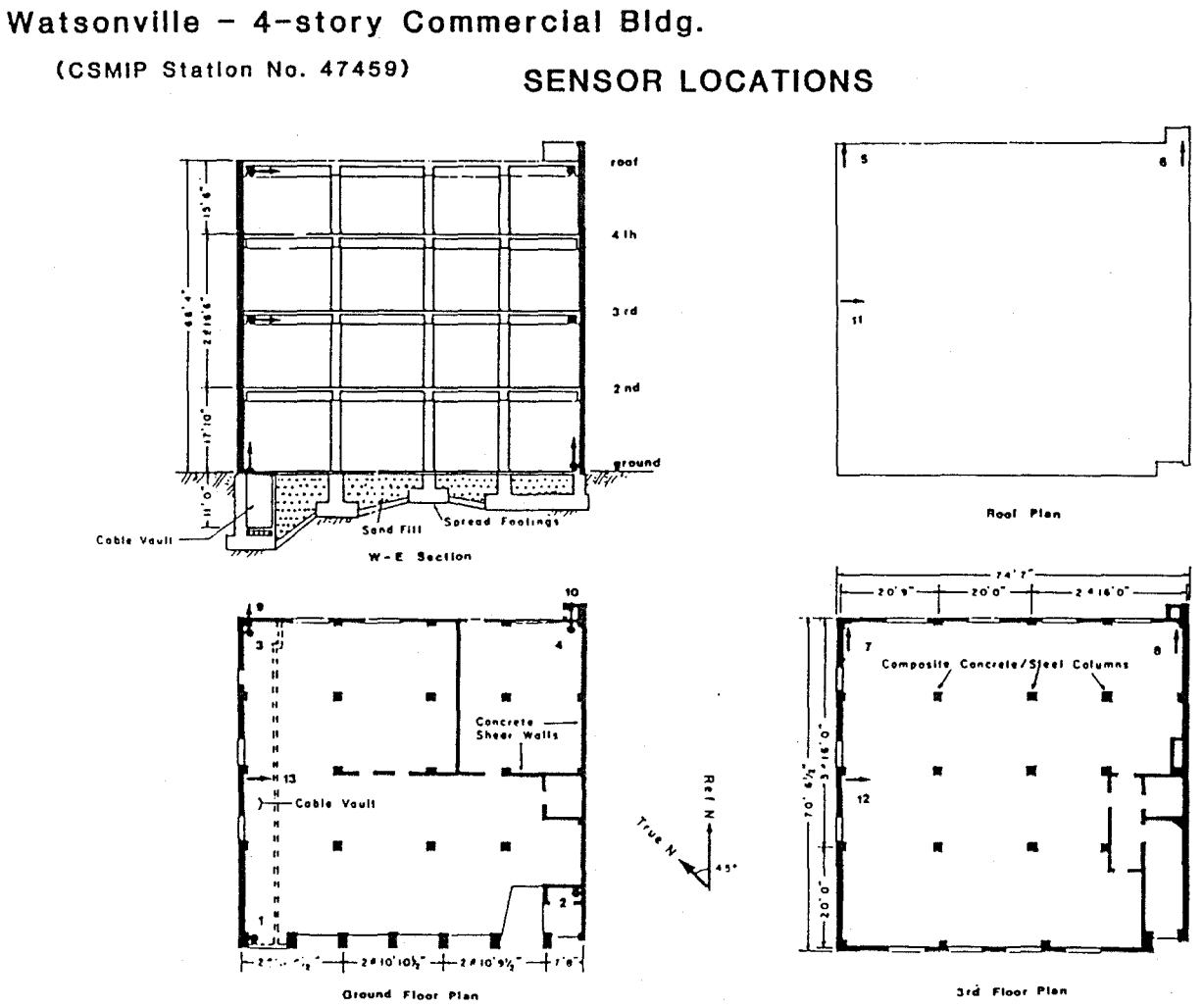

Figure 7.1 Plan views of building and sensor locations

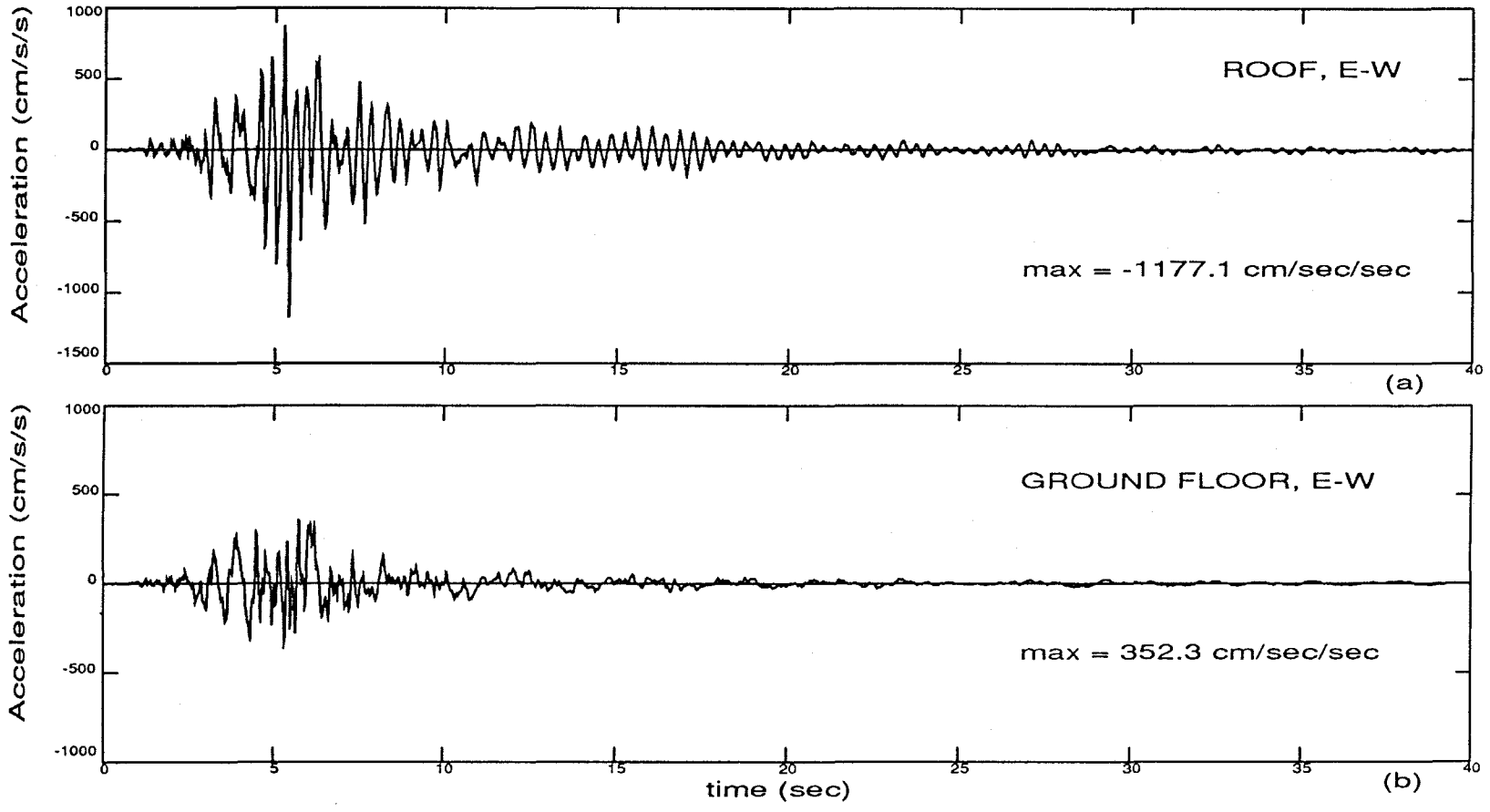

Figure 7.2. Time histories of acceleration (E-W) of (a) roof and (b) ground floor.

is employed. A three-stage identification approach for hysteretic system proposed by C. Loh and S. Chung [19] was also applied to analysis of this building. In this thesis, the building will be analyzed by means of a different approach, which is based on a different view. It will be investigated using the previously-presented methods. Only the E-W response (first 40.96 seconds) will be studied herein.

7.1.2 Fourier Amplitude Ratio (FAR)

As in the examination of the three-degree-of-freedom system in chapter 2, the Fourier Amplitude Ratio will be used for preliminary study in this investigation.

Fourier Amplitude Spectra (FAS) of the roof and basement accelerations and their ratio (FAR) are shown in Figure 7.3. A few peaks can be seen in Figure 7.3(c). However, it can be seen from 7.3(a) that the response is mainly dominated by frequency components lower than *4Hz*.

The imaginary part of Fourier Transform Ratios of the roof and third floor accelerations to the basement are shown in Figure 7.4. It can be observed that below *5Hz* the roof and third floor vibrate in phase, namely, in the first mode. Since all other modes are in a higher-frequency range and contribute little to the system response, it is concluded that the first mode dominates this response.

7.1.3 E-W Vibration Modes

Based on the above observation, a single mode analysis is applied. That is, all displacement coordinates are approximated as

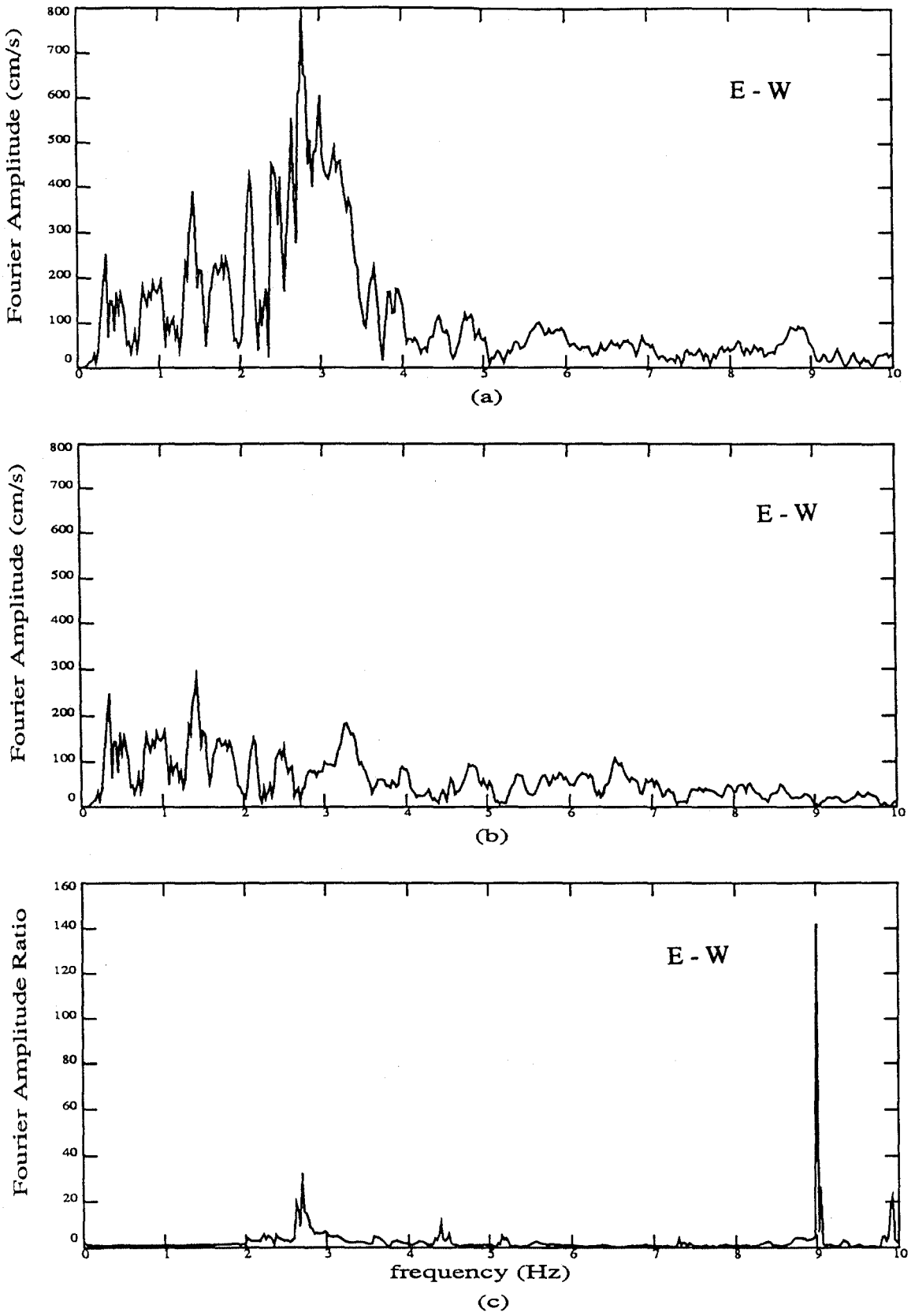

Figure 7.3. Fourier Amplitudes (FA) and their ratio
(a) FA of roof; (b) FA of basement; (c) ratio

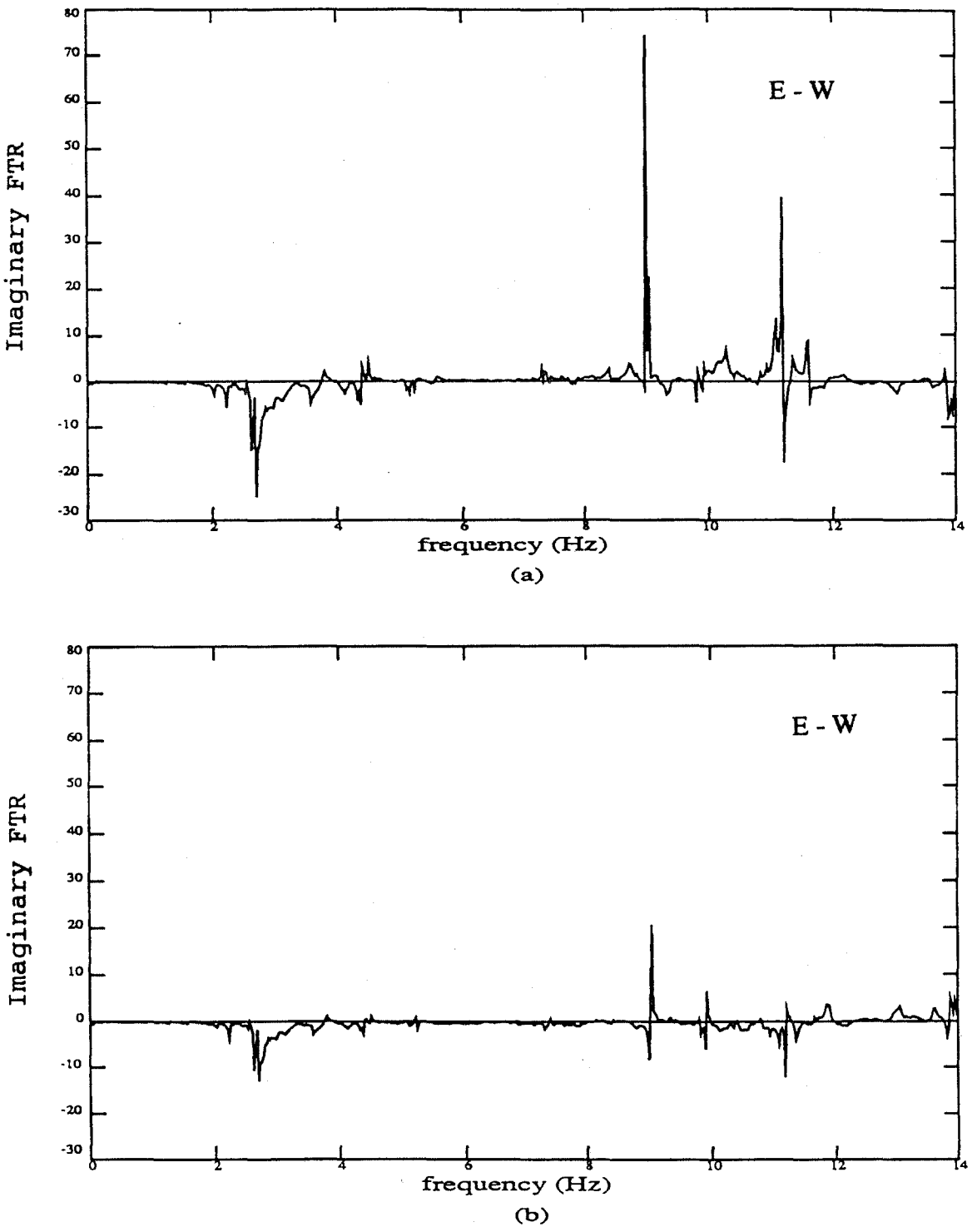

Figure 7.4. Imaginary part of Fourier Transform Ratio
(a) roof ; (b) 3rd floor

$$\mathbf{x}(t) \approx \Phi_1 (A_1)\, u_1(t) \qquad (7.1)$$

where $\mathbf{x}(t)$ is displacement coordinate vector, Φ_1 is the first-mode shape vector, u_1 is modal coordinate and A_1 is the amplitude of u_1.

Let the value of Φ_1 at roof be unit value. Then, u_1 will be equal to the roof displacement. From the modal relation (7.1), the system can be uncoupled and described as a SDOF system. The corresponding modal equation will be amplitude-dependent.

Using a single mode approach, the effective restoring force per unit mass between roof and base can be obtained directly from the absolute acceleration of the roof. This is plotted in Figure 7.5(a). Nonlinear behavior of the structure in this earthquake can easily be observed from this figure.

7.1.4 Modal Response

1. Correction of long period errors

Figure 7.6(a) shows the time history of the E-W relative displacement at roof. Long period components are observed in this response. They are obviously not structural response since the building is a low aspect ratio structure that cannot have such a low stiffness. According to reference [11], it is a long period error. Appearance of long period errors can be found in the above-mentioned reference.

The original accelerogram provided by CDMG was filtered by a bandpass filter with ramps at *0.08-0.16* and *23.0-25.0 Hz*. In order to eliminate the low frequency error, the high-pass cutoff frequency needs to be increased. According to the treatment presented in the above reference, different high-pass cutoff frequencies can be selected until

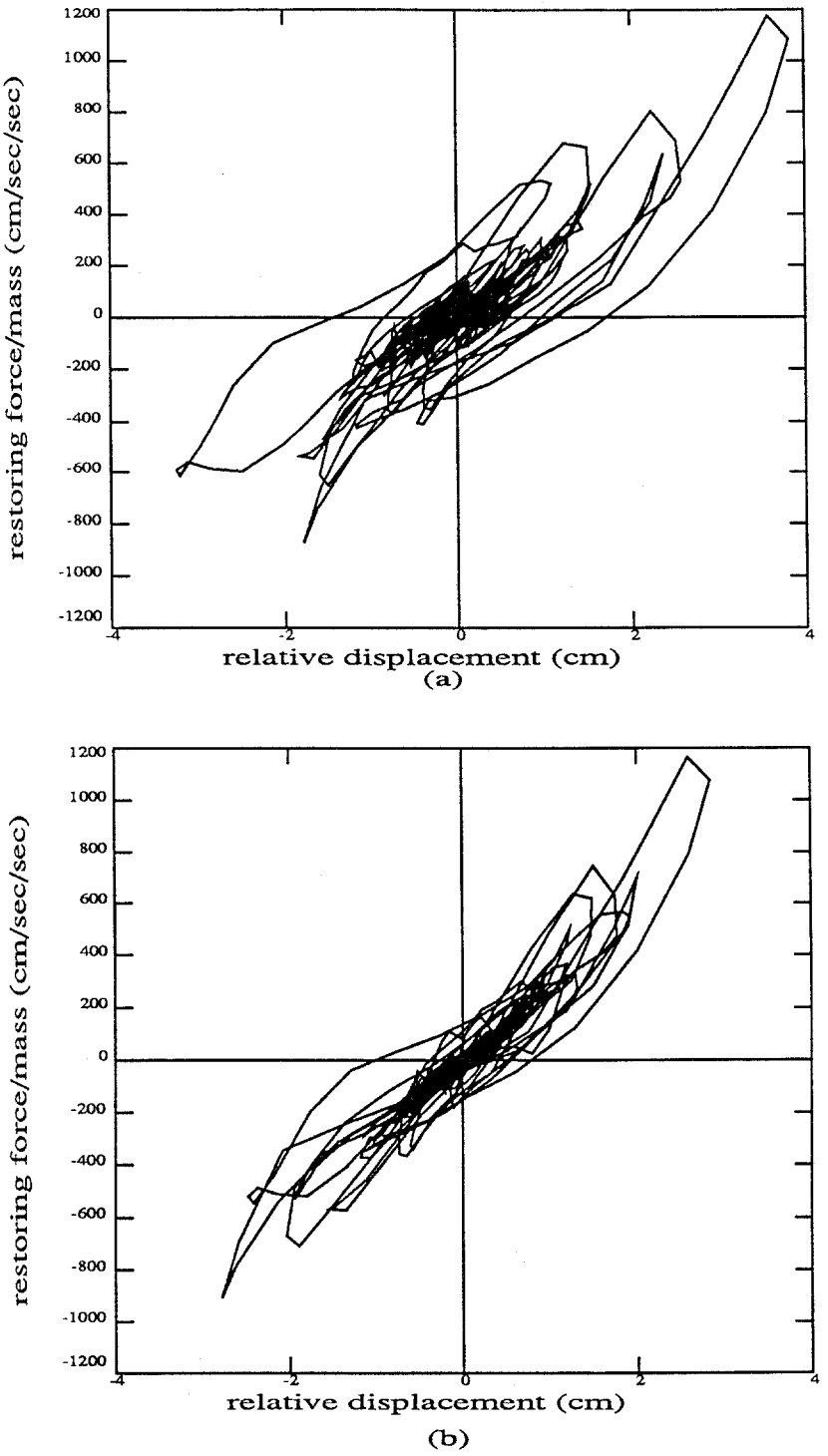

Figure 7.5. Restoring force per mass. (a) unfiltered;

(b) filtered from 0.7-23Hz.

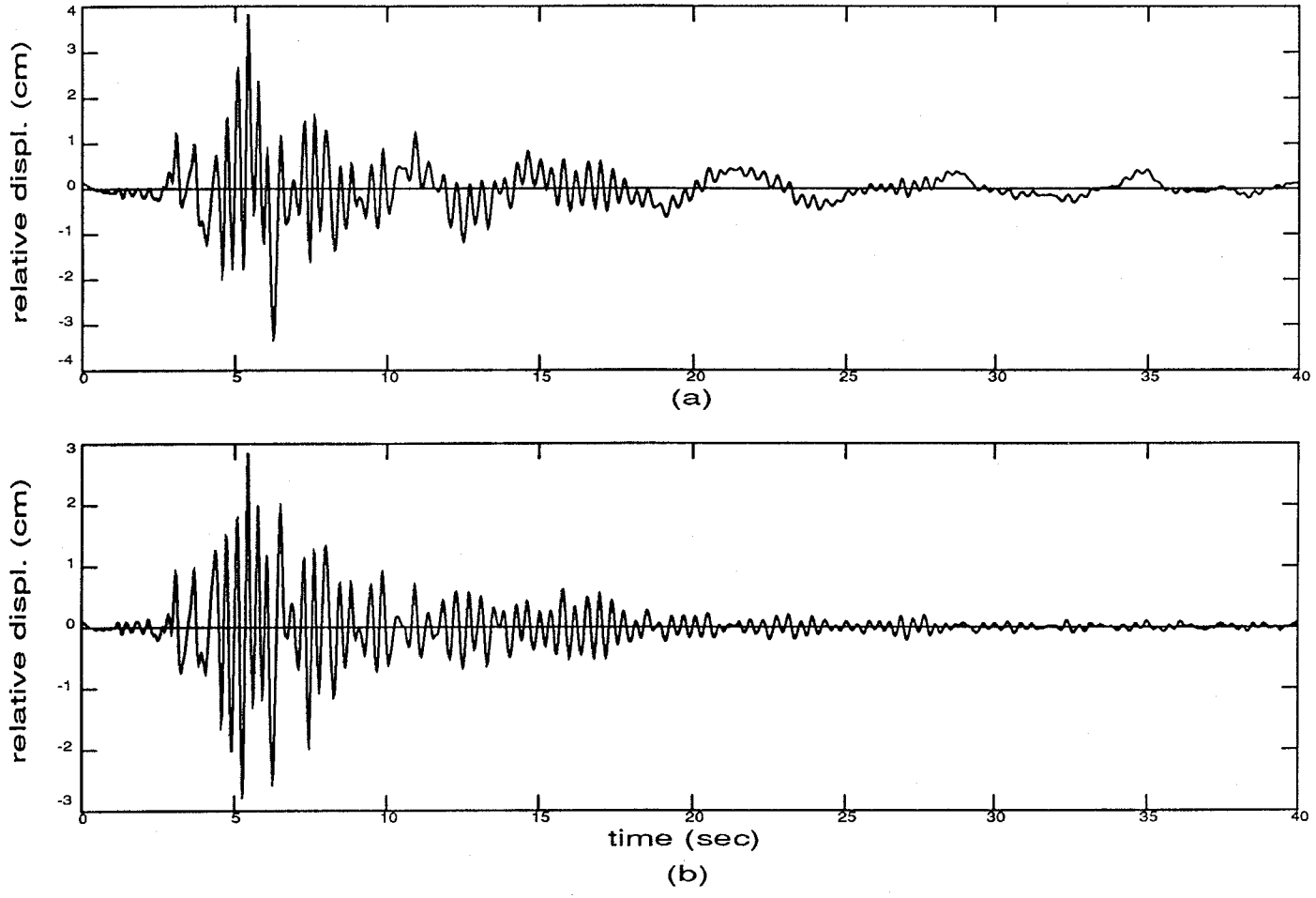

Figure 7.6. Relative displacement of roof. (a) unfiltered displacement with long period error; (b) displacement filtered from 0.7-23Hz.

the long period errors disappear from the response time history. For the recorded response data of the four-story building, a cutoff frequency of *0.7Hz* is chosen. The corrected relative displacement and restoring force per mass are plotted in Figure 7.6(b) and Figure 7.5(b). It can be seen that the long period error has disappeared from the response data and that the displacement drift in the restoring force diagram has been eliminated.

2. Elimination of the influence of higher modes

As mentioned, a single mode approach will be used to analyze the seismic response of the four-story building. To eliminate the influence of higher modes, a low-pass filter is used. Based on inspection of the Fourier Amplitude Ratio (Figure 7.3), the low-pass cutoff frequency is chosen to be *8.5 Hz*. All frequency components higher than this value are removed.

7.1.5 Modal Identification

A corrected modal response is obtained by applying a bandpass filter of *0.7-8.5Hz*. Applying both previously-presented identification methods to the measured roof response, the equivalent modal frequency, effective modal damping coefficient and modal participation factor are identified. Truncated at fourth order, these results may be expressed as

$$\omega_1^2(A) = 295.2 - 16.9A^2 + 2.1A^4 \qquad (7.2)$$

$$\alpha_1(A) = 2.93 + 0.03A^2 - 0.03A^4 \qquad (7.3)$$

$$\beta_1(A) = 1.33 - 0.13A^2 + 0.02A^4. \qquad (7.4)$$

The natural frequency and damping ratio of this mode are calculated from the results of $\omega_1^2(A)$ and $\alpha_1(A)$ respectively. The results and $\beta_1(A)$ are plotted in Figure 7.7. It can be seen in Figure 7.7(a) that the system has softening behavior in the low amplitude range and becomes stiffer in the large amplitude range. This result is consistent with what is observed in the restoring force diagram (Figure 7.5). It confirms that a polynomial function of ω_1^2 (A) with at least the fourth order is needed to describe the curve of natural frequency in the Figure 7.7(a). Therefore, the system is assumed to have fifth order to describe such stiffness characteristics.

The Figure 7.7(a) shows that the linear natural frequency is *2.73Hz* and that the modal frequency drops down to *2.58Hz* when modal amplitude is *2cm* and goes up to *2.75Hz* when *2.8cm*. In the reference [79], the equivalently linear natural frequency over the entire duration of 40seconds is *2.72Hz*, which is in the range of amplitude-dependent modal frequency. In this reference, time windows (*0-10second, 10-20second* and *20-40second*) were used to investigate the extent of nonlinearity, which shows that the modal frequency tends to decrease as the response amplitude increases. This result explores the nonlinearity of the system. However, it doesn't mean a conflict with the observation in this thesis since the reference used only three wide time windows. It is believed that the same conclusion can be obtained if the number of time window tends to be the same as the half-cycle number of the response and the width of the windows to be the same as the half-cycle width.

For successive approximation model, the first-order terms, $\varpi_{11}(A)$, α_1 (A), and β_1 (A), are already obtained at the first stage of the procedures where ω_1^2 (A) is $\varpi_{11}(A)$, i.e.

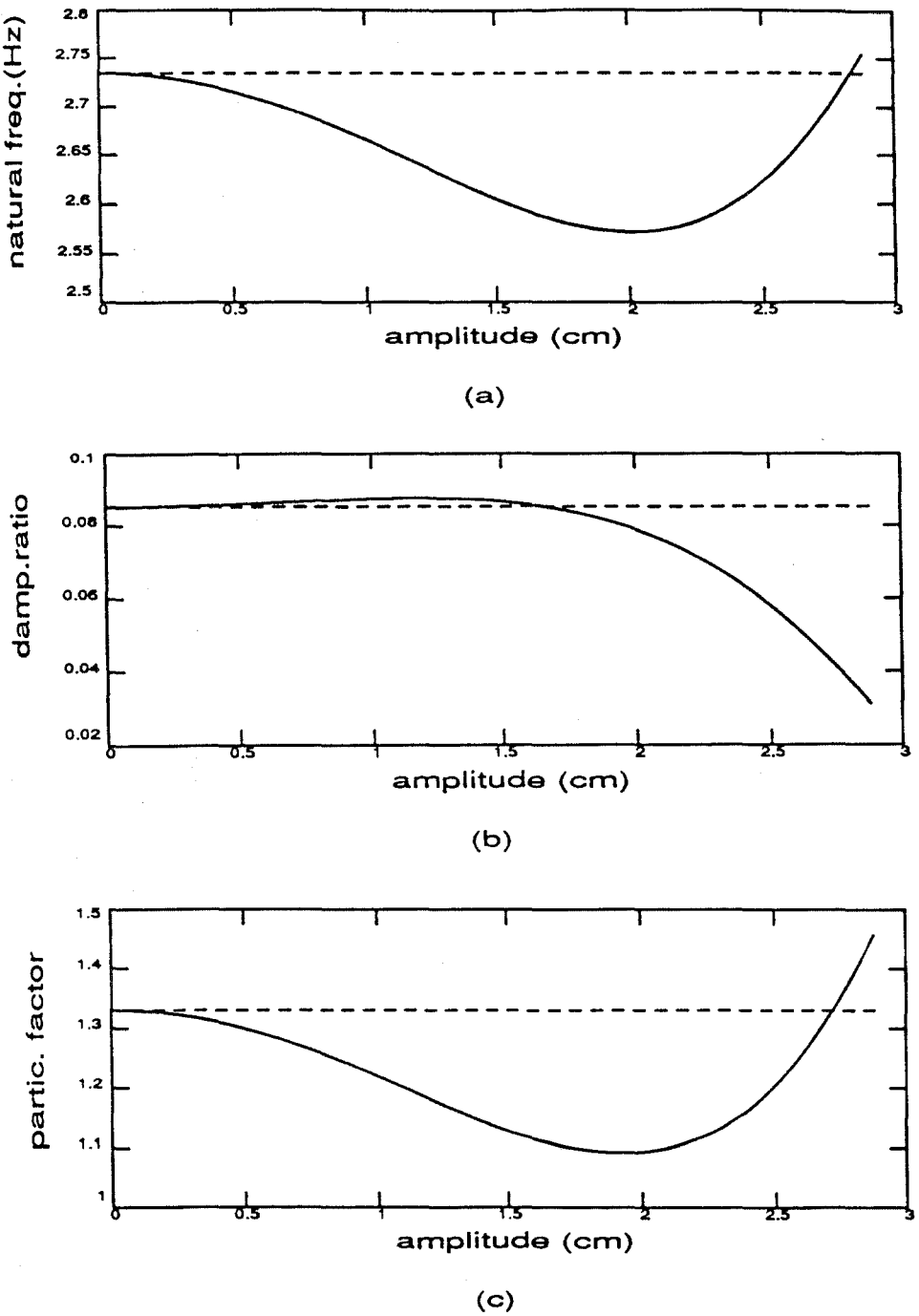

Figure 7.7. Identified modal parameters
solid line - nonlinear modal parameters
dashed line - linear modal parameters
(a) natural frequency;
(b) damping ratio;

$$\varpi_{11}(A) = \omega_1^2(A) = 295.23 - 16.9A^2 + 2.10A^4 . \qquad (7.5)$$

Furthermore, applying the process (Equation 5.18-21) for a cubic-order approximation yields

$$\varpi_{31}(A) = -1.64 + 0.68A^2 + 0.21A^4 . \qquad (7.6)$$

With the cubic-order approximation, the total absolute error between the calculated and measured displacements, ε, is calculated. Further approximation to fifth order results in little improvement in this error. Therefore, the higher-order terms are ignored. The final successive approximation modal equation is

$$\ddot{u}_1 + \alpha_1(A)\dot{u}_1 + \varpi_{11}(A)u_1 + \varpi_{31}(A)u_1^3 = -\beta_1(A)\ddot{z} \qquad (7.7)$$

where all coefficients are given above (7.3-7.6). The modal displacement calculated by this equation and the measured response are plotted in Figure 7.8.

For simplified expansion modal equation, since it is already known that the system needs a model with at least fifth order, the modal equation is assumed to be

$$\ddot{u}_1 + \alpha_1(A)\dot{u}_1 + \overline{\kappa}_{11}u_1 + \overline{\kappa}_{31}u_1^3 + \overline{\kappa}_{51}u_1^5 + \tilde{\kappa}_{51}(A)u_1^5 = -\beta_1(A)\ddot{z} . \qquad (7.8)$$

$\overline{\kappa}_{11}$ and $\overline{\kappa}_{31}$ are given from $\omega_1^2(A)$. $\overline{\kappa}_{51}$ and $\tilde{\kappa}_{51}(A)$ are determined through the process (equation 6.21b-6.23b). The results are

$$\overline{\kappa}_{11} = 295.2, \qquad \overline{\kappa}_{31} = -16.9, \qquad \overline{\kappa}_{51} = 3.2,$$
$$\tilde{\kappa}_{51}(A) = 0.7A^2 - 0.1A^4 . \qquad (7.9)$$

The modal response calculated by equation (7.8) is plotted in Figure 7.9. The

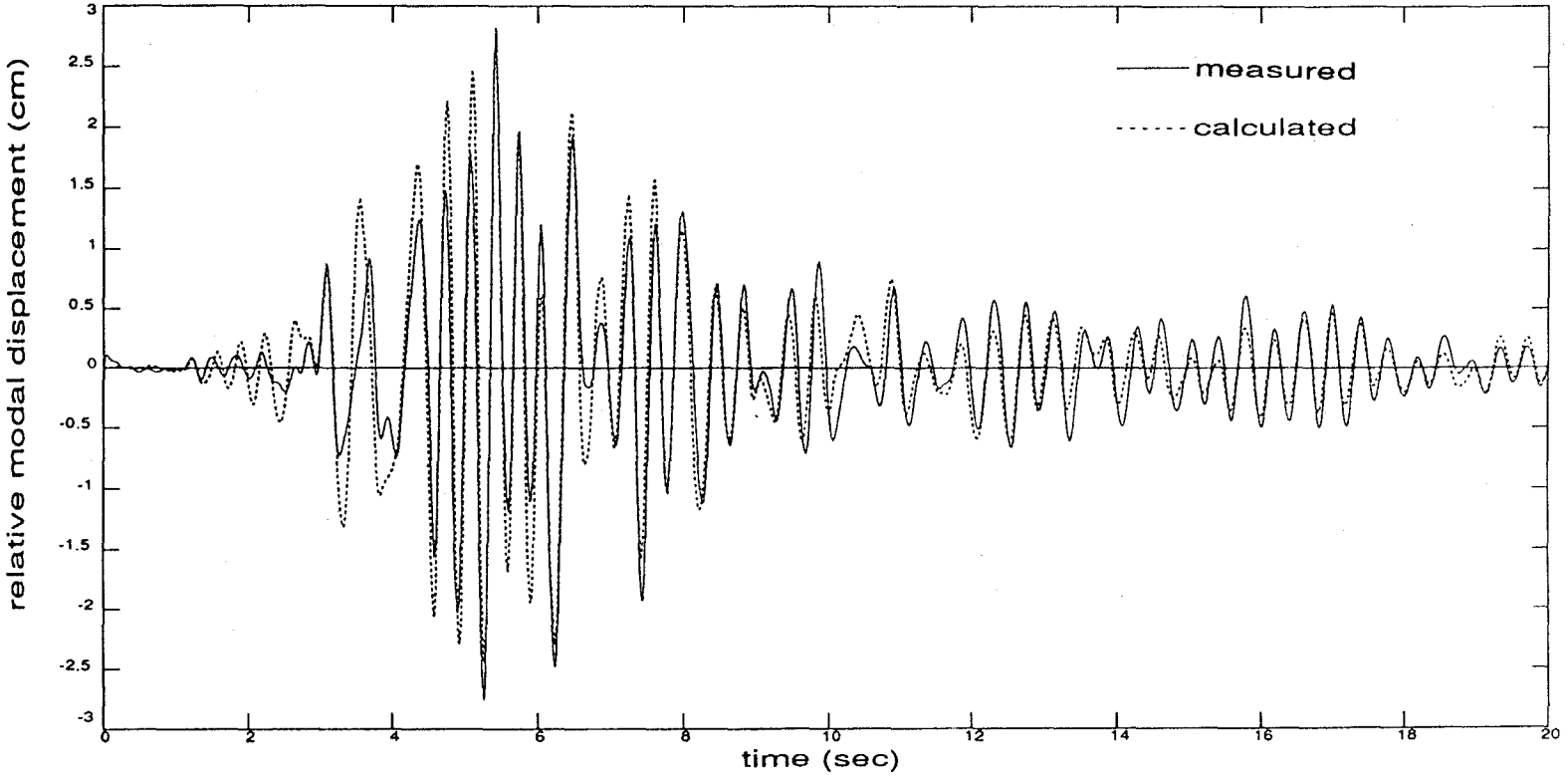

Figure 7.8. Comparison of calculated and measured relative modal displacements. Succesive approximation method was used in identification.

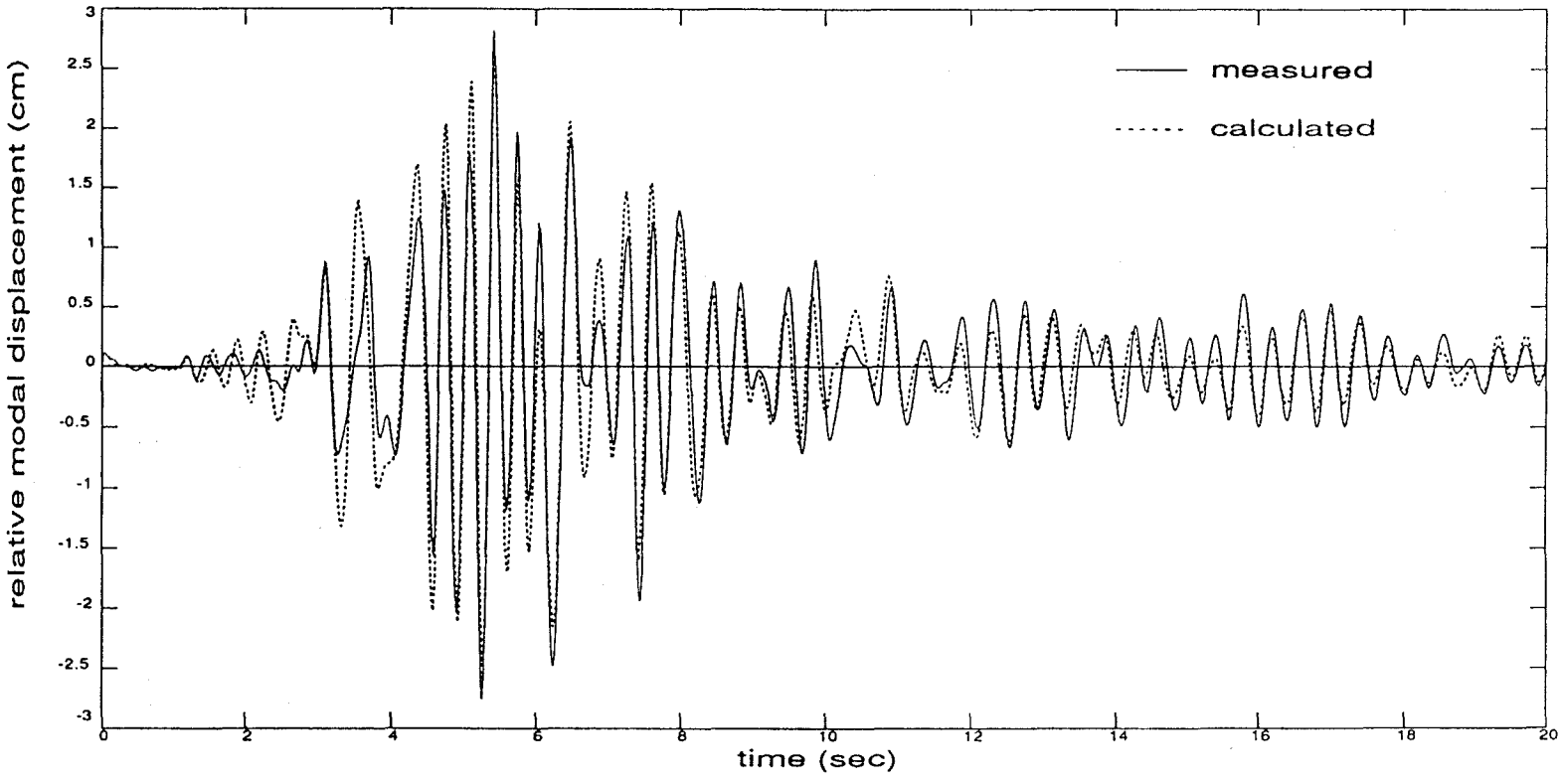

Figure 7.9. Comparison of calculated and measured relative modal displacements. Simplified model method was used in identification.

measured modal response is also shown in this figure for comparison.

Using measured modal displacements at the roof and third floor levels, the mode shape may be calculated by equation (5.24). The result is

$$\begin{cases} roof & \phi_{21}(A) = 1.00 \\ 3rd\ floor & \phi_{11}(A) = 0.65 - 0.02A^2 + 0.00A^4. \end{cases} \qquad (7.10)$$

ϕ_{11}(A) is plotted in Figure 7.10 (a). It can be seen from the figure (a) that the modeshape component changes with amplitude. When the amplitude is approximately *2cm*, the difference between the linear and nonlinear mode shapes is greatest. This difference is about 9% of the linear modeshape component value. The mode shape associated with *A* = *2cm* and linear mode shape are shown in Figure 7.10 (b).

7.2 FORTY-SEVEN-STORY BUILDING (N-S Direction)

7.2.1. Building Description and Measurement

The second building to be investigated is located in San Francisco. It was constructed in 1978-79. The lateral force resisting system consists of moment-resisting steel frames braced in the transverse direction. The foundation is a reinforced concrete mat supported by composite concrete and steel piles. Accelerometers were installed in this building in the basement, and at the podium level (*2nd*), 16*th*, 39*th* and 44*th* floors. The plan view of the building and the location of accelerometers installed are shown in Figure

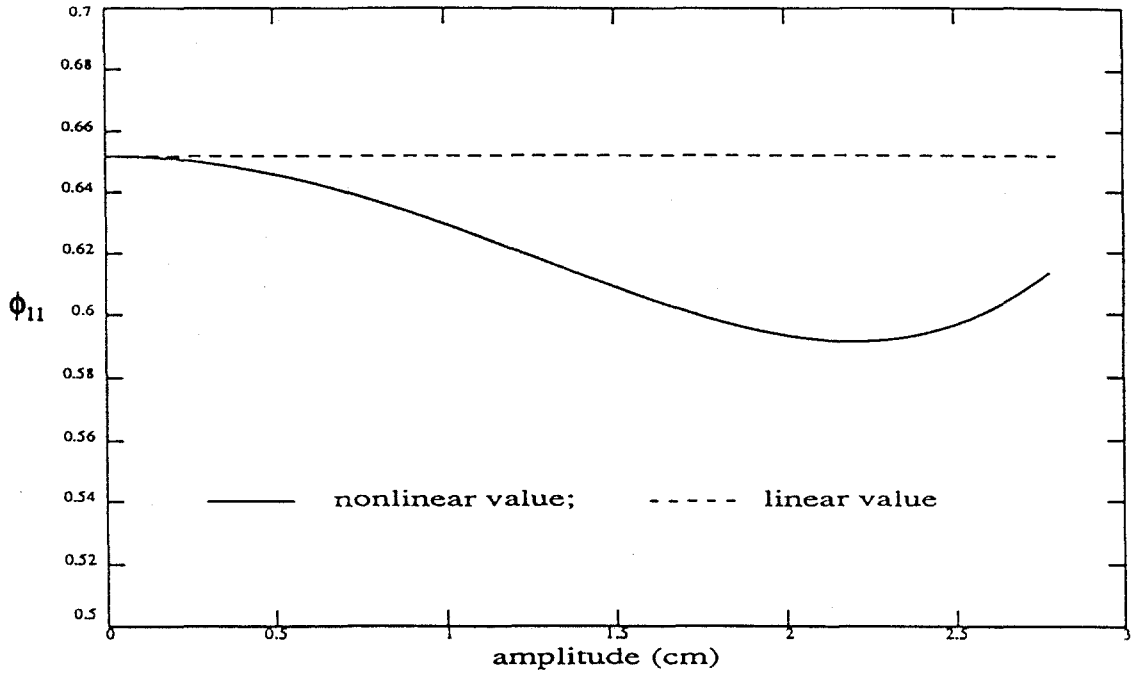

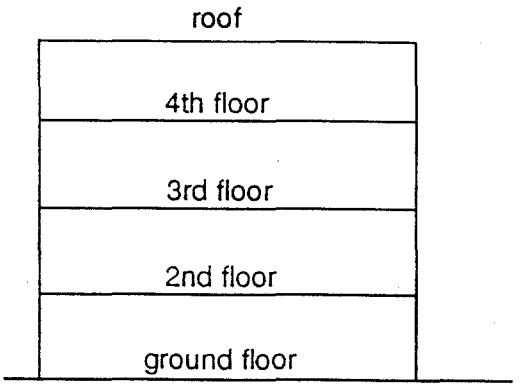

Watsonville 4-story Building

(b)

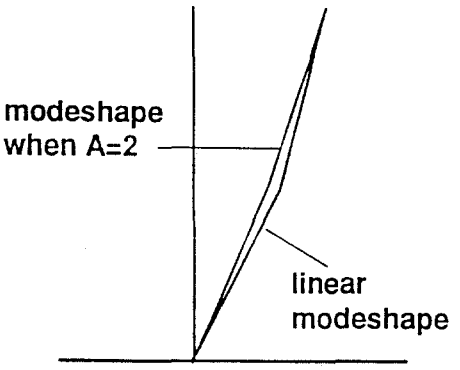

First mode

(c)

Figure 7.10 Identified first mode shape
(a) component value at 3rd floor; (b) structure;
(c) comparison of linear mode shape and mode shape when roof amplitude A = 2 cm.

7.11. Seismic responses in three directions (N-S, W-E, Up-Down) can be recorded during earthquakes.

The displacement time histories of the building at the *44th,* *39th,* *16th,* floors, podium level and basement in N-S direction are shown in Figure 7.12. The time histories of acceleration in this direction at roof and basement are shown in Figure 7.13. The roof peak acceleration in N-S direction is *0.48g*. Only dynamic properties in N-S direction of the structure will be investigated.

7.2.2 N-S Vibration Modes

The Fourier Amplitude Ratios of accelerations of the *44th,* *39th,* *16th* and 2nd floors to basement in N-S direction are shown in Figure 7.14. From Figure 7.14, it can be seen that there are three predominant resonances in the N-S direction below *1Hz* and that three resonances are well separated. Based on this observation, a basis for applying the modal approach to analyze this system is found.

Figure 7.15 shows the imaginary part of Fourier Transform ratios. It can be seen that the imaginary values of Fourier Transform ratios for all degree-of-freedoms at about *0.2Hz* are negative and that the values of roof and *39th* floor are positive and others are negative near *0.6Hz*. This means that all degree-of-freedoms are moving in phase if the system vibrates at about *0.2Hz* but that the upper and lower portions of the building are vibrating out of phase near *0.6Hz*. Therefore, it can be inferred that *0.2Hz* is the first mode and that *0.6Hz* is the second mode.

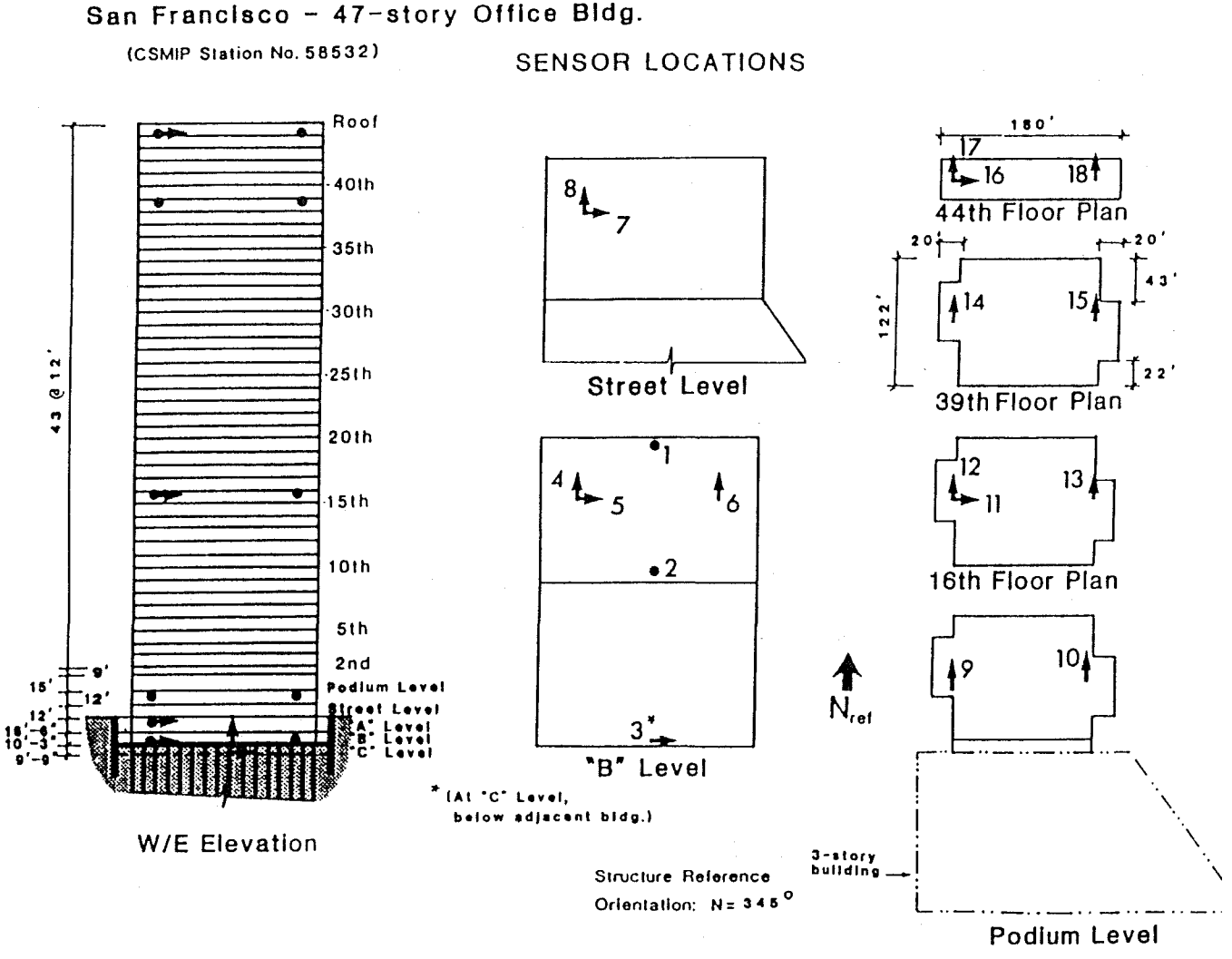

Figure 7.11 Plan views of building and sensor locations

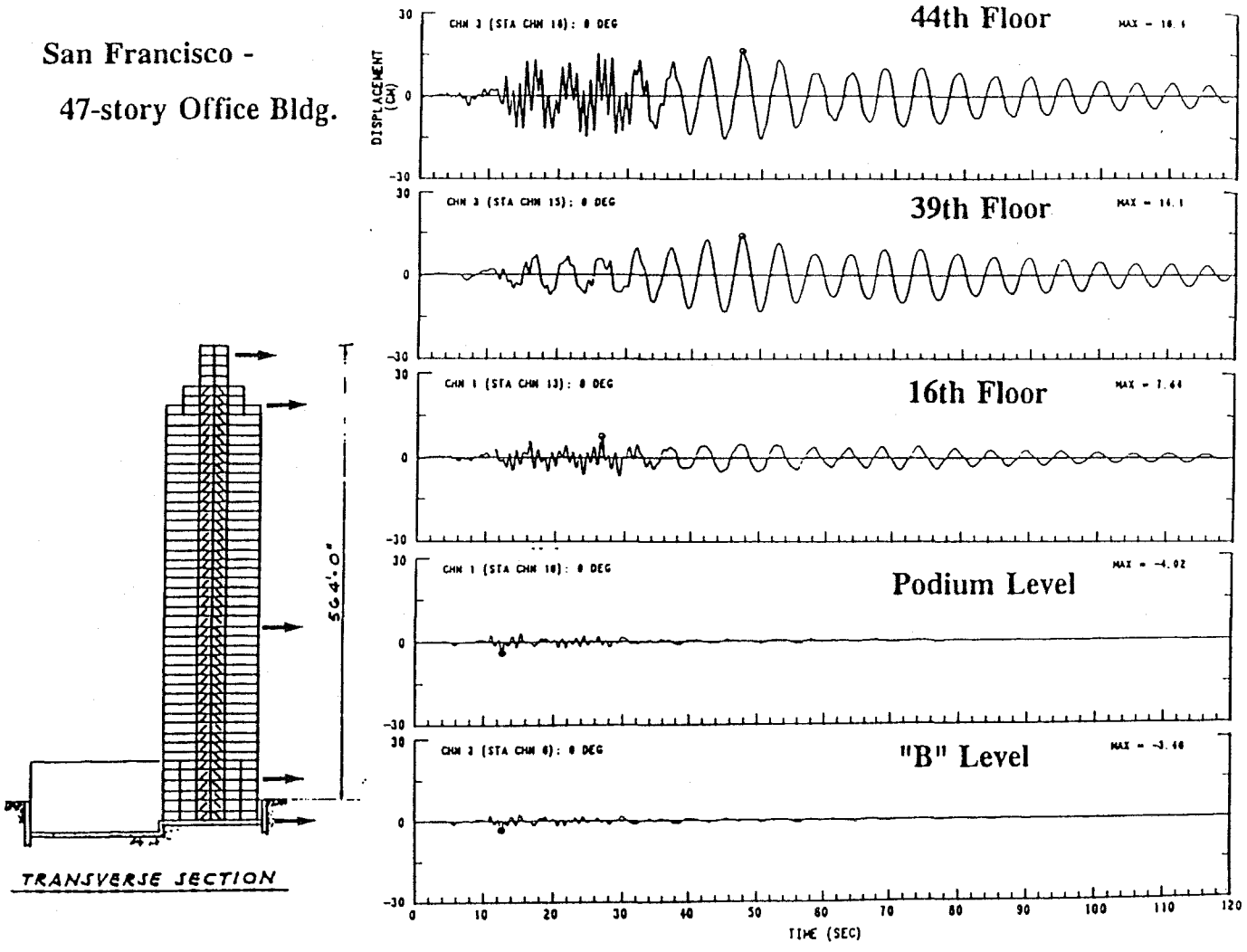

Figure 7.12 N-S section of building and displacements

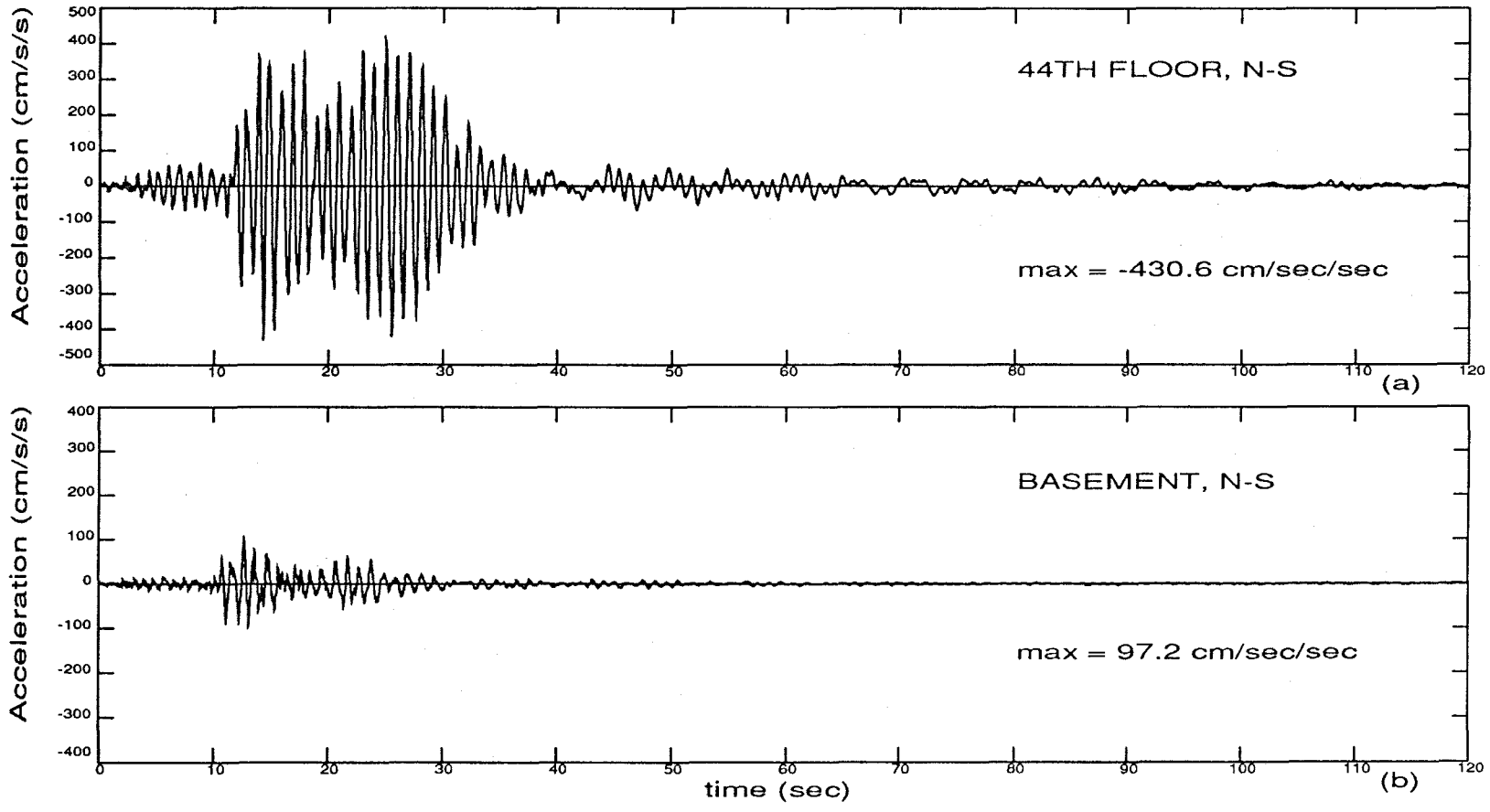

Figure 7.13. Time histories of acceleration (N-S) of (a) 44th floor and (b) basement.

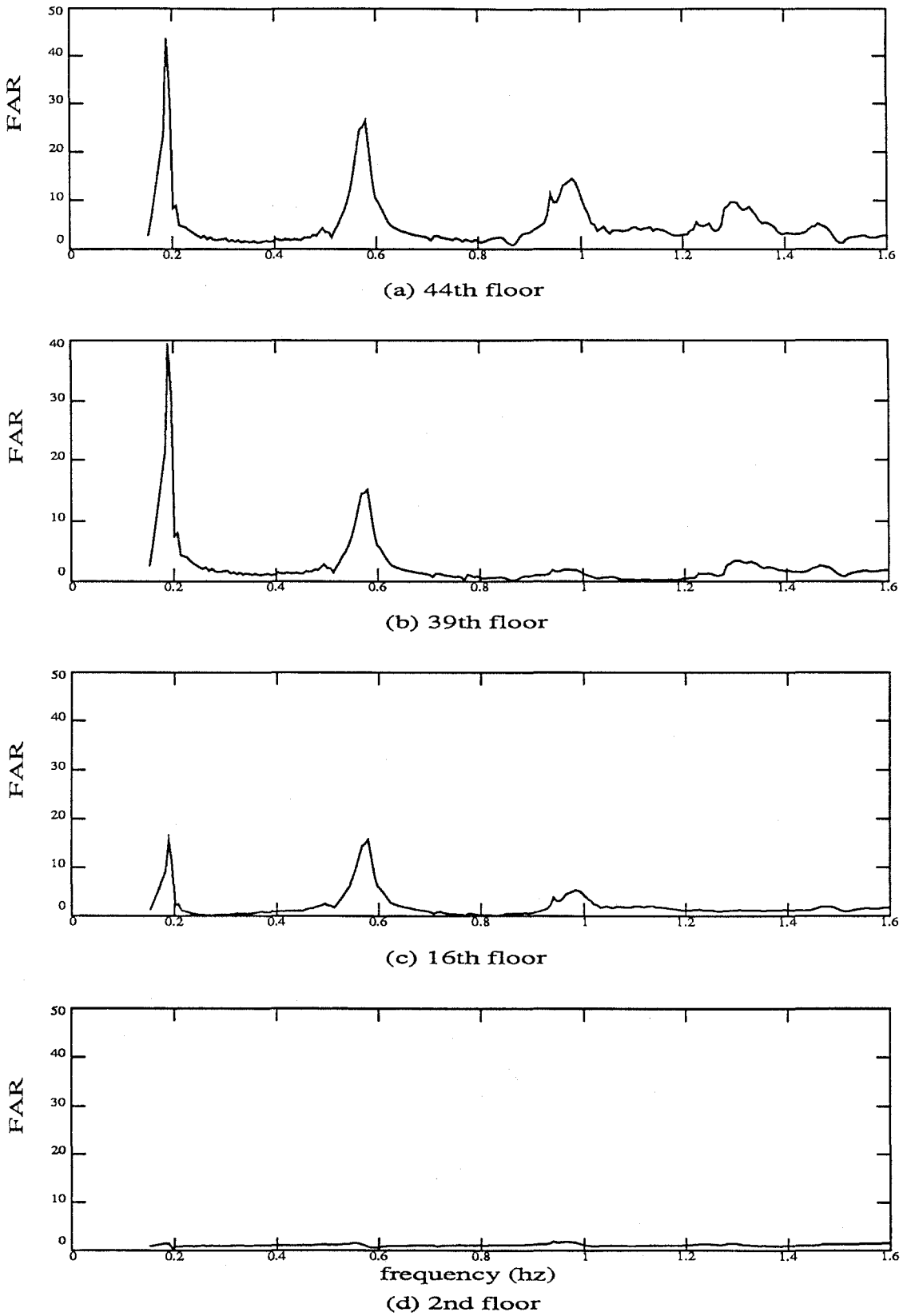

Figure 7.14. Fourier Amplitude Ratios of Structural Response

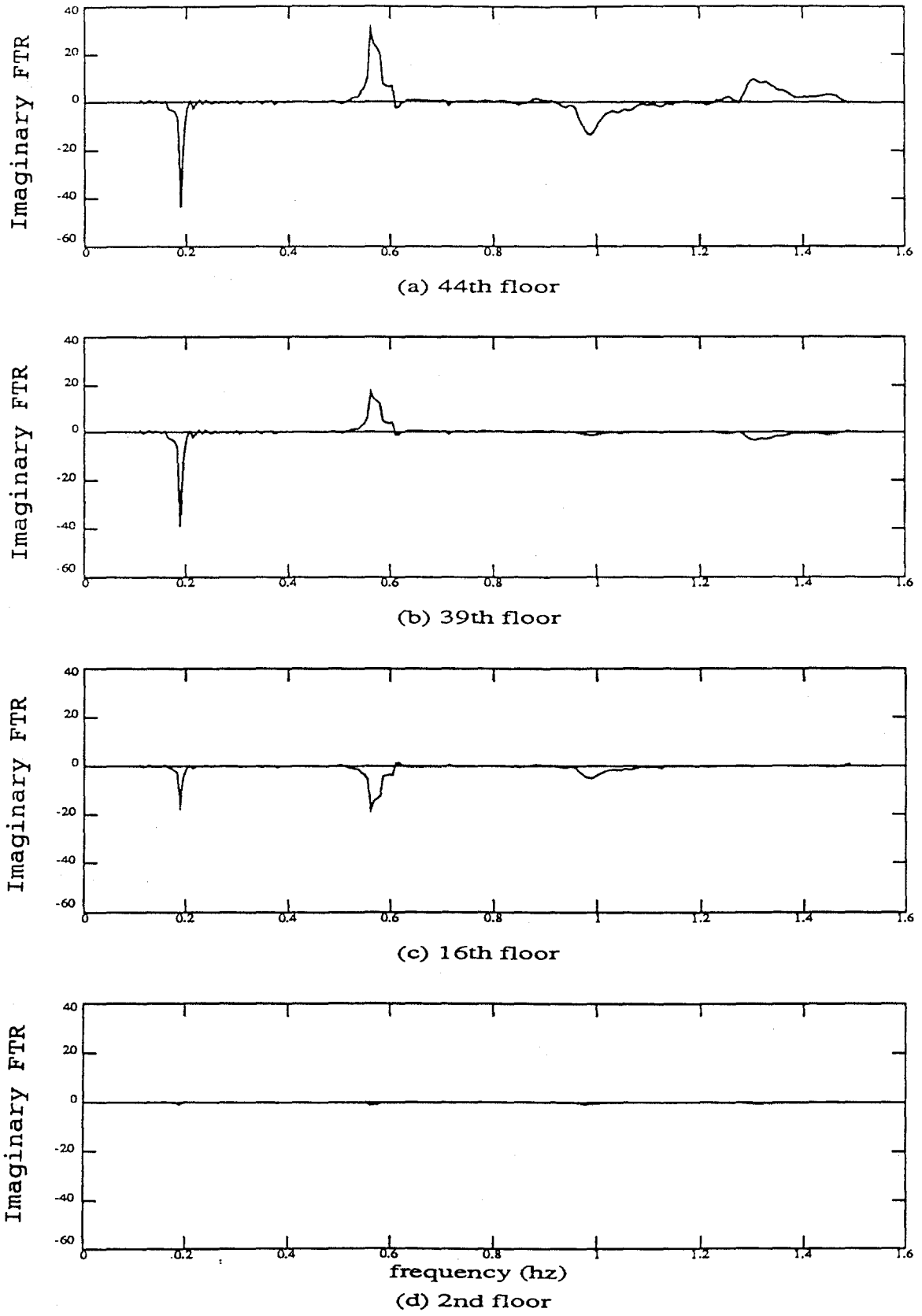

Figure 7.15. Imaginary part of Fourier Transform Ratio

For the peak near *1Hz* in Figure 7.15, all imaginary values are negative. This is obviously not the first mode, since these floor values do not appear to be monotonously increasing, in order from base to top floor, and *0.2Hz* is already confirmed to be the first mode. It is believed that the instrumentation is not sufficient to measure the third modeshape. However, it can be assumed based on the order of peaks that the vibration of *1Hz* is the third mode. This may be supported by the observation that the value of FAR at the 39th floor is very small, from which it may be speculated that there are degrees of freedom between the 16th and 39th floors which have a positive imaginary Fourier Transform ratios value.

7.2.3 Modal Identification

The modal responses of three N-S modes are estimated by band-pass filtering. The cutoff frequencies of the band-pass filters for estimation of three modes are *0.12 - 0.27Hz*, *0.5 - 0.7Hz*, and *0.85 - 1.05Hz* respectively. The frequency bands can nearly cover three resonance peaks. Since the peaks are well separated and the widths of the peaks are narrow (relatively speaking), such estimation of the modal response is appropriate. These measured data are used in identification. The modeshape at the 44th floor is defined to be unity for all modes. Thereby, the modal coordinates will be equal to the modal displacements at the 44*th* floor.

Using both identification methods described in chapters 5 and 6 and the modal response of 44th floor, the modal frequencies of three modes are identified. Truncating the polynomial expressions at the fourth order, the three modal frequencies are found to

be:

$$\omega_1^2(A_1) = 1.44 - 0.00A_1^2 + 0.00A_1^4 \qquad (7.11)$$

$$\omega_2^2(A_2) = 13.15 - 0.18A_2^2 + 0.01A_2^4 \qquad (7.12)$$

$$\omega_3^2(A_3) = 39.60 - 0.03A_3^2 + 0.00A_3^4 \qquad (7.13)$$

where A_1, A_2, A_3 are amplitudes of the first, second and third modal responses respectively and the 0.00 means that the result is zero to two places of decimals. The natural frequencies are calculated and shown in Figure 7.16 as solid lines. The corresponding linear natural frequencies are shown as dashed lines. From these figures, the characteristics of each mode can be extracted. It can be seen that all three modal frequencies change with amplitude. However, the change is relatively small, which shows that the three modes are very weakly nonlinear. Furthermore, it can be seen that the first and third modal frequencies monotonously decrease with modal amplitude and that the second modal frequency decreases with low amplitude but increases with larger amplitude. It represents that the first and the third modes are weakly softening and that the second mode is weakly softening for low amplitudes but hardens somewhat for large amplitudes. The modal frequencies of all three modes are lower than the corresponding linear frequencies.

In the first stage of both modal identifications, modal damping coefficients and modal participation factors are also determined as well as equivalent linear natural frequencies. The effective modal damping coefficients of the three modes are obtained as

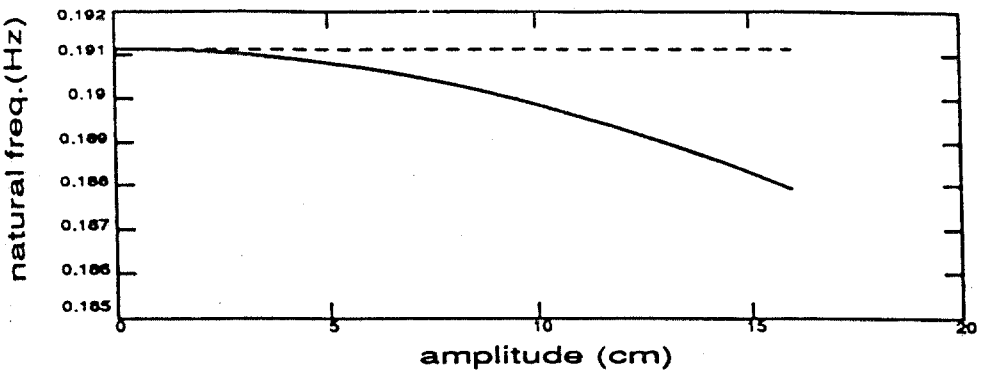

(a)

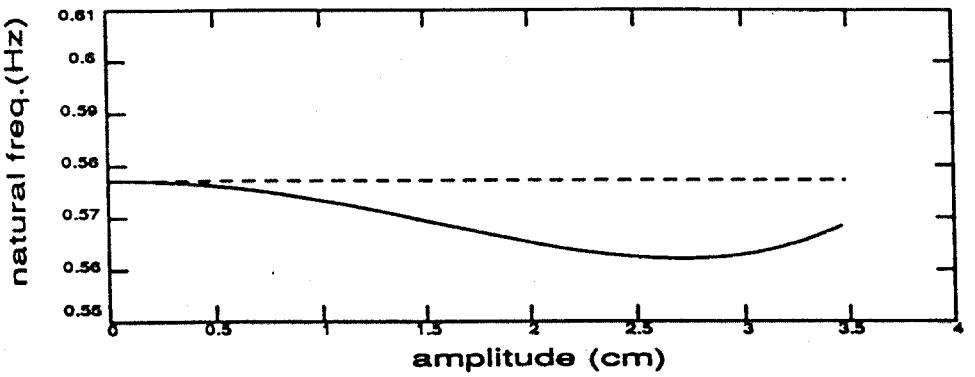

(b)

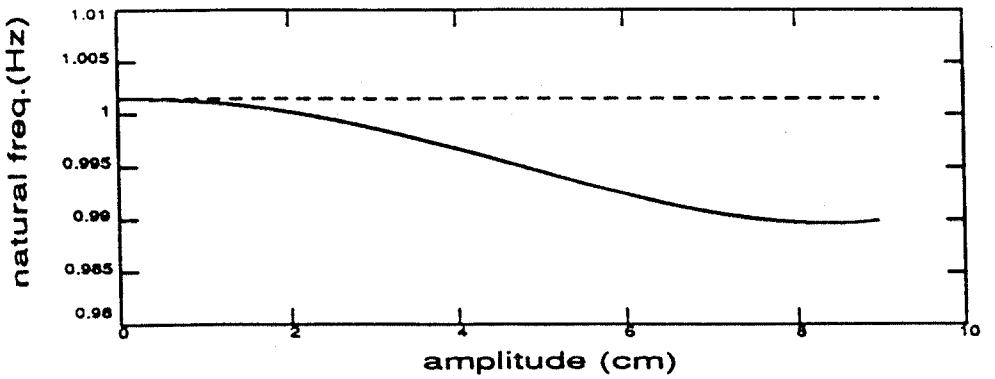

(c)

Figure 7.16. Identified natural frequencies

solid line - nonlinear natural frequency

dashed line - linear natural frequency

(a) 1st mode; (b) 2nd mode; (c) 3rd mode

$$\alpha_1 (A_1) = 0.04 - 0.00A_1^2 + 0.00A_1^4 \quad (7.14)$$

$$\alpha_2 (A_2) = 0.09 + 0.02 A_2^2 + 0.00A_2^4 \quad (7.15)$$

$$\alpha_3 (A_3) = 0.32 - 0.00A_3^2 + 0.00A_3^4 \quad (7.16)$$

The effective modal participation factors are

$$\beta_1 (A_1) = 1.59 + 0.00A_1^2 + 0.00A_1^4 \quad (7.17)$$

$$\beta_2 (A_2) = -0.50 - 0.02 A_2 + 0.00A_2^4 \quad (7.18)$$

$$\beta_3 (A_3) = 0.62 - 0.01A_3^2 + 0.00A_3^4 \quad (7.19)$$

The modal damping ratios are calculated. The functions of modal damping ratio and participation factor are shown in Figure 7.17 and 7.18 as solid lines. The corresponding linear values are shown as dashed lines. Figure 7.17 shows that the modal damping of the first and third modes are lower than the linear values and decrease with modal amplitudes and that the damping of the second mode is greater than the linear damping when the modal amplitude is less than *3cm* and lower than that when greater than *3cm.* It is also shown that the damping of the second mode increases when amplitude is less than *2cm* and decreases when greater than *2.5cm.* However, the result would be unreasonable if it was extrapolated from the curve that the damping will be negative when the amplitude is greater than *3.5cm.* Because the data used in modal identification does not contain the information beyond the response, the extrapolation of structural behavior beyond this range may be not true.

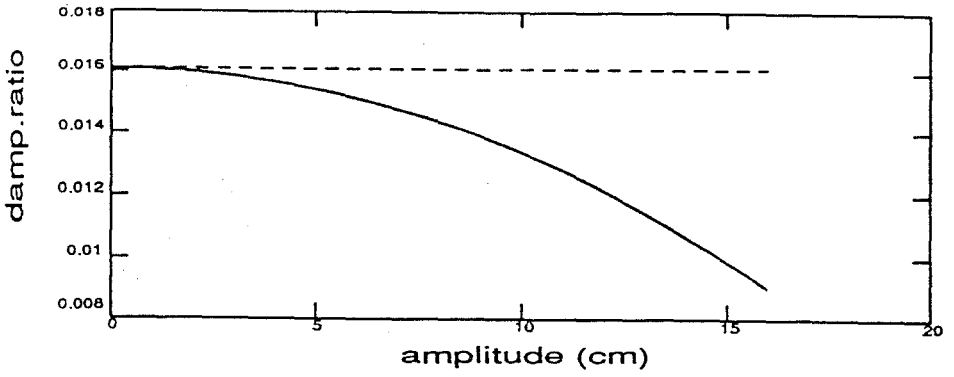

(a)

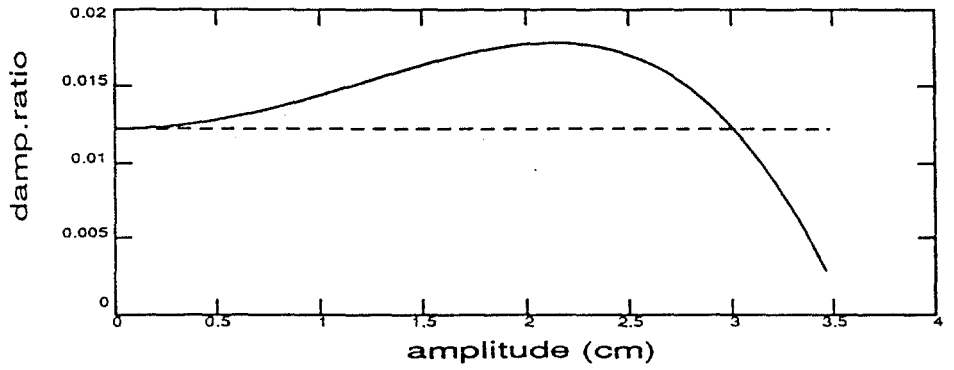

(b)

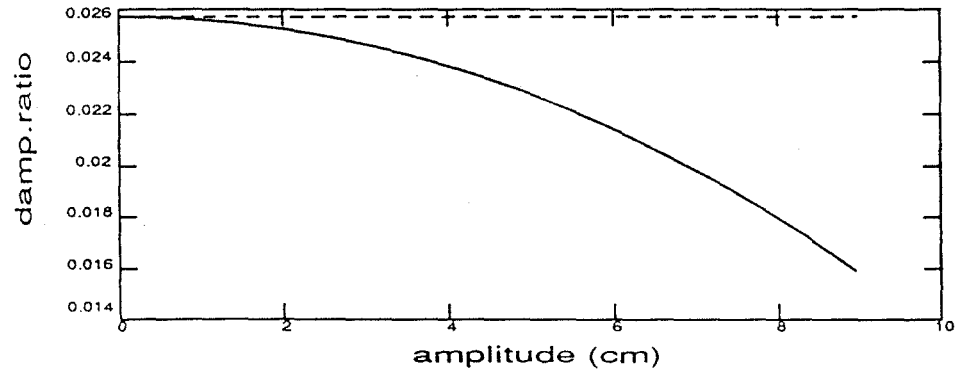

(c)

Figure 7.17. Viscous damping factors (ratios)
solid line - value of nonlinear system
dashed line - linear value of the system
(a) 1st mode; (b) 2nd mode; (c) 3rd mode

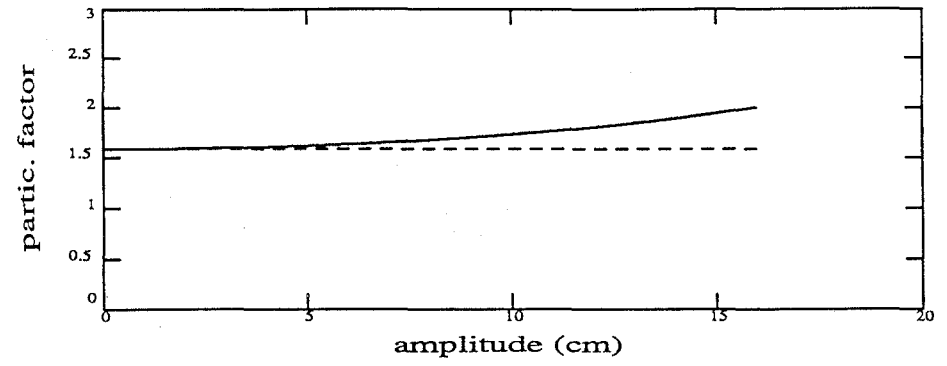

(a)

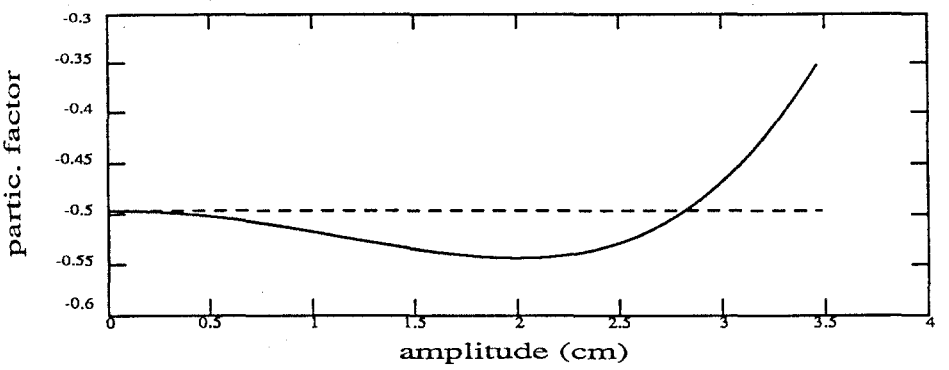

(b)

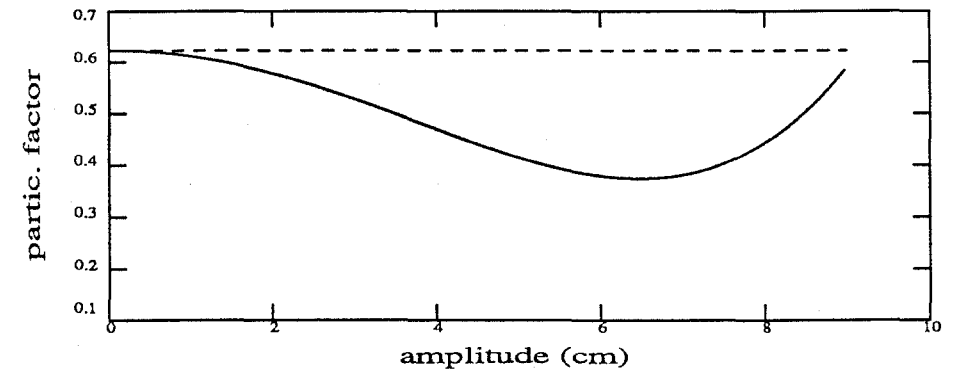

(c)

Figure 7.18. Identified participation factors
solid line - nonlinear participation factors
dashed line - linear participation factors
(a) 1st mode; (b) 2nd mode; (c) 3rd mode

For the successive approximation modal equation and the simplified expansion modal equation, other parameters of the equations besides $\alpha_j(A_j)$ and $\beta_j(A_j)$ need to be determined.

In the simplified expansion model identification, since it has already shown from the identified $\omega_j^2(A_j)$'s that the system is very weakly nonlinear, a nonlinear model up to cubic-order will be sufficient to describe the system. Therefore, it is assumed that the modal equation is of the form:

$$\ddot{u}_j + \alpha_j(A_j)\dot{u}_j + \overline{\kappa}_{1j}u_j + \overline{\kappa}_{3j}u_j^3 + \tilde{\kappa}_{3j}(A_j)u_j^3 = -\beta_j(A_j)\ddot{z} \quad (7.20)$$

where j denotes number of mode, j = 1, 2, 3 and where $\alpha_j(A_j)$ and $\beta_j(A_j)$ are known. By the simplified expansion model identification procedure, $\overline{\kappa}_{1j}$ and $\overline{\kappa}_{3j}$ are obtained from $\omega_j^2(A_j)$, and $\tilde{\kappa}_{3j}(A_j)$, truncated at the fourth order, are determined by the process (6.32-6.34). This yields

$$\overline{\kappa}_{11} = 1.44,\ \overline{\kappa}_{31} = -0.00,\ \tilde{\kappa}_{31}(A_1) = 0.00A_1^2 + 0.00A_1^4 \quad (7.21)$$

$$\overline{\kappa}_{12} = 13.14,\ \overline{\kappa}_{32} = -0.18,\ \tilde{\kappa}_{32}(A_2) = 0.00A_2^2 + 0.00A_2^4 \quad (7.22)$$

$$\overline{\kappa}_{13} = 39.60,\ \overline{\kappa}_{33} = -0.03,\ \tilde{\kappa}_{33}(A_3) = -0.00A_3^2 + 0.00A_3^4. \quad (7.23)$$

It can be seen that all nonlinear terms are very small as expected since the system behaves nearly linearly during the earthquake. The modal displacements calculated from these modal equations are plotted (dashed lines) and compared with the filtered measured responses (solid lines) in Figure 7.19, 7.20 and 7.21. The combined three-mode response calculated from the modal equations are shown in Figure 7.22 in correspondence with the

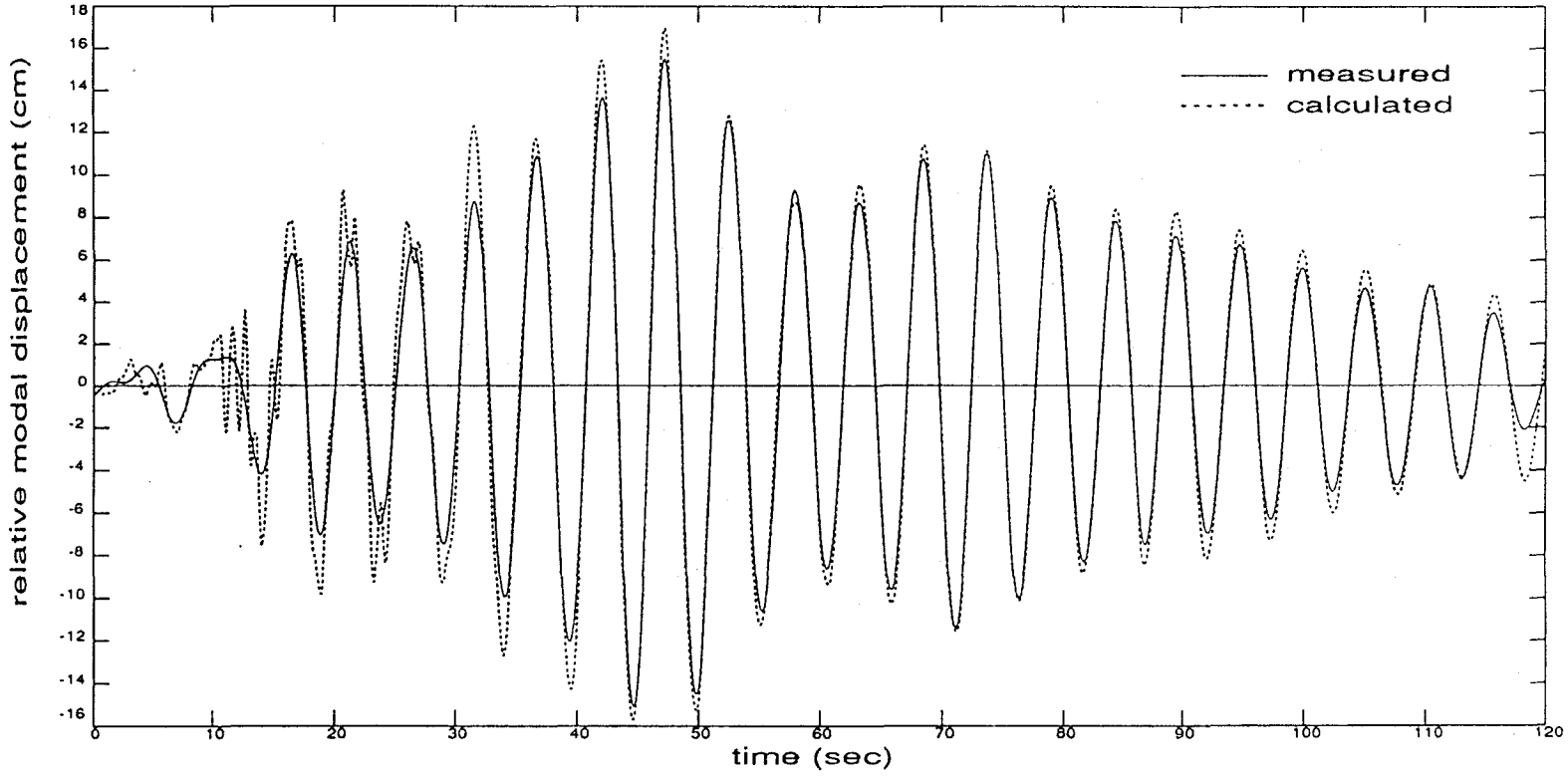

Figure 7.19. Comparison of calculated and measured relative modal displacements: first N/S mode identified by simplified model method.

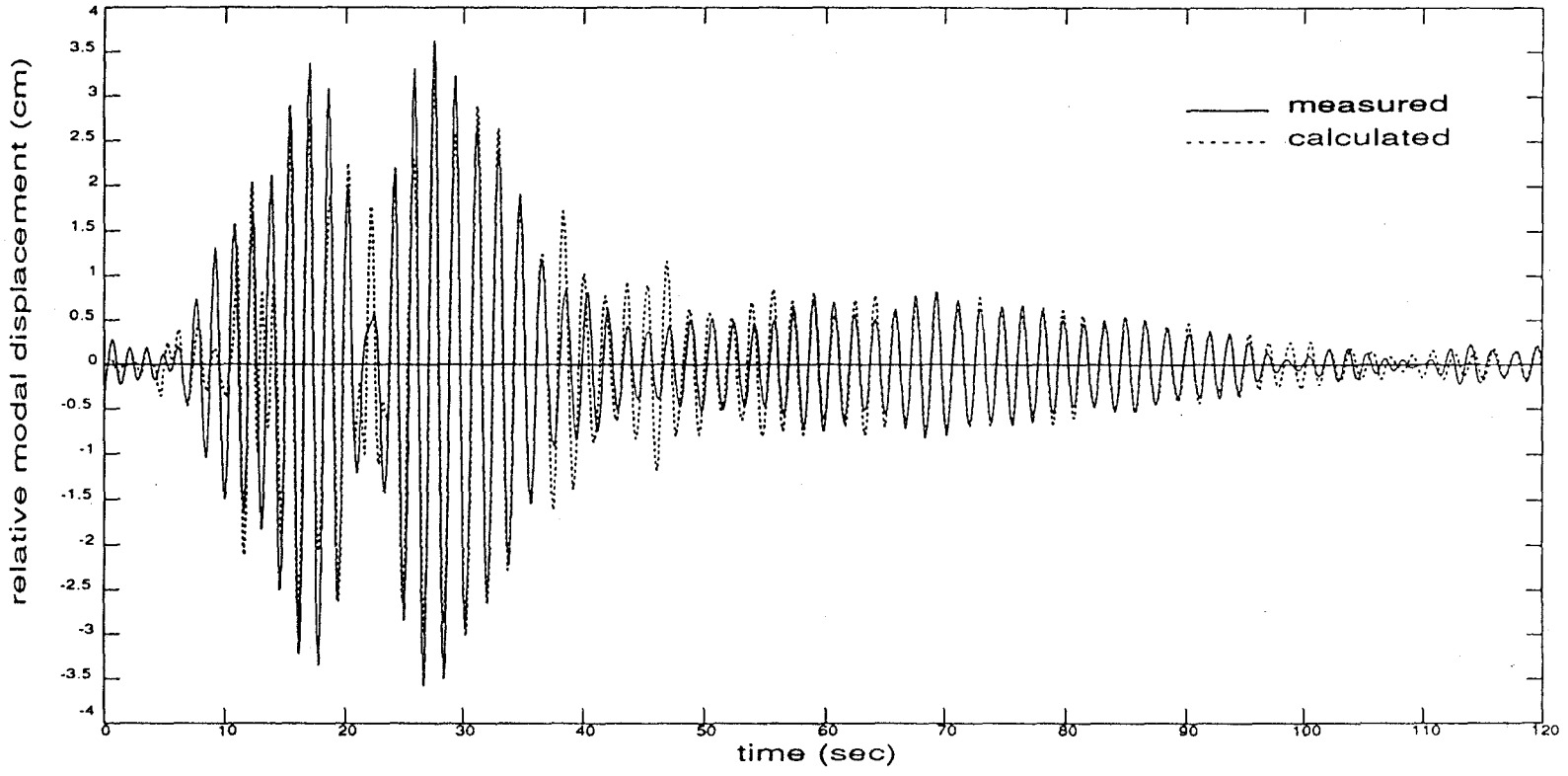

Figure 7.20. Comparison of calculated and measured relative modal displacements: second N/S mode identified by simplified model method.

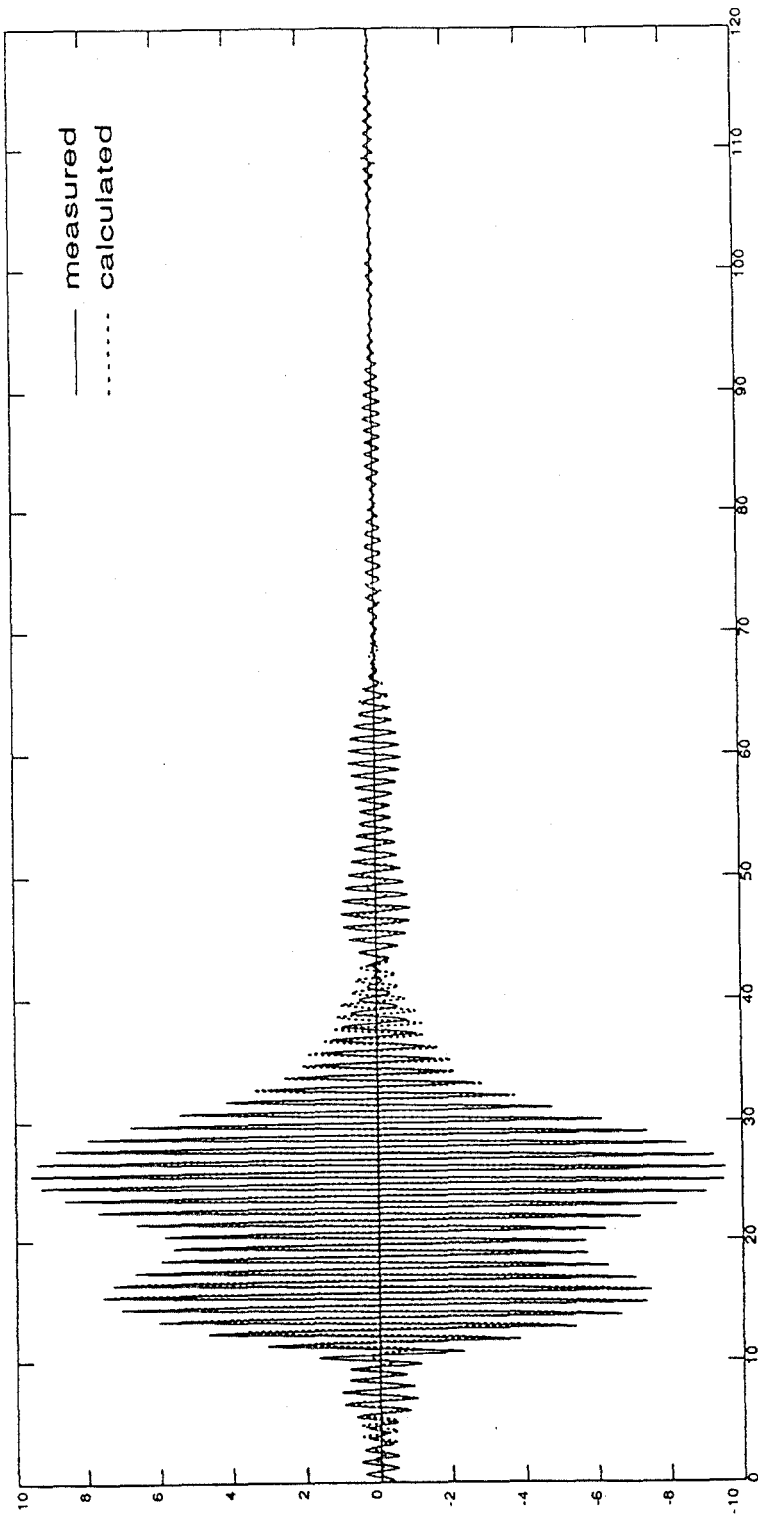

Figure 7.21. Comparison of calculated and measured relative modal displacements: third N/S mode identified by simplified model method.

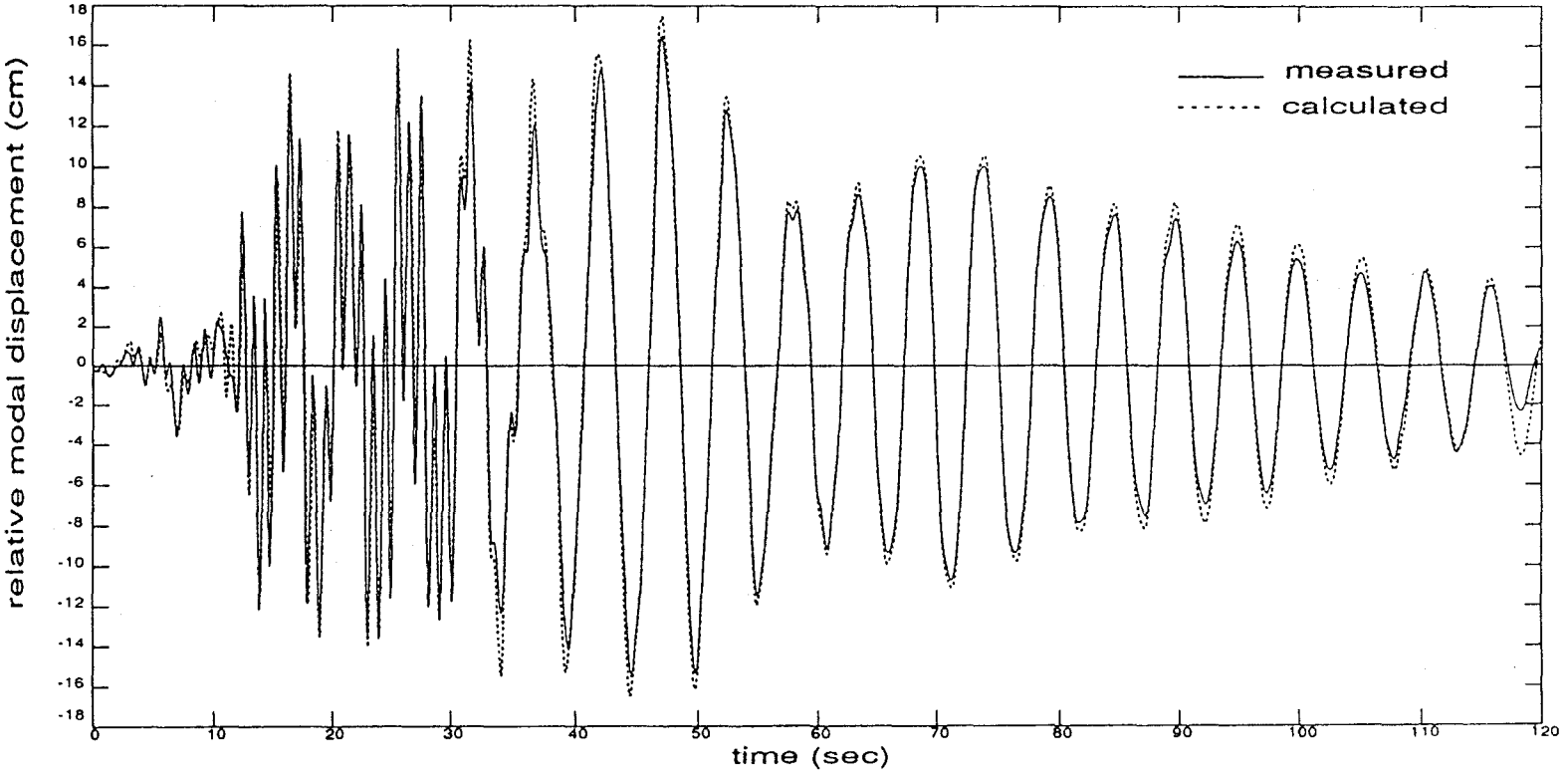

Figure 7.22. Comparison of combined 3 calculated relative modal displacements (by simplified model method) and measured relative displacement.

measured response. The results show that the first three modes dominate the response of the system and that these modal equations can describe the system response quite well.

In the successive approximation procedure, $\varpi_{1j}(A_j)$ (instead of $\omega_j^2(A_j)$), $\alpha_j(A_j)$ and $\beta_j(A_j)$ obtained above (7.11-7.19) are used to derive the modal equations. Applying the successive approximation method for a cubic-order approximation leads to the following results

$$\varpi_{31}(A_1) = \varpi_{32}(A_2) = 0.00 + 0.00A_{1,2}^2 + 0.00A_{1,2}^4 \qquad (7.24)$$

$$\varpi_{33}(A_3) = -0.57 + 0.02A_3^2 + 0.00A_3^2 . \qquad (7.25)$$

These equations imply that the cubic terms for the first and second modes do not result in any improvement. It is not surprising since all modes are very weakly nonlinear and so the first terms are a very good approximation. According to the successive approximation approach, the modal equation of the first and second modes are respectively

$$\ddot{u}_j + \alpha_j(A_j)\dot{u}_j + \varpi_{1j}(A_j)u_j = -\beta_j(A_j)\ddot{z} \qquad (7.26)$$

where j = 1, 2 and $\varpi_{1j}(A_j)$, $\alpha_j(A_j)$ and $\beta_j(A_j)$ are given above. The third modal equation is

$$\ddot{u}_3 + \alpha_3(A_3)\dot{u}_3 + \varpi_{13}(A_3)u_3 + \varpi_{33}(A_3)u_3^3 = -\beta_3(A_3)\ddot{z} . \qquad (7.27)$$

The total three-mode displacement response predicted by these modal equations is shown in Figure 7.23.

Using the equation (5.24) and the modal responses of all stations, the mode shapes

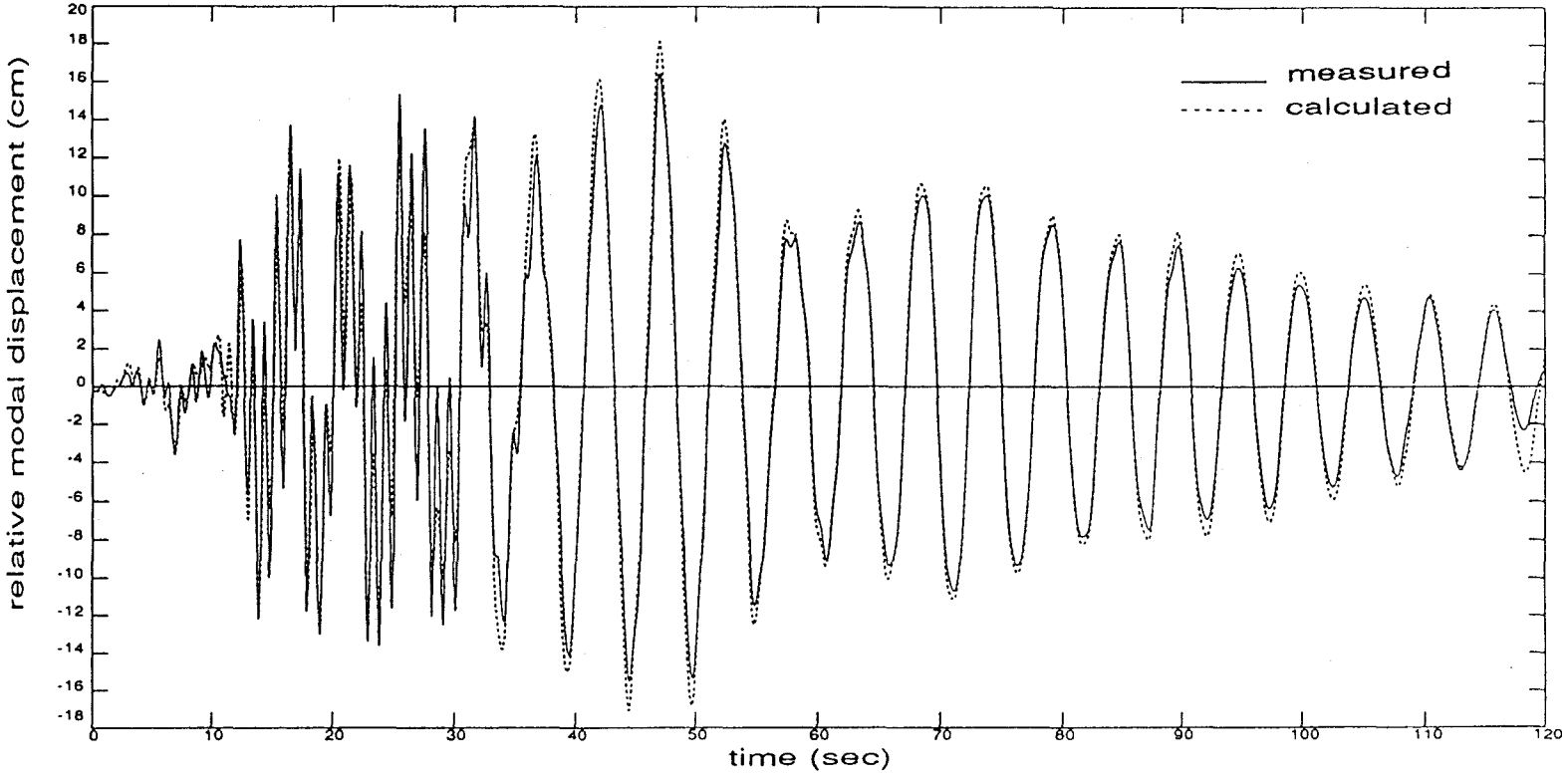

Figure 7.23. Comparison of combined 3 calculated relative modal displacements (by succesive approximation method) and measured relative displacement.

of the three modes are obtained as

$$\text{1st mode}\begin{cases}\text{44th floor} & \phi_{41}(A) = 1.00 \\ \text{39th floor} & \phi_{31}(A) = 0.91 - 0.00A_1^2 + 0.00A_1^4 \\ \text{16th floor} & \phi_{21}(A) = 0.36 - 0.00A_2^2 - 0.00A_1^4 \\ \text{2nd floor} & \phi_{11}(A) = 0.02 - 0.00A_1^2 + 0.00A_1^4 \end{cases} \quad (7.28)$$

$$\text{2nd mode}\begin{cases}\text{44th floor} & \phi_{42}(A) = 1.00 \\ \text{39th floor} & \phi_{32}(A) = 0.56 - 0.02A_2^2 + 0.00A_2^4 \\ \text{16th floor} & \phi_{22}(A) = -0.63 - 0.03A_2^2 + 0.00A_2^4 \\ \text{2nd floor} & \phi_{12}(A) = -0.04 + 0.00A_2^2 - 0.00A_2^4 \end{cases} \quad (7.29)$$

$$\text{3rd mode}\begin{cases}\text{44th floor} & \phi_{43}(A) = 1.00 \\ \text{39th floor} & \phi_{33}(A) = 0.11 - 0.00A_3^2 + 0.00A_3^4 \\ \text{16th floor} & \phi_{23}(A) = 0.40 - 0.00A_3^2 - 0.00A_3^4 \\ \text{2nd floor} & \phi_{13}(A) = 0.06 + 0.00A_3^2 - 0.00A_3^4 \end{cases} . \quad (7.30)$$

These functions are shown in Figures 7.24 (a), 7.25 (a) and 7.26 respectively for the first, second and third modes. The corresponding linear mode shape values are also drawn for comparison. The first and second mode shapes associated with the maximum modal amplitudes

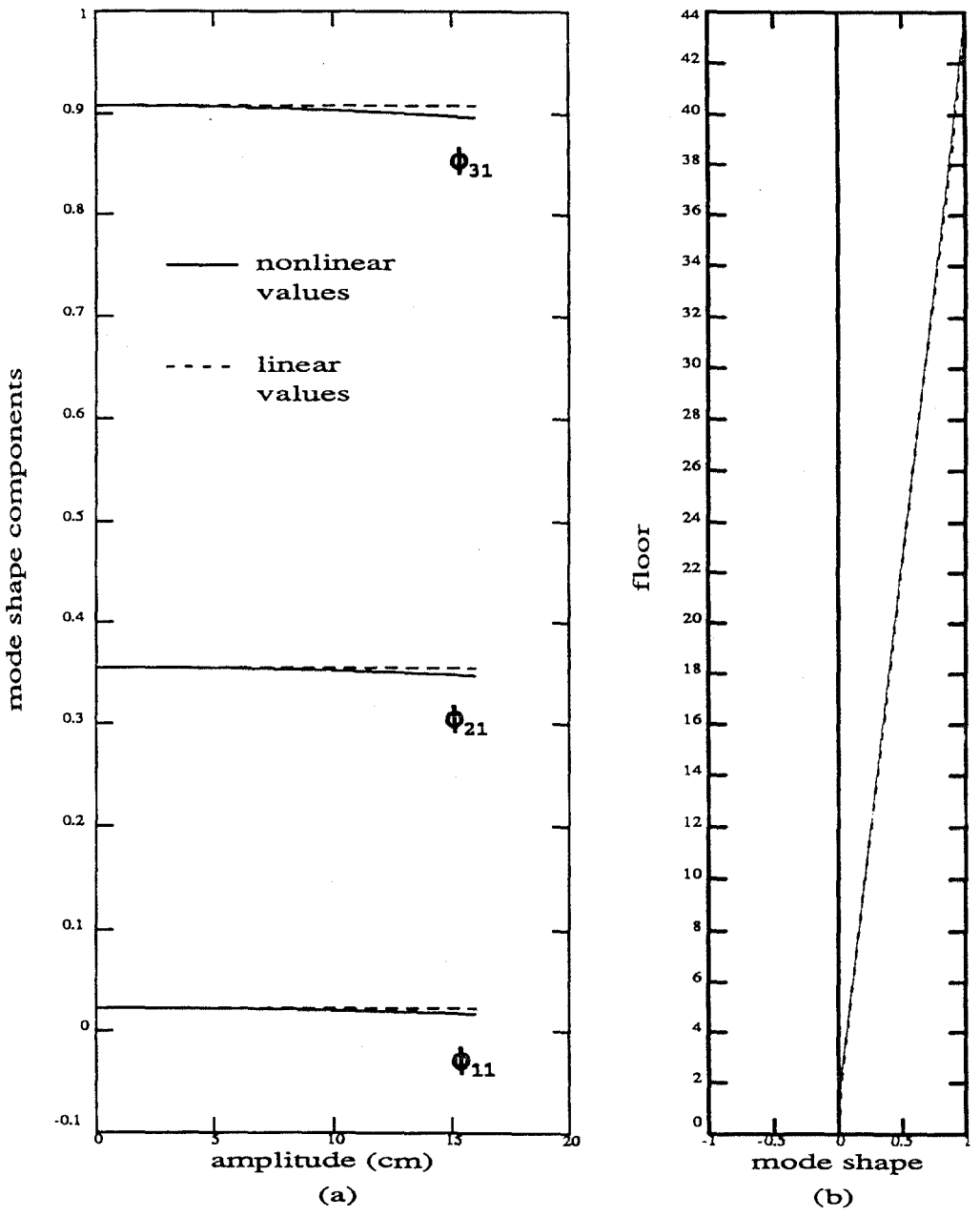

Figure 7.24. Identified first mode shape

(a) mode shape components

(b) mode shape configuration

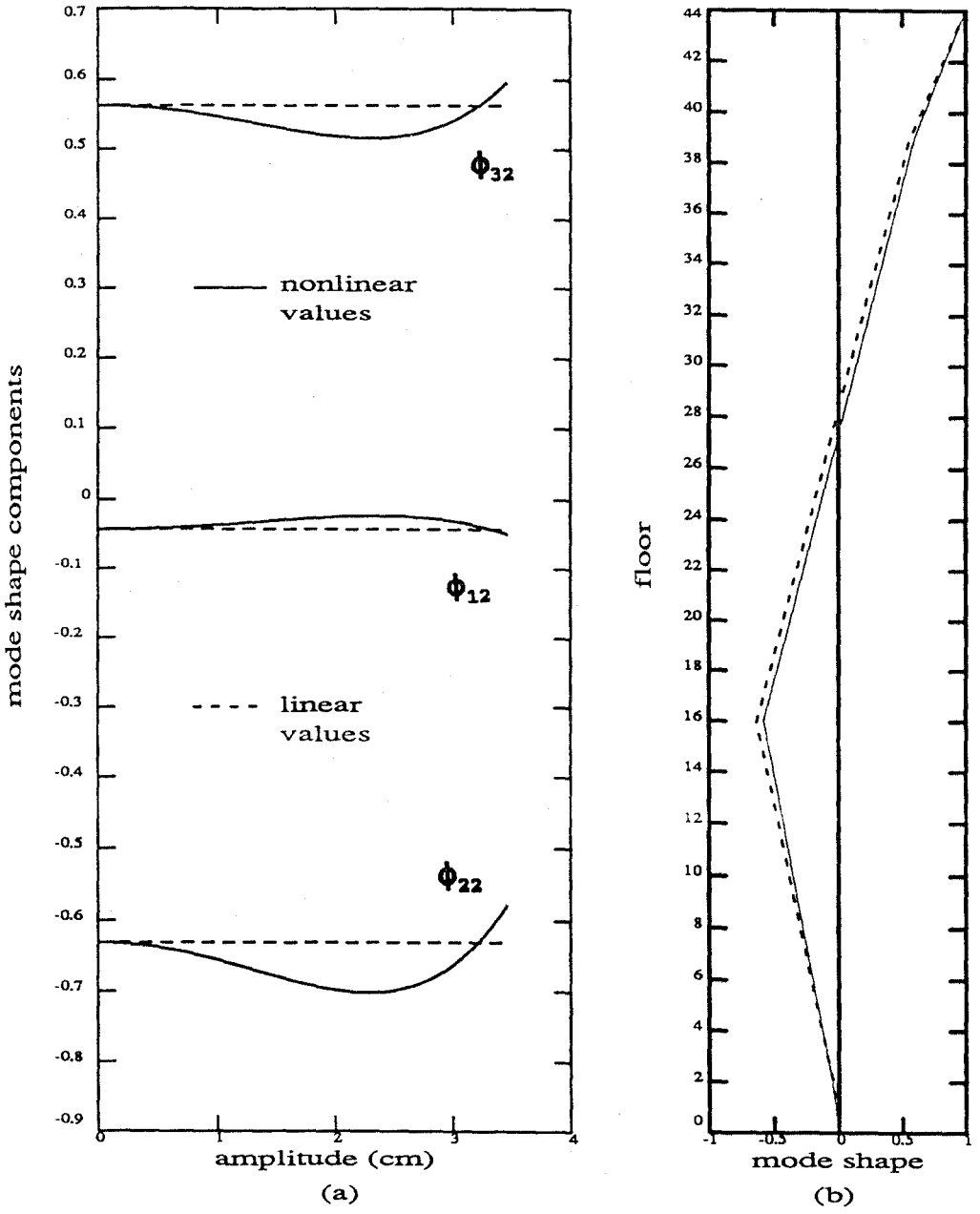

Figure 7.25. Identified second mode shape

(a) mode shape components

(b) mode shape configuration

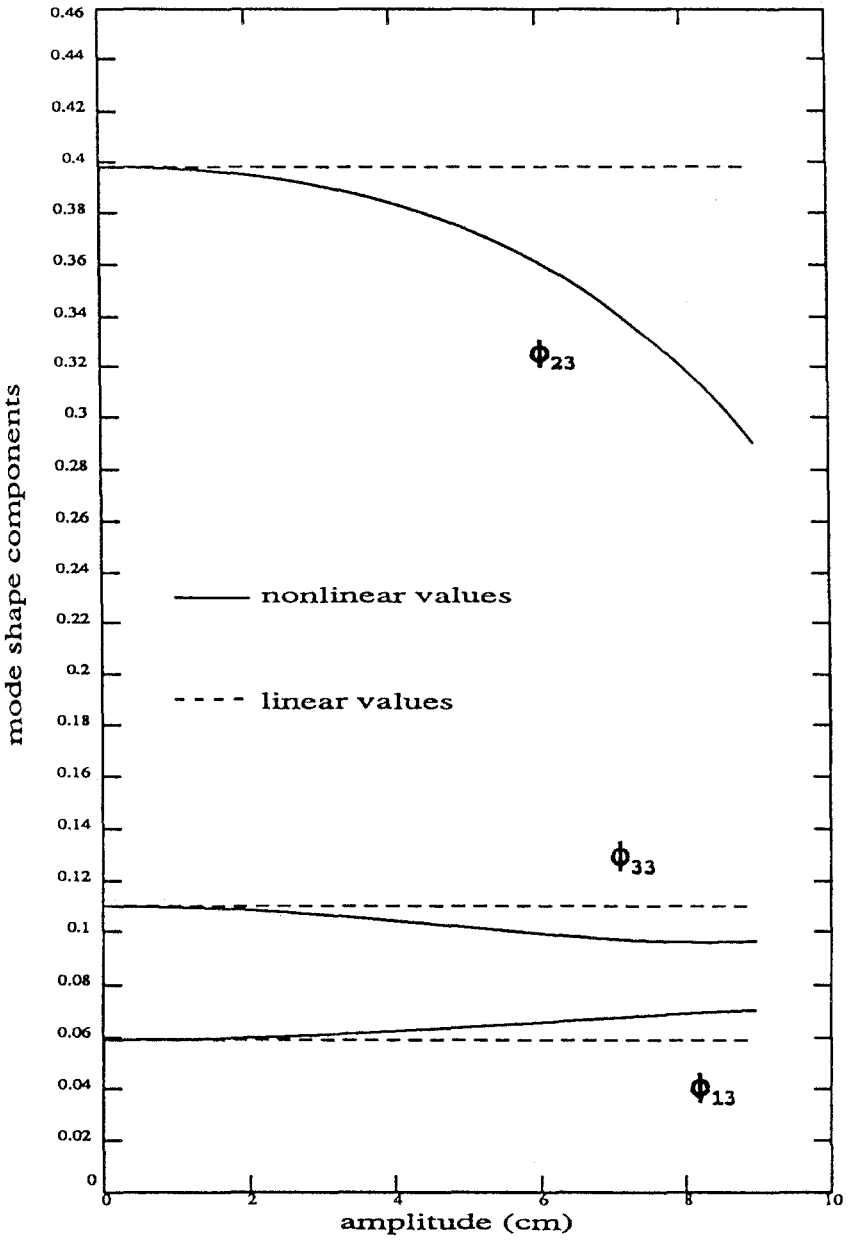

Figure 7.26. Identified third modeshape components

and the corresponding linear ones are shown in Figure 7.24 (b) and 7.25 (b). The third mode shape is not shown since it cannot be represented due to the lack of necessary measurement station.

From Figure 7.24(a) it can be seen that all first-mode shape components monotonously decrease when amplitude increases. The biggest difference between the nonlinear mode and linear mode shapes occur at the instant of maximal modal displacement. Figure 7.24(a) shows that the first nonlinear mode shape changes little. The linear and nonlinear mode shapes are nearly the same, which is shown in Figure 7.24(b). The second nonlinear-mode shape at maximal displacement is slightly different from the linear one. From 7.25(a), the biggest difference in this vibration event between linear and nonlinear mode occurs around $A \approx 2.2cm$. For the third mode, as seen from 7.26, the biggest difference occurs at maximal displacement and ϕ_{23} (16th) floor changes in a large amount.

7.3 SUMMARY

The seismic responses of a 47-story building (N-S) in San Francisco and a 4-story building (E-W) in Watsonville to the Loma Prieta earthquake were analyzed using the modal approach. Both previously proposed modal identification methods incorporating two amplitude-dependent nonlinear modes were used.

It has been found that the dynamic behavior of the 47-story building was dominated by its first three modes. Since these modes are well separated, each mode can be identified separately by the proposed methods. Using these methods, all modal parameters (natural frequencies, effective modal damping coefficients, modal participation factors and mode shapes)

were identified and modal equations were established from the recorded response data. In these results, all nonlinear terms are very small. This shows that the response of the structure in Loma Prieta earthquake was almost linear. Since the nonlinear performance in the response was very small, only the tentative nonlinear dynamic properties of the structure could be extracted from the recorded data. Since very limited information about system nonlinearities is included in the data, the resulting modal parameters and modal equations can describe the system only in the small amplitude range of vibration. The dynamic behavior of three modes in the linear and weakly nonlinear vibration range are shown in the corresponding figures of the modal parameters and represented by mathematical expressions. Changes of modal parameters with modal amplitude can be found in these figures. By these modal parameters and the modal equations, response characteristics of the structure within the observed vibration range can be assessed for a future earthquake. However, the dynamic performance of the structure beyond this vibration range may not be accurately predicted by the identified results.

The 4-story building was found to have strong nonlinear behavior during the Loma Prieta earthquake. This is supported by the identified results since modal equations determined by two approaches have significant nonlinear terms. By amplitude-dependent models and the corresponding identification methods, nonlinear dynamic properties of the structure were extracted and represented quantitatively. The investigation showed that the response of the structure to the Loma Prieta earthquake was dominated by only one mode. The modal parameters of this mode were found by the identification procedure and the properties of these parameters were shown by corresponding curves. Since all other modes are higher (at least three times higher) than *9Hz* and the major earthquake energy components are lower than *5Hz* (from

Figure 7.3a), the identified model can be used to assess dynamic behavior and to predict response of the system subjected to other earthquake.

Some advantages of the amplitude-dependent model and corresponding modal identification have been demonstrated through their applications. First, nonlinearities in the mode can be identified through the results, since modal stiffness is represented by the modal frequency and the modal restoring force is given by the modal equation. Second, nonlinear behavior of a mode can be described quantitatively since the modal parameters are expressed as functions of amplitude. By this approach, the dynamic characteristics of a system at any vibration level can be assessed. If a vibration of the system is beyond the level of the data used for identification, the modal parameters can still be predicted by extension of the functions. Meanwhile, the linear modal parameters of a system can be identified as the limit value of nonlinear modal parameters as modal amplitude tends to zero. In addition, it has been already shown by the analysis of the 47-story building that the presented modal identification is also applicable to linear systems.

CHAPTER 8

CONCLUSIONS

The purpose of this study has been to develop a deeper understanding of mode-like behavior of nonlinear systems in real structural vibrations and the application of these properties in dynamic analysis of nonlinear structures.

A study of mode-like properties and of identification of nonlinear vibrating systems has been presented in this thesis. A new nonlinear modal analysis methodology that is suitable for use with multi-degree-of-freedom nonlinear systems with a small number of resonant modes is proposed. The nonlinear modal analysis approach presented is applicable to the dynamic analysis of structures whose vibration amplitude may vary over a large range.

The study consists of forward modal analysis and backward modal analysis. Forward analysis is the analysis process of calculating modal frequencies and mode shapes (instantaneous and amplitude-dependent) for nonlinear systems in which the equations of motion of the system are already known *a priori* using the mass matrix and stiffness restoring force functions of the system. Backward analysis (modal identification) is the process of identification of modal frequencies, mode shapes (amplitude-dependent) and modal equations using excitation and response data from vibration measurements.

The study has clarified basic concepts of nonlinear modes (rigorous and

approximate), discussed the range of application of nonlinear modes, presented a methodology for using the modal approach in nonlinear structural analysis, and proposed approximate analysis approaches. For applications to more general nonlinear systems, the studies of nonlinear mode-like behavior presented in this work were performed using approximate analysis techniques.

For the calculation of nonlinear modal frequencies and mode shapes in the forward analysis case, approximate methods in which all modal quantities are evaluated as functions of displacement or modal amplitude are presented. Among these approaches, amplitude-dependent modal quantities are obtained as approximations of instantaneous values and the generalized method unifies the Galerkin's method and the peak method. The forward analysis leads to a new understanding of nonlinear modes and shows that modal frequencies and mode shapes of nonlinear systems are dependent upon modal response level (amplitude). The example of a three-degree-of-freedom system with cubic stiffness nonlinearity demonstrates that the variation of modal frequency and mode shape with modal amplitude may be significant and cannot be ignored in general.

An important property of forced nonlinear vibrating systems, that in resonance the system assumes the displacement configuration of the free vibration mode shape, provides a basis for the application of free vibration modes to the analysis of forced vibration. Amplitude-dependent modal equations that are parametric differential equations with amplitude-dependent coefficients are derived in the case of a single resonance using the amplitude-dependent modal relationship. The amplitude-dependent modal equation is suitable for any level of vibration and overcomes the limitation on application of constant-

coefficient models.

The amplitude-dependent model of modal equations is extended to the multiple resonance case where each resonance is treated as a mode. Two specific amplitude-dependent models which are suitable for identification from recorded vibration data are proposed. The successive approximation model is an asymptotic approach from a linear approximation to high-order nonlinear approximation. All coefficients of the model are functions of modal amplitude. The simplified expansion model is based on a modified Taylor expansion of the modal restoring force function in which one term remains amplitude-dependent and others are simplified to be constant. The former model can be expected to have fewer lower-order terms than the latter for a satisfactory match with a response data. The latter model is expected to be able to describe more stronger nonlinearities than the former since the former presents an equivalent weakly nonlinear system.

For these two models, two identification algorithms, the successive approximation model method and the simplified expansion model method, are presented. Both identification procedures are performed in the time domain, one mode at a time. Modal separation is based on separation of the resonant responses using frequency filtering. Each "modal response" is used to estimate coefficient functions in the modal equations. Both methods give unique identification results. The procedures also determine modal frequency and mode shape as functions of modal amplitude.

The mode-like behavior of a three-degree-of-freedom system with a cubic nonlinearity is examined using both forward and backward modal analysis methods. Both

modal identification procedures are applied to modeling of the first mode of the system. The successive approximation modal equation and the simplified expansion modal equation are identified from given response data. The responses calculated with these modal equations give a good match to the data. This shows that both identification procedures are effective. The identified modal equations were used to predict the response to a different loading and gave satisfactory results. This demonstrates that the proposed models of modal equation are efficient for describing modal response of different levels.

The modal identification approaches presented are also applied to investigate the seismic response of a forty-seven-story building and a four-story building. The studies show that behavior of the forty-seven-story building during the Loma Prieta earthquake was almost linear and that the response was dominated by the first three modes. The four-story building established a significant nonlinear behavior during the Loma Prieta earthquake and the response was dominated by one mode. The modal frequencies, mode shapes and modal equations of these two buildings are identified from the response data. The dynamic behavior of the structures is represented in terms of these modal frequencies and modal shapes. The modal equations can be used to predict the response of these structures to future loadings. These applications demonstrate that the modal approaches presented are feasible and effective in real engineering analysis and that the methods are applicable over a large vibration level range.

It is believed that the work presented in this thesis will be helpful for better understanding of mode-like behavior of nonlinear systems and provide a useful tool for nonlinear structural dynamic analysis.

This thesis elaborates the studies on the mode-like properties of elastic nonlinear systems and modal identification of nonlinear systems with elastic nonlinear models. For inelastic nonlinear systems, the approach may be used as an approximation. For example, the proposed model can be used to describe the backbone of restoring force loop of hysteretic systems. However, it cannot explore the hysteretic characteristics of structures. For an improvement of the structural seismic modal analysis, mode-like behavior of hysteretic nonlinear systems may be further investigated. In addition, inelastic systems with other nonlinearities may be studied for more understanding of nonlinear mode-like behavior. The methodology described from chapter 2 through 4 may be used for forward modal analysis.

REFERENCE

[1] Distefano, Nestor; Rath, Amitav "System Identification Nonlinear Structural Seismic Dynamics," Computer Methods in Applied Mechanics and Engineering 5 (1975) 353-372

[2] Distefano, Nestor; Rath, Amitav "Sequential Identification of Hysterestic and Viscous Models Structural Seismic Dynamics," Computer Methods in Applied Mechanics and Engineering 6 (1975) 219-232

[3] Udwadia, F. E.; Marmarelis, P. Z. "The Identification of Buildings. I The Linear Case," Bulletin of Seismology Society of America, Vol. 66, 1976

[4] Udwadia, F. E.; Marmarelis, P. Z. "The Identification of Buildings. II The Nonlinear Case." Bulletin of Seismology Society of America, Vol. 66, 1976

[5] McVerry, G. H. "Frequency Domain Identification of Structural Models from Earthquake Records." Report No. EERL 79-02, EERL, California Institute of Technology, Pasadena, California, October 1979

[6] Abdel-Ghaffar, A. M.; Scott, R. F. "Experimental Identification of the Dynamic Response Characteristics of an Earth Dam," Proceedings of the 2nd U.S. National Conference on Earthquake Engineering, 1979

[7] Beck, J. L.; Jennings, P. C. "Structural Identification Using Linear Models and Earthquake Records," International Journal of Earthquake Engineering and Structural

Dynamics, Vol. 8, 1980

[8] Toussi, S. and Yao, J. "Hysteretic Identification of Multi-Story Buildings." Report No. CE-STR-81-15, School of Civil Engineering, Purdue University, May 1981.

[9] Toussi, S. and Yao, J. "Identification of Hysteretic Behavior for Existing Structures." Report No. CE-STR-80-19, School of Civil Engineering, Purdue University, December 1980.

[10] Beck, J. L. "System Identification Applied to Strong Motion Records from Structures." Earthquake Ground Motion and Its Effects on Structures, ASME, AMD-Vol.53, New York, 1982

[11] Cifuentes, Arturo O. "System Identification of Hysteretic Structures." Earthquake Engineering Research Laboratory Ph.D. thesis 1984.

[12] Cifuentes, Arturo O.; Iwan, W.D. "Nonlinear System Identification Based on Modeling of Restoring Force Behavior." Soil Dynamics and Earthquake Engineering 1989, v 8 no.1

[13] Beck, J. L.; Jayakumar, P "Pseudo-Dynamic Testing and Model Identification," Proceedings of the 3rd U.S. National Conference on Earthquake Engineering, Charleston, South Carolina, August 1986

[14] Beck, J. L.; Jayakumar, P "Application of System Identification to Pseudo-Dynamic Test Data from a Full-Scale Six-Story Steel Structure," Proceedings of the International Conference on Vibration Problems in Engineering, Xian, China, June 1986

[15] Beck, J. L. " Determining Models of Structures from Earthquake Records." Report no.

EERL 78-01 Earthquake Engineering Research Laboratory, California Institute of Technology, Pasadena, CA 1987.

[16] Iwan, Wilfred D. "A Model For System Identification of Degrading Structures." Earthquake Engineering and Structural Dynamics. v 14 877-890 (1986)

[17] Loh, Chin-hsiung; Chin-Huang "Identification Study on Base Isolation Systems by Full-Scale Buildings." Proceedings of JACE no.455/I-21 1992-10

[18] Loh, Chin-hsiung; Tou, Iat-ChunLee, "A System Identification Approach to the Detection of Changes in Structural Parameters."

[19] Loh, Chin-hsiung; Chung, Sheng-Tsai "A Three-Stage Identification Approach for Hysteretic Systems." Earthquake Engineering and Structural Dynamics. v 22 129-150 (1993)

[20] Lu, S. L.; Frederick, D. "The Random Structural Response of a MDF System With Stiffness and Strength Degradation." Proceedings of the 8th International Modal Analysis Conference, 1990

[21] Hart, Gary C.; Yao, James T. P. "System Identification in Structural Dynamics." J. Engineering Mechanics Division pp. 1089-1104, Dec 1977.

[22] Yun, Chung-Bang; Shinozuka, Masanobu "Identification of Nonlinear Structural Dynamic Systems." J. Struct. Mech., 8 (2), 187-203 (1980)

[23] Distefano, Nestor; Rath, AmitavYun, "Modeling and Identification in Nonlinear Structural Dynamics," Report EERC, University of California, Berkeley, Calif., 1974.

[24] Kim, K. Steven ; Shin, Young S. :"Application of a New Gilbert Transform Method to Nonlinearity Identification." Proceedings of the 8th International Analysis Conference,

1990

[25] Gifford, S. J. ; Tomlinson, G. R. "Understanding Multi-degree of Freedom Nonlinear Systems via Higher Order Frequency Response Functions." Proceedings of the 8th International Analysis Conference, 1990.

[26] Hong, J. Y.; Kim, Y. C. Powers, D. J. "On Modeling the Nonlinear Relationship Between Fluctuations With Nonlinear Transfer Functions. " Proceedings of the IEEE, v 68 No.8 August 1980.

[27] Vanherok, P.; Wyckaert, K.; Brussel, H. V. "Parametric Identification of Non-Linear Mechanical Systems From Measurements in Time and Frequency." Proceedings of the 8th International Analysis Conference,1990.

[28] Frachebourg, A. "Using Voterra Model With Impact Excitation: A Simple Solution to Identify Nonlinearities." Proceedings of the the 8th International Modal Analysis Conference, 1990.

[29] Worden, K.; Tomlinson, G. R. "Application of the Restoring Force Surface Method to Nonlinear Elements." Proceedings of the 8th International Modal Analysis Conference 1990.

[30] Bendat, Julius S. ; Palo, Paul A. "Practical Techniques for Nonlinear System Analysis/Identification." Sound and Vibration, June 1990

[31] Bendat, J. S., " Nonlinear System Analysis and Identification from Random Data." Wiley-Interscience, New York, 1990

[32] Kan, C. D.; Chen, H. M. ; Yang, J. S. "Error Analysis of Linear And Nonlinear System Identification." Proceedings of the 8th International Modal Analysis Conference, 1990

[33] Bella, David F.; Pardon, Gerard C. " Using Multiple Input/Output Analysis To Estimate Parameters of Linear Systems With Additional Nonlinear Components" Proceedings of the 8th International Modal Analysis Conference, 1990

[34] Hunter Jr, Norman F. "Analysis of Nonlinear Systems Using Arma Models" Proceedings of the 8th International Modal Analysis Conference, 1990

[35] Nam, S. W.; Kim, S. B.; Powers, E. J. " Nonlinear System Identification with Random Excitation Using Discrete Third-Order Volterra Series" Proceedings of the 8th International Modal Analysis Conference, 1990

[36] Benhafsi, Y; Penny, J.; Friswell, M. I. "A Method of System Identification For Nonlinear Vibrating Structures" Proceedings of the 8th International Modal Analysis Conference, 1990

[37] Tang, Jiashi "Parameter Identification of Nonlinear System in the Frequency Domain" Proceedings of the 8th International Modal Analysis Conference, 1990

[38] Masri. S. F.; Caughey, T. K. "A Nonparametric Identification Technique for Nonlinear Dynamic Problems." J. Applied Mechanics Jun 1979 v 46 pp. 433-447

[39] Masri, S. F.; Caughey, T. K. "Identification of Nonlinear Structural Dynamic Systems." J. Structural Mechanics 1980.

[40] Masri, S. F.; Sassi, H. ; Caughey, T. K. "Nonparametric Identification of Nearly Arbitrary Nonlinear Systems." J. Applied Mechanics Sept 1982 v 49 pp. 619-628

[41] Masri, S. F. ; Miller, R. K.; Saud, A. F.; Caughey, T. K. "Identification of Nonlinear Vibrating Structures: Part I-Formulation." J. Applied Mechanics v 54 pp. 918-922 Dec 1987.

[42] Masri, S. F. ; Miller, R. K.; Saud, A. F.; Caughey, T. K. "Identification of Nonlinear Vibrating Structures: Part II-Formulation." J. Applied Mechanics v 54 pp. 923-929 Dec1987.

[43] Bendat, J. S. ; Palo, P. A. and Coppolino, R. N., "A General Identification Technique for Nonlinear Differential Equations of Motion." Probablistic Engineering Mechanics, 1990

[44] Worden, K. ; Wright, J. R.; Al-Hadid, M. A. ; Mohammad, K. S. "Experimental Identification of Multi-Degree-of-Freedom Nonlinear Systems Using Restoring Force Methods." Modal Analysis v 9 no.1 January 1994

[45] Ma, Xiaojiang; Yuan, Jingxia; Liu, Peide "A New Nonlinear Modal Parameters Identification Method" Proceedings of 8th International Modal Analysis Conference

[46] Simon, M.; Tomlinso, G. R. "Use of the Hilbert Transform in Modal Analysis of Linear and Non-Linear Structures." J. Sound and Vibration (1984) 96 (4), 421-436

[47] Vinh, T.; Liu, H. "Extension of Modal Analysis to Non-Linear Systems." Proceedings of the 8th International Analysis Conference.

[48] Setio, S.; Setio, H. D.; Jezequel, L. " Modal Analysis of Nonlinear Multi-Degree-of-Freedom Structures." Int. J. Analytical and Experimental Modal Analysis v 7 no.2 April 1992

[49] Jezequel, L.; Setio, H. D.; Setio, S. "Nonlinear Modal Synthesis in Frequency Domain." Proceedings of the 8th International Modal Analysis Conference

[50] Geng, Chia-Yen "Generalized Modal Identification of Linear and Nonlinear Dynamic

Systems." Report no. EERL 87-05 Earthquake Engineering Research Laboratory, California Institute of Technology, Pasadena, CA 1987.

[51] Huang, L. ; Iwan, W. D. "A Single Mode Method for the Analysis and Identification of Nonlinear MDOF Systems." Proceedings of the 10th International Modal Analysis Conference 1992.

[52] Vakakis, Alexander F. "Analysis and Identification of Linear and Nonlinear Normal Model in Vibrating Systems." Ph.D. Thesis, California Institute of Technology, Pasadena, CA 1992

[53] Rosenberg, R. M. "Normal Modes of Nonlinear Dual-Mode System." J Applied Mechanics, Jun 1960 pp. 263-268

[54] Rosenberg, R. M. " On Normal Vibrations of a General Class of Nonlinear Dual-Mode Systems." J. Applied Mechanics Jun 1961 pp. 275-283

[55] Rosenberg, R. M. "The Normal Modes of Nonlinear n-Degree-of-Freedom System." J. Applied Mechanics 1962.

[56] Atkinson, C. P. "A Study of the Nonlinearly Related Modal Solutions of Coupled Nonlinear Systems by Superposition Techniques." J. Applied Mechanics Jun 1965 pp. 359-364

[57] Chi, Cheng-Ching; Rosenberg, R. M. "On Damped Non-Linear Dynamic Systems With Many Degrees of Freedom." J. Non-linear Mechanics 1985 v 20 pp. 371-384

[58] Yen, David H. Y. "On the Normal Modes of Non-Linear Dual-Mass Systems." J. Nonlinear Mechanics v 9 pp. 45-53 1974.

[59] Rosenberg, R. M. "Steady-State Forced Vibrations." Int. J. Non-Linear Mechanics 1966 v

1 pp. 95-108

[60] Pak, C. H.; Rosenberg, R. M. "On the Existence of Normal Mode Vibrations in Nonlinear Systems." May 1967

[61] Johenson, T. L.; Rand, R. H. "On the Existence and Bifurcation of Minimal Normal Modes." J. Non-Linear Mechanics v 14 pp. 1-12 1979.

[62] Atkinson, C. P. "On the Stability of the Linearly Related Modes of Certain Nonlinear Two-Degree-of-Freedom System." J. Applied Mechanics, March 1961 pp. 71-77

[63] Rand, R. " A Higher Order Approximation for Nonlinear Normal Modes in Two DOF Systems. Int.J. Nonlinear Mech.6,pp.545-547 1971b

[64] Rand, Richard H. "A Direct Method for Non-Linear normal Modes." J. Non-linear Mechanics v 9 pp. 363-368 1974.

[65] Month, L.; Rand, R. " The Stability of Bifurcating Periodic Solutions in a Two DOF Nonlinear System" J. Appl. Mech., pp.782-783 1980

[66] Caughey, T. C.; Vaka kis, A.; Sivo, J. M. "Analytical Study of Similar Normal Modes And Their Bifurcations in a Class of Strongly Nonlinear Systems."

[67] Shakal, A.; Huang, M. etc. "CSMIP Strong-Motion Records from the Santa Cruz Mointains (Loma Prieta), California Earthquake of 17 October 1989." Report No.OSMS 89-06, California Strong Motion Instrument Program, California Department of Conservation, Division of Mines and Geology, November 17, 1989

[68] Szemplinska-Stupnicka, W. "A Study of Main and Secondary Resonances in Nonlinear Multi-Degree-Of-Freedom Vibration Systems." J. Nonlinear Mechanics, Vol.10, pp.289-304, 1975

[69] Szemplinska-Stupnicka, W. "The Modified Single Mode Method in the Investigations of the Resonant Vibrations of Nonlinear System." J. Sound and Vibration 1979.

[70] Knight Jr, Norman F. " Nonlinear Structural Dynamic Analysis Using a Modified Modal Method." AIAA J. v 23 no.10

[71] Nickell, R. E. "Nonlinear Dynamics By Mode Superposition" Computer Methods In Applied Mechanics And Engineering 7(1976)107-129

[72] Noor, Ahmed K. " Recent Advances in Reduction Methods For Nonlinear Problems" Computers & Structrures v 13 pp. 31-44 1981

[73] Stricklin, James A.; Haisler, Walter E. " Formulations and Solution Procedures For Nonlinear Structural Analysis." Computers & Structures v 7 pp. 125-136 1977

[74] Mohraz, Bijan; Elghadamsi, Fawzi E; Chang, Chi-Jen " An Incremental Mode-Superposition for Non-linear Dynamic Analysis." Earthquake Engineering And Structural Dynamics v 20 1991

[75] Bathe, Klaus-Jurgen; Gracewski, Sherly " On Nonlinear Dynamic Analysis Using Substructuring and Mode Superposition" Computers & Structures. v 13 pp. 699-707, 1981

[76] Morris, Nicholas F. "The Use of Modal Superposition In Nonlinear Dynamics." Computers & Structures v 7 pp. 65-72 1977

[77] Press, W. H.; Flannnery, B. P.; Teukolsky, S. A.; Vetterling, W. T. "Numerical Recipes." Cambridge University Press, 1986

[78] Nayfeh, A. H.; Mook, D. T. "Nonlinear Oscillations." John Willey, New York, 1979

[79] Hashimoto, P. S.; Tiong, L. W.; Steele, L.K.; Johnson, J.J; Beck, J.L. " Stiffness and

Damping Properties of a Low Aspect Ratio Shear Wall Building Based on Recorded Earthquake Responses." Report Nureg/Gr-0612, 1993